UNIVERSITY OF TRENTO

International PhD Program in Biomolecular Sciences

Department of Cellular, Computational and Integrative Biology – CIBIO

XXXI Cycle

Analysis of the role of arginine methylation in the pathogenesis of Huntington's disease

Supervisor

Manuela Basso

Laboratory of Transcriptional Neurobiology

Department of Cellular, Computational and Integrative Biology, University of Trento

Ph.D. Thesis of

Alice Migazzi

Academic Year 2017/2018

Declaration of original authorship

I Alice Migazzi confirm that this is my own work and the use of all material from other sources has been properly and fully acknowledged.

Contents

Abstract

Huntington's disease (HD) is a fatal neurodegenerative disorder characterized by progressive loss of striatal and cortical neurons. HD is caused by an abnormal polyglutamine (polyQ) expansion in Huntingtin protein (HTT). HTT controls vesicular trafficking along axons in neurons through interaction with components of the molecular motor machinery. Arginine methylation is one of the most abundant post-translational modifications (PTMs) and is catalyzed by protein arginine methyltransferases (PRMTs). Recent evidence supports a key role for arginine methylation in neurodegeneration and particularly in polyglutamine diseases. However, whether HTT is methylated at arginine residues has not been investigated yet and the role of arginine methylation in HD pathogenesis remains to be fully elucidated.

In this thesis, I show that vesicle-associated HTT is methylated *in vivo* at two evolutionarily conserved arginine residues, namely R101 and R118. Methylation of HTT at R118 is catalyzed by Protein Arginine Methyltransferase 6 (PRMT6), which localizes on vesicles together with HTT, whereas further analyses are required to identify the enzyme(s) responsible for R101 methylation. Interestingly, loss of PRMT6-mediated R118 methylation reduces the association of HTT with vesicles, impairs anterograde axonal transport and exacerbates polyQ-expanded HTT toxicity. Conversely, PRMT6 overexpression improves the global efficiency of anterograde axonal transport and rescues cell death in neurons expressing polyQ-expanded HTT. These findings establish a crucial role of arginine methylation as a modulator of both normal HTT function and polyQ-expanded HTT toxicity and identify PRMT6 as a novel modifier of HD pathogenesis. Importantly, defects in HTT methylation may contribute to neurodegeneration in HD and promoting arginine methylation of HTT might represent a new therapeutic strategy for HD.

List of abbreviations

AD	Alzheimer's disease
ADMA	Asymmetric dimethylarginine
Adox	Adenosine-2′,3′-dialdehyde
ALS	Amyotrophic lateral sclerosis
APP	Amyloid precursor protein
AR	Androgen receptor
ATP	Adenosine triphosphate
BDNF	Brain-derived neurotrophic factor
CBP	CREB binding protein
Cdk5	Cyclin-dependent kinase 5
CREB	cAMP-response element binding protein
DIV	Days *in vitro*
DRPLA	Dentatorubral-pallidoluysian atrophy
EGFP	Enhanced green fluorescent protein
Ezh2	Enhancer of zeste 2
FUS	Fused in Sarcoma
GABA	γ-aminobutyric acid
GAPDH	Glyceraldehyde 3-phosphate dehydrogenase
HAP1	Huntingtin-associated protein 1
HAP40	Huntingtin-associated protein 40
HAT	Histone acetyltransferase
HD	Huntington's disease
HDACs	Histone deacetylases
HEAT	Huntingtin, Elongation factor 3, protein phosphatase 2A and TOR1
HIP1	Huntingtin interacting protein 1
HIP14	Huntingtin interacting protein 14
HTT	Huntingtin

IGF-1	Insulin-like growth factor 1
JHD	Juvenile Huntington's disease
JMJD6	Jumonji Domain-Containing Protein 6
KHC	Kinesin heavy chain
KIF5C	Kinesin Family Member 5C
KLC	Kinesin light chain
MMA	Monomethylarginine
MSNs	Medium-sized projection spiny neurons
MTA	Methylthioadenosine
NF-kB	Nuclear factor-kB
NMDA	N-methyl-D-aspartate
NMDAR	NMDA receptor
NRSE	Neuron-restrictive silencer elements
PEST	Proline (P)-, glutamic acid (E)-, serine (S)-, and threonine (T)-enriched
PGC1-α	Peroxisome proliferator-activated receptor gamma coactivator 1-alpha
PLA	Proximity ligation assay
PolyQ	Polyglutamine
PRC2	Polycomb repressive complex 2
PRD	Proline-rich domain
PRMTs	Protein arginine methyltransferases
PRMT2	Protein arginine methyltransferase 2
PRMT6	Protein arginine methyltransferase 6
PTMs	Post-translational modifications
REST/NRSF	Repressor Element-1 Transcription Factor/Neuron Restrictive Silencer Factor
SAH	S-adenosylhomocysteine
SAHH	S-adenosylhomocysteine hydrolase
SAM	S-adenosylmethionine
SBMA	Spinal and bulbar muscular atrophy

SCA	Spinocerebellar ataxia
SDMA	Symmetric dimethylarginine
SGK	Serum- and glucocorticoid kinase
SH3	Src Homology 3
Sp1	Specificity protein 1
Suz12	Suppressor of zeste 12
TFIID	Transcription Factor II D
TrkB	Tyrosine receptor kinase B
UPS	Ubiquitin-proteasome system

List of figures

Figure **Page**

1. Introduction

1.1 Huntington's Disease

Huntington's disease (HD), also known as Huntington's chorea, is an autosomal dominant, progressive and fatal neurodegenerative disorder. It is named after George Huntington, the American physician who wrote the first detailed description of this hereditary disease in 1872. HD is caused by an abnormal expansion of a CAG trinucleotide repeat in the coding region of *IT15* gene (also called *HD* or *HTT* gene), which encodes a polyglutamine (polyQ) tract in the Huntingtin (HTT) protein (The Huntington's Disease Collaborative Research Group, 1993). HD is the most common condition belonging to the family of polyglutamine diseases, which comprises nine genetically inherited late-onset neurodegenerative diseases, i.e. spinal and bulbar muscular atrophy (SBMA), dentatorubral-pallidoluysian atrophy (DRPLA) and spinocerebellar ataxia (SCA) type 1, 2, 3, 6, 7 and 17. HD is characterized by a triad of late-onset motor, cognitive and psychiatric symptoms. There are currently no disease-modifying treatments available, and HD patients die within 15-20 years after the appearance of symptoms (Ross and Tabrizi 2011).

1.1.1 Clinical features of Huntington's Disease

1.1.1.1 Epidemiology

HD is the most common monogenic neurological disorder in the developed world (Bates et al. 2015). In the past, the true prevalence of HD was most probably underestimated; nowadays the wider availability of genetic testing for the identification of the CAG repeat expansion allows to obtain more accurate estimates (Ghosh and Tabrizi 2018). Prevalence studies combining both genetic testing and neurological evaluations indicate that 10.6–13.7 individuals per 100,000 (or 1 in 7,300) are affected in Western populations, the incidence being around 4.7-6.9 new cases per million per year (Bates et al. 2015). Remarkably, there is geographic and ethnic variation in the prevalence of HD between populations: HD occurs at much higher rates in populations of European ancestry, whereas lower frequencies are observed in Asian and African populations (Kay, Hayden, and Leavitt 2017). These

higher rates correlate with the genetic differences at the *HTT* locus, with longer average CAG repeat lengths in individuals of European descent compared to other populations (**Figure 1**). However, the overall worldwide prevalence of HD is still unclear, since HD remains significantly understudied outside the developed countries (Kay, Hayden, and Leavitt 2017).

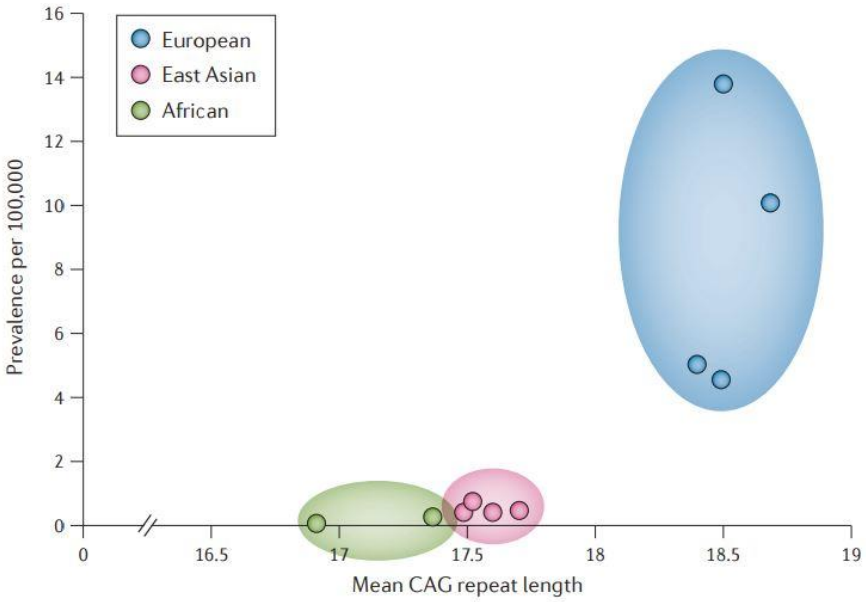

Figure 1: Ethnic variation in the prevalence of Huntington's Disease. Longer CAG repeats in individual of European ancestry are thought to give rise to higher frequencies of CAG expansion, higher rates of *de novo HTT* mutation, and hence higher HD prevalence (Bates et al., 2015).

1.1.1.2 Genetics

The genetic mutation responsible for HD was discovered in 1993 by a collaborative research group, thanks to genetic linkage studies in a Venezuelan population living near Lake Maracaibo, where the prevalence of the disease is particularly high (around 700 in 100,000 people). HD is caused by the expansion of an instable CAG repeat in the first exon of *HTT* gene, which lies on the short arm of chromosome 4 (Gusella *et al.*, 1983; The Huntington's Disease Collaborative Research Group, 1993). The CAG repeat expansion leads to the production of an extended polyQ tract in the N-terminus of HTT protein. HD is a monogenic autosomal dominant disorder, therefore each child of an affected parent has 50% chance of inheriting the

disease. In healthy individuals, the CAG sequence is repeated 10 to 35 times, with an average of 18 CAG repeats across the population; expansions over 40 repeats cause HD with full penetrance, whereas people with 36 to 39 repeats might or might not develop HD symptoms due to reduced penetrance (Ghosh and Tabrizi 2018). Longer CAG repeat length correlates with greater severity, more rapid disease progression and younger age at onset. Accordingly, rare juvenile forms of HD (JHD) occur when the *HTT* gene bears more than 55 CAG repeats, with patients developing symptoms before the age of 20 years (Andrew et al. 1993). Unstable trinucleotide repeats tend to further expand during meiosis from generation to generation, especially when the disease gene is inherited from the father, resulting in progressively younger age of onset in children, a phenomenon known as genetic *anticipation*. Therefore, individuals carrying intermediate (or pre-mutation) alleles with CAG repeats ranging from 27 to 35 may still transmit the disease to their offspring (Zuccato, Valenza, and Cattaneo 2010). Sporadic cases of HD caused by de novo mutations represent at least 5–8% of diagnosed patients (Bates et al. 2015) and may thus arise from the pathological expansion of intermediate alleles.

1.1.1.3 Symptoms and disease progression

HD is characterized predominantly by adult-onset motor symptoms, which initiate with chorea (defined as short-lived, involuntary, excessive movements), dystonia, and movement incoordination, and culminate in impaired voluntary movement, bradykinesia, and rigidity in the final stages of the disease. These symptoms are preceded in the early stages by subtle cognitive impairment, which then progresses to subcortical and frontal dementia in advanced stages (Ross and Tabrizi 2011). In addition, HD patients are largely affected by psychiatric symptoms, including depression, anxiety, personality changes and psychosis. A marked incidence of suicide among HD patients has also been reported, and suicide is considered the second most common cause of death in HD (Ghosh and Tabrizi 2018). Moreover, as disease progresses, a wide range of systemic symptoms become evident, including body weight loss, skeletal muscle atrophy, osteoporosis, endocrine and metabolic abnormalities, cardiac dysfunction, testicular atrophy, and defective hematopoiesis (Marques Sousa and Humbert 2013). The average age of onset is 45 years, when patients develop clear motor symptoms, and divides the course of HD into 'premanifest' and 'manifest' phases

(**Figure 2**); the period before diagnosable signs and symptoms appear can be further subdivided into a presymptomatic phase, when HD patients are indistinguishable from healthy individuals, and a prodromal phase, where subtle motor, cognitive and behavioural changes are present (Ross et al. 2014). After the appearance of definitive motor and cognitive symptoms, the disease progresses slowly and inexorably over 15-20 years, when death occurs mainly due to respiratory failure.

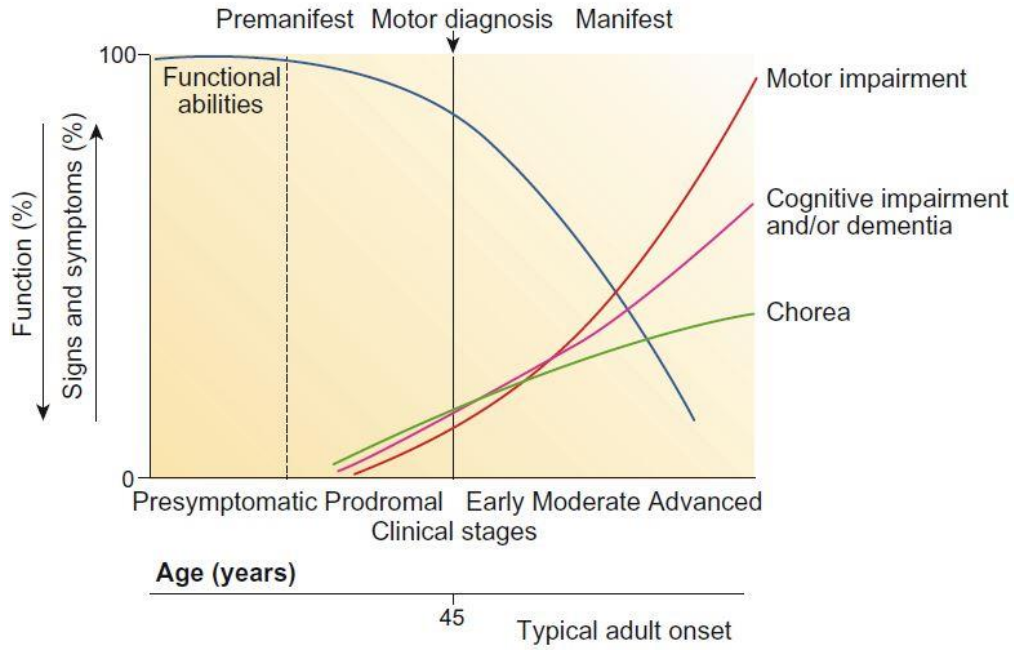

Figure 2: Natural history of clinical Huntington's Disease. The period before the appearance of diagnosable signs and symptoms is termed 'premanifest'. Subtle signs and symptoms begin in the 'prodromal' phase. Manifest HD is characterized by slow progression of motor and cognitive defects, with chorea often prominent early but plateauing or even decreasing later. Fine motor impairments such as incoordination, bradykinesia and rigidity progress more steadily (Ghosh and Tabrizi, 2018).

1.1.1.4 Neuropathology

Most clinical features of HD arise from degeneration of the brain, despite the ubiquitous expression of wild-type and mutant HTT throughout the organism. Furthermore, there are no pronounced regional differences in HTT expression within the brain (Strong et al. 1993), yet selective neuronal vulnerability is observed, with primary and prominent damage in the caudate and putamen (Zuccato, Valenza, and Cattaneo 2010). In fact, the motor abnormalities observed in HD patients derive from

the massive degeneration of the striatum, which can shrink to as little as 10% of its normal volume in later stages of the disease (Subramaniam and Snyder 2011). The degree of striatal neuronal loss correlates with disease severity and progression of HD. Intriguingly, neuronal dysfunction and degeneration in affected brain regions is also cell-specific. Within the striatum, the most severely affected neurons (up to 95% neuronal loss) are γ-aminobutyric acid (GABA)-ergic medium-sized projection spiny neurons (MSNs) projecting to the globus pallidus and the substantia nigra (Ross and Tabrizi 2011), whereas interneurons are relatively spared even in advanced stages of HD (Ferrante et al. 1985). As the disease progresses, degeneration of other brain regions is observed, such as cerebral cortex, subcortical white matter, thalamus, subthalamic nucleus (**Figure 3**). By the late stages of the disease, widespread brain atrophy is observed in HD patients. Selective vulnerability of specific tissues or cell types of the nervous system is a common feature of neurodegenerative disorders, but the underlying mechanisms are still poorly understood. The expression and location of the affected protein do not explain the selective neurodegeneration. Therefore, it is likely that both cell-autonomous and non-cell-autonomous pathways of degeneration contribute to selective striatal damage.

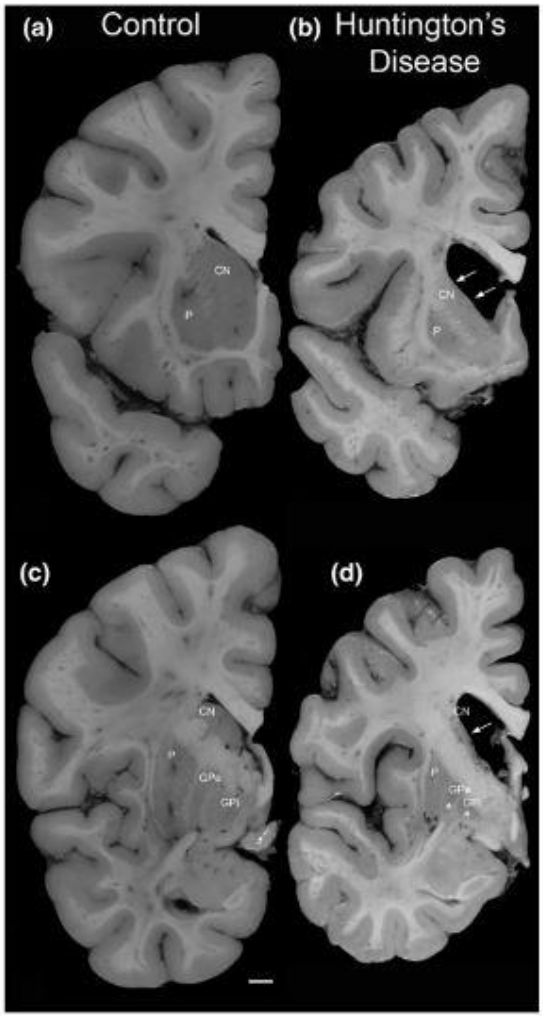

Figure 3: Neuropathology of Huntington's Disease. Coronal sections through the human brain of a healthy control (a,c) and a Grade 3/4 HD patient (b,d). Major shrinkage of the caudate nucleus and putamen (white arrows) as well as the globus pallidus (white asterisks) are observed in HD. Shrinkage of the cerebral cortex is also evident. CN, caudate nucleus; GPe, globus pallidus external segment; GPi, globus pallidus internal segment and P putamen. Scale bar, 1 cm (Waldvogel et al. 2014).

1.1.2 Huntingtin protein

1.1.2.1 Huntingtin structure

HTT is a large 348 kDa protein of 3144 amino acids encoded by the *IT15* gene, that consists of 67 exons and whose locus spans around 180 kb. HTT is highly conserved throughout evolution, from mammals to the oldest still living deuterostome, the sea urchin (Tartari et al. 2008), with the highest degree of conservation among vertebrates (Schulte and Littleton 2011). Given that the pathogenic mutation is found in exon1 of HTT, most research focused on the very N-terminal region of the protein, resulting in 97% of the protein being largely uncharacterized (Saudou and Humbert 2016). Furthermore, the high molecular weight and the flexibility of HTT hindered the production of crystals and the efforts to elucidate its structure (Zuccato, Valenza, and Cattaneo 2010). However, recently Guo and colleagues revealed by cryo-electron microscopy the first high-resolution (4Å) structure of full-length human HTT in a complex with Huntingtin-associated protein 40 (HAP40), providing new insights into HTT three-dimensional architecture (Guo et al. 2018). HTT is organized as a succession of ordered domains, known as HEAT (Huntingtin, Elongation factor 3, protein phosphatase 2A and TOR1) repeats, separated by intrinsically disordered regions (Bates et al. 2015) bearing many proteolysis-susceptible PEST (proline (P)-, glutamic acid (E)-, serine (S)-, and threonine (T)-enriched) sequences (Caterino et al. 2018). HTT is mostly α-helical and consists of three major domains: an amino-terminal and a carboxy-terminal domain comprising multiple HEAT repeats connected to each other by a smaller bridge domain (**Figure 4**) (Guo et al. 2018).

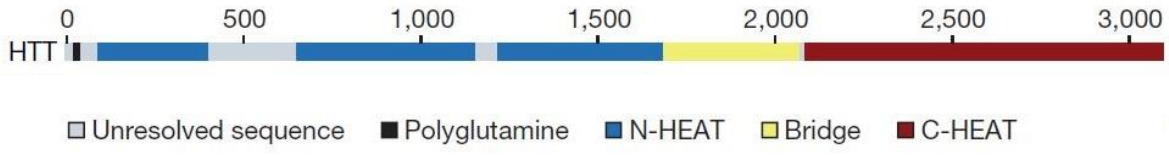

Figure 4: Schematics of Huntingtin structure. HTT is organized in three major domains: one N-terminal and a C-terminal domain composed of several HEAT repeats (N-HEAT and C-HEAT, respectively) and a smaller bridge domain connecting them (adapted from Guo et al., 2018).

The N-terminal portion of HTT is the most recently evolved, with the polyQ-containing exon1 being poorly conserved in evolution, whereas the C-terminal region is well conserved among all animals (Zuccato, Valenza, and Cattaneo 2010). The first appearance of the polyQ tract dates back to the sea urchin, which has a NHQQ sequence biochemically similar to the 4Q repeats found in other vertebrates (Tartari et al. 2008). The polyQ stretch has progressively expanded in mammals, with humans having the longest and most polymorphic tract. PolyQ sequences in proteins are thought to be involved in the stabilization of protein-protein interactions. (Schaefer, Wanker, and Andrade-Navarro 2012). However, it remains unclear how the variability of the polyQ repeat affects the normal function of HTT (Saudou and Humbert 2016). At the N-terminal, the polyQ stretch is preceded by a segment of 17 residues (N17) strongly conserved in vertebrates (Tartari et al. 2008) and followed by a proline-rich domain (PRD). N17 is an amphipathic membrane-binding α-helix that can reversibly target HTT to the endoplasmic reticulum, Golgi and endosomes (Atwal et al. 2007; Rockabrand et al. 2007) and determines HTT intracellular localization between the nucleus and the cytoplasm by acting as a nuclear export signal (Maiuri et al. 2013). Moreover, N17 influences the aggregation properties of the polyQ stretch (Jayaraman et al. 2012) and contains several regulatory post-translational modification sites that modulate HTT clearance and subcellular localization (Atwal et al. 2011; Steffan et al. 2004; Thompson et al. 2009). The PRD represents a recently evolved region of the protein as it is found only in mammals (Tartari et al. 2008), and it mediates the interaction of HTT with several partners containing Src homology 3 (SH3) or tryptophan (WW) domains (Harjes and Wanker 2003).

HTT contains around 37 well conserved HEAT repeats (Guo et al. 2018) clustered into three to five α-rod domains arranged in a solenoid-like structure that is critical to mediate protein-protein interactions (**Figure 5**) (Saudou and Humbert 2016). Importantly, it has been observed that α-rods in different portions of the protein bind to each other creating intramolecular interactions (Palidwor et al. 2009), suggesting that HTT can adopt multiple three-dimensional conformations. In this way, by combining both intra- and intermolecular interactions HTT acts as a molecular scaffold for several protein complexes and coordinates numerous cellular functions. Furthermore, HTT contains a highly conserved nuclear export signal (NES) in the C-terminus (Xia et al. 2003) and a karyopherin β2-dependent proline-tyrosine nuclear

localization sequence (PY-NLS) in the N-terminus spanning between amino acids 174 and 207 (Desmond et al. 2012), indicating that HTT shuttles to and from the nucleus. Finally, HTT undergoes multiple post-translational modifications which are mostly located in the unstructured regions between HEAT repeats (**Figure 5**) and will be discussed in detail later in this thesis.

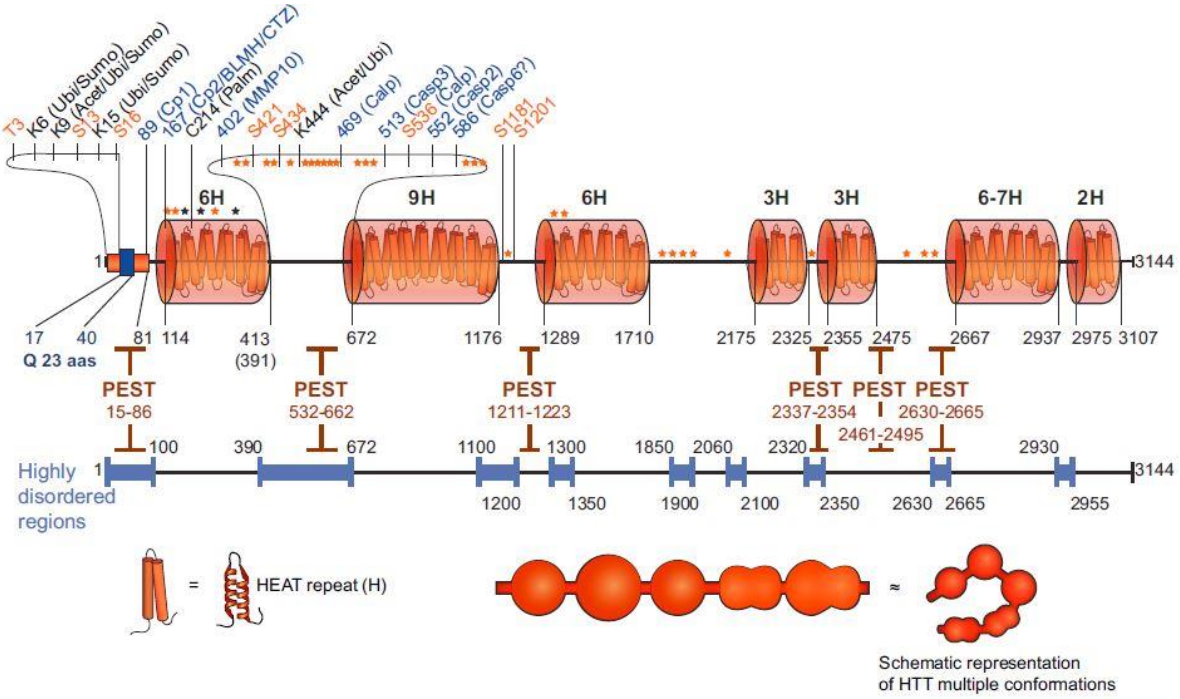

Figure 5: Structure of human Huntingtin protein. In human HTT several HEAT repeats are separated by highly disordered regions containing many PEST sequences. Orange amino acids: phosphorylation sites identified by mass spectrometry and confirmed by other approaches. Black amino acids: other post-translational modifications. Blue amino acids: cleavage sites. Orange and black stars: phosphorylation and acetylation sites identified by mass spectrometry with no further confirmations. H indicates the number of predicted HEAT repeats organized in larger domains. Ubi, ubiquitin; Sumo, sumoyl; Acet, acetyl; Palm, palmitoyl; MMP10, metalloproteinase 10; Calp, calpain; Casp3/2/6, caspase 3/2/6 (Saudou and Humbert, 2016).

1.1.2.2 Biological functions of wild-type Huntingtin

Soon after the discovery of *HTT* gene in 1993, it was established that HTT is ubiquitously expressed throughout the body. HTT protein and transcripts are found in most tissues at different concentrations, with the highest levels of expression in the nervous system, particularly in the brain, and testes (Li et al. 1993; Strong et al. 1993;

Sharp et al. 1995). Within the brain, HTT expression is not restricted to specific regions or cellular subtypes; it is found in several types of neurons as well as in glial cells, although at lower levels (Landwehrmeyer et al. 1995). In addition, HTT is expressed starting from the early embryonal stages up into adulthood. Importantly, HTT knockout in mice causes lethality at embryonic day (E) 7.5, before gastrulation and development of the nervous system (Zeitlin et al. 1995; Nasir et al. 1995; Duyao et al. 1995), indicating that in higher vertebrates HTT is essential for embryogenesis. Besides the widespread spatial and temporal expression pattern of HTT, the subcellular localization of HTT adds a further layer of complexity. HTT is primarily cytoplasmatic and particularly abundant in the perinuclear region, yet it is associated with many organelles, including the nucleus, Golgi apparatus, endoplasmic reticulum, mitochondria and endosomes, as well as with microtubules (DiFiglia et al. 1995; Hoffner, Kahlem, and Djian 2002; Hilditch-Maguire et al. 2000). Finally, HTT has a large and complex structure and more than 350 HTT partners have been identified with different biochemical and bioinformatic approaches. This strongly supports the idea that HTT serves as a major protein interaction hub, tethering multiple interactors into molecular complexes (Guo et al. 2018; Saudou and Humbert 2016). For all these reasons, HTT is a protein with pleiotropic functions that has been implicated in diverse cellular processes, such as cell survival, transcription, axonal transport, trafficking of endosomes and organelles, vesicular recycling, synaptic activity, cell division, autophagy. However, a thorough understanding of HTT biological functions is still lacking. The most studied are described hereafter.

Huntingtin function during embryonic development

Complete genetic inactivation of HTT in mice results in gastrulation defects and embryonic lethality before day 8.5 (Zeitlin et al. 1995; Nasir et al. 1995; Duyao et al. 1995). This appears to be the consequence of defective organization of the extraembryonic tissue in the absence of HTT, as chimeric embryos with wild-type extraembryonic tissues are rescued from early death (Dragatsis, Efstratiadis, and Zeitlin 1998). Interestingly, HTT knockout in *Drosophila* melanogaster does not recapitulate the same phenotype, suggesting that an expanded polyQ region after protostome-deuterostome divergence may have conferred new relevant molecular functions to wild-type HTT (Zuccato, Valenza, and Cattaneo 2010). Indeed,

experiments in mice with 50% reduction in HTT levels have revealed that at post-gastrulation stages HTT is a key player in the development of the nervous system. These mice display defects in the epiblast, which will later give rise to the central nervous system, reduced neurogenesis and structural aberrations of the cortex and striatum, and they die shortly after birth (White et al. 1997). The role of wild-type HTT in brain maturation might involve the regulation of neuroblasts proliferation, differentiation and/or survival in specific areas: chimeric embryos created by injection of $HTT^{-/-}$ cells in the blastocyst show few HTT-depleted cells in the cortex, striatum, basal ganglia and thalamus (Reiner et al. 2001). The underlying molecular mechanisms may be linked to HTT-mediated regulation of the mitotic spindle orientation in replicating neural progenitors (Godin et al. 2010). These studies reveal that HTT is required at different stages of embryogenesis and that 50% decrease in HTT levels causes early developmental abnormalities. However, interestingly polyQ-expanded HTT rescues embryonic lethality in HTT-null mice, indicating that the CAG expansion does not interfere with the developmental function of wild-type HTT and that mutant HTT can compensate for the absence of endogenous HTT; this is consistent with the normal development and late-onset symptoms of HD patients who carry only one fully functional allele (Cattaneo, Zuccato, and Tartari 2005).

Huntingtin has antiapoptotic activity

Wild-type HTT has pro-survival properties that have been demonstrated by several *in vitro* and *in vivo* studies. Evidence supporting the antiapoptotic activity of HTT was first provided by *in vitro* experiments showing that overexpression of wild-type HTT protects brain-derived cells from various pro-apoptotic stimuli, such as serum starvation, death receptors (Rigamonti et al. 2000; Rigamonti et al. 2001), excitotoxicity (Leavitt et al. 2006) and polyglutamine-expanded HTT itself (Ho et al. 2001). These observations were confirmed by *in vivo* studies showing that upon lowered HTT levels, ectopic expression of wild-type HTT confers protection from excitotoxicity-induced neurodegeneration in a dose-dependent manner (Zhang et al. 2003; Leavitt et al. 2006). In contrast, cells depleted of HTT showed higher vulnerability to apoptotic cell death and increased caspase-3 activity (Zhang et al. 2006). Similarly, morpholino-mediated knockdown of HTT in zebrafish embryos caused strong activation of caspase-3 and massive induction of cell death particularly

in the mid-/hindbrain region, together with central nervous system underdevelopment (Diekmann et al. 2009). Moreover, conditional HTT knockout in mouse forebrain resulted in progressive apoptotic neuronal death in cortex, striatum and hippocampus, delineating a key role of HTT in neuronal homeostasis and survival in the adult brain (Dragatsis, Levine, and Zeitlin 2000). It has been shown that HTT exerts its protective effect by inhibiting the assembly of a functional apoptosome complex, thereby blocking the activation of caspase-3 and caspase-9 (Rigamonti et al. 2000; Rigamonti et al. 2001). In addition, HTT physically interacts with caspase-3 and inhibits its proteolytic activity (Zhang et al. 2006). Others have reported that HTT hinders Fas-induced programmed cell death by preventing caspase-mediated cleavage and activation of p21-activated-kinase 2 (Pak2) (Luo and Rubinsztein 2009). Finally, HTT also interferes with caspase-8 activation and cell death by sequestering huntingtin interacting protein 1 (HIP1) and inhibiting the formation of the HIP1-HIPPI pro-apoptotic complex (Gervais et al. 2002). Interestingly, these apoptosis-inhibitory activities of wild-type HTT are partially lost upon polyQ expansion. Altogether, these observations indicate that HTT promotes cell survival.

Huntingtin modulates transcription

Profound gene expression alterations have been observed both in human HD brains and HD mouse models, suggesting that HTT has a role in transcriptional regulation. HTT is mainly found in the cytoplasm but localizes also in the nucleus and influences transcription in a variety of ways, such as directly interacting with transcription factors, scaffolding transcriptional complexes and shuttling transcription factors or transcriptional regulators to the nucleus (Saudou and Humbert 2016). Notably, polyQ tracts are enriched in eukaryotic transcription factors and are known to mediate the binding between transcription factors and transcriptional regulators, thereby contributing to transcriptional activation; indeed, polyQ-containing proteins are able to recruit other regulatory proteins with polyQ stretches or glutamine-rich activation domains (Atanesyan et al. 2012). Accordingly, wild-type HTT binds several transcription factors, including nuclear factor-kB (NF-kB)(Takano and Gusella 2002), specificity protein 1 (Sp1) (Dunah et al. 2002; Li et al. 2002), p53 and most notably with cAMP-response element (CREB)-binding protein (CBP) (Steffan et al. 2000). HTT can also bind to some nuclear receptors, which are highly expressed in the brain and

transcriptionally regulate a large number of physiological processes (Futter et al. 2009). HTT interacts with both positive and negative transcriptional regulators, such as the co-activator TAFII130 (Dunah et al. 2002) and the Repressor Element-1 Transcription Factor/Neuron Restrictive Silencer Factor (REST/NRSF) (Zuccato et al. 2003). TAFII30 is part of the Transcription Factor II D (TFIID), a multisubunit general transcription factor that binds to the TATA box in the core promoter of genes. The fact that HTT binds both TAFII130 and Sp1 suggests that it acts as a scaffold that allows the association of Sp1 to the basal transcription machinery (Harjes and Wanker 2003). REST/NRSF activity as a transcriptional silencer is particularly relevant in neurons because it recognizes and binds to neuron-restrictive silencer elements (NRSE) that control the expression of many genes essential for neuronal development and function, including the gene encoding for brain-derived neurotrophic factor (BDNF). Importantly, wild-type HTT sequesters REST/NRSF in the cytoplasm, preventing the formation of an active co-repressor complex in the nucleus and its binding to NRSE, thereby promoting *BDNF* transcription and neuronal survival (Zuccato et al. 2003).
HTT might additionally regulate transcription by acting as a transcriptional cofactor. By chromatin immunoprecipitation, Benn and collaborators have demonstrated that HTT occupies gene promoters and directly binds DNA in vivo in a polyQ-dependent fashion (Benn et al. 2008). Finally, HTT is involved in epigenetic regulation of gene expression by interacting with the epigenetic silencer polycomb repressive complex 2 (PRC2). Wild-type HTT binds two PRC2 subunits, namely Suppressor of zeste 12 (Suz12) and Enhancer of zeste 2 (Ezh2), and facilitates H3K27me3 deposition by PRC2 (Seong et al. 2010).

1.1.2.2.1 Huntingtin and axonal transport

Overview of axonal transport

Axonal transport, also called axoplasmic transport, is essential for neuronal survival and function. Neurons are polarized cells with axons that can reach up to one meter in length, therefore a proper communication between the soma and the axon terminal is required. Intracellular transport is critical to ensure efficient signal transmission between neuronal cells and allows neurons to react to both trophic and stress stimuli. Moreover, axonal transport has an important role in neuronal metabolism, given that the axon largely depends on the biosynthetic and catabolic

activities of the cell body. Although axonal mRNA localization and local protein synthesis have been demonstrated, most of the axonal proteins are produced in the cell body and need to be actively transported along axons. Axoplasmic transport supplies axons and axon terminals with newly synthetized mRNAs, proteins, lipids, synaptic vesicles and organelles, such as mitochondria providing a local energy source. At the same time, proteins vesicles and organelles, such as mitochondria and autophagosomes, are removed from the periphery and transported back to the soma for clearance and recycling of the molecular components. Axonal transport is carried out by molecular motors that drive the different cargoes along cytoskeletal tracks formed by parallel and polarized microtubules.

Microtubules assemble thanks to the polymerization of α-tubulin/β-tubulin dimers and they form a unipolar array in the axon, with the slower growing 'minus' end oriented toward the soma and the faster growing 'plus' end facing the axon tip (Maday et al. 2014). The movement of cargoes from the cell body toward the axon terminal is called *anterograde* transport, whereas the transport of material toward the cell body is called *retrograde* transport. Specific ATP-driven motor proteins mediate transport in the two directions: kinesins (mainly kinesin-1) are the major drivers of anterograde transport, whereas the cytoplasmic dynein complex is the major motor responsible for retrograde transport, together with its activator dynactin (Millecamps and Julien 2013) (**Figure 6**). Finally, axonal transport can be divided into fast axonal transport and slow axonal transport. Fast axonal transport is involved in the movement of membrane-bound organelles, such as mitochondria, vesicular cargoes, signalling endosomes and autophagosomes; on the other hand, slow axonal transport is responsible for the travelling of cytoskeletal proteins (microtubules and neurofilaments) and soluble cytoplasmic proteins, including enzymes (Maday et al. 2014). Considering the crucial role of axonal transport for the growth, homeostasis and survival of the neuron, it is not surprising that defects in axoplasmic transport have been associated to several neurodegenerative diseases.

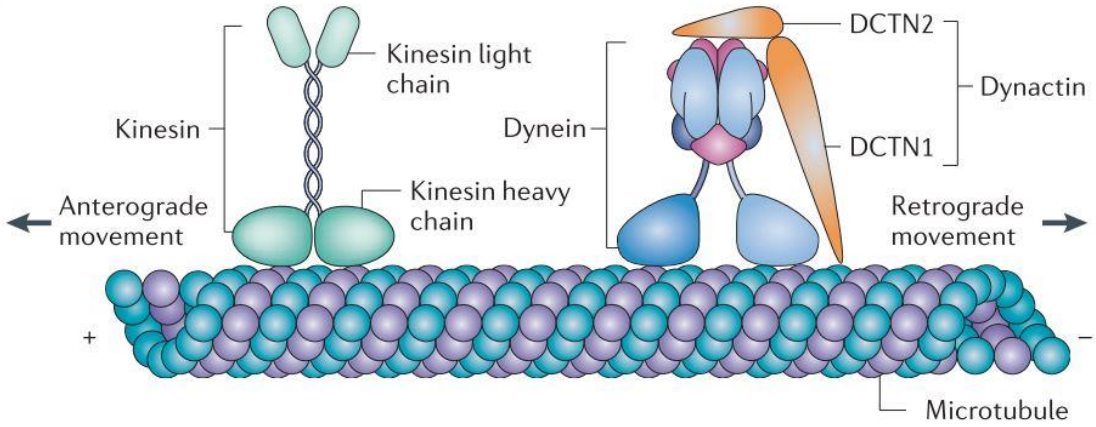

Figure 6: Microtubule-based axonal transport is mediated by specific motor proteins. Axonal transport of most cargoes is mediated by ATP-driven kinesin and dynein complexes. Kinesin is composed of two heavy chains and two light chains and transports cargoes in the anterograde direction. Dynein complexes comprise the dynein heavy, intermediate, intermediate light and light chains and several dynactin subunits and move cargoes retrogradely (adapted from Millecamps and Julien 2013).

Role of Huntingtin in vesicle and organelle trafficking

The first work suggesting that HTT could play a role in vesicle trafficking was published in 1995 by DiFiglia and colleagues, who detected the presence of HTT in cortex-derived synaptosomes and showed association of HTT with vesicles and microtubules along with widespread cytoplasmic HTT localization in neurons (DiFiglia et al. 1995). Soon after it was also reported that HTT and Huntingtin-associated protein 1 (HAP1) are anterogradely and retrogradely transported in rat sciatic nerve (Block-Galarza et al. 1997). Additional evidence was provided by earlier studies in *D. melanogaster* showing that HTT silencing in neurons causes axonal transport defects in larval nerves, a phenotype that was further aggravated upon reduction of kinesin heavy chain (KHC) or kinesin light chain (KLC) expression (Gunawardena et al. 2003). Similarly, defects in fast axonal trafficking of mitochondria were observed in embryonic mouse striatal neurons expressing less than 50% of normal HTT levels, indicating that wild-type HTT is involved in axonal transport in mammals as well (Trushina et al. 2004). HTT regulates the bidirectional transport of various organelles

along microtubules by acting as a scaffold that coordinates the function of the molecular motor machinery (Caviston and Holzbaur 2009). HTT interacts directly with dynein and indirectly via HAP1 with the p150^{Glued} subunit of dynactin (Engelender et al. 1997; Li et al. 1998; Gauthier et al. 2004; Caviston et al. 2007) and the kinesin-1 member KIF5C (Colin et al. 2008; McGuire et al. 2005; Twelvetrees et al. 2010). Thanks to these interactions HTT facilitates dynein/dynactin-mediated retrograde transport and kinesin-driven anterograde transport (**Figure 7**). HTT controls the movement of various different cargoes, including BDNF-containing vesicles, synaptic precursor vesicles, endosomes and lysosomes, autophagosomes, vesicles containing GABA-receptors, and amyloid precursor protein (APP)-positive vesicles (Saudou and Humbert 2016).

HTT promotes anterograde transport of BDNF-containing vesicles along cortical axons and their delivery at the cortico-striatal synapses (Gauthier et al. 2004). Upon release, BDNF binds and activates TrkB receptors, which are in turn endocytosed and transported to the soma of striatal neurons, thereby stimulating pro-survival pathways. Importantly, it has been shown that the HTT-dynein complex regulates the retrograde transport of TrkB-signalling endosomes in striatal dendrites (Liot et al. 2013). These two coordinated functions of HTT are crucial for the survival of striatal neurons, because they do not produce BDNF themselves and hence they depend almost exclusively on the neurotrophic support provided by the transport of BDNF through the cortico-striatal connections.

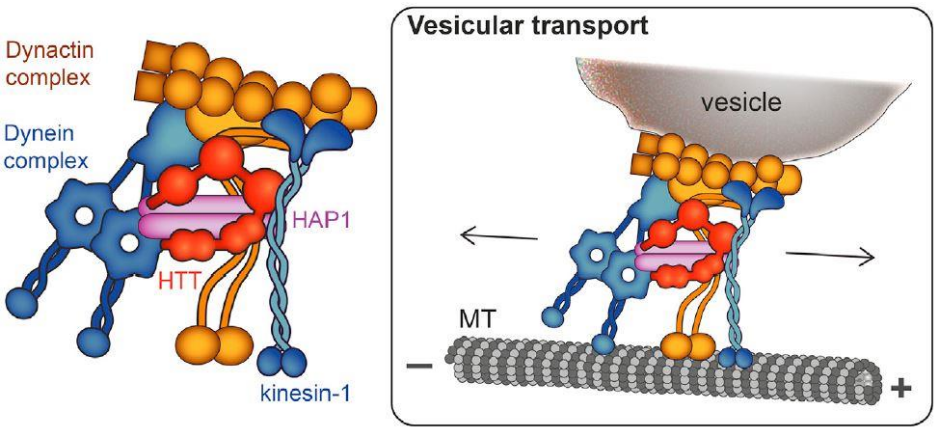

Figure 7: Huntingtin scaffolds molecular motors and controls axonal transport in both directions. HTT scaffolds dynein/dynactin and kinesin complexes and regulates axonal trafficking of various organelles both in the anterograde and retrograde direction (adapted from Saudou and Humbert 2016).

The proposed mechanism underlying the enhancement of the efficiency and velocity of vesicular transport by HTT involves its ability to bind and scaffold the glycolytic enzyme glyceraldehyde 3-phosphate dehydrogenase (GAPDH) on vesicles (Zala et al. 2013b). Indeed, HTT depletion both *in vitro* and *in vivo* results in reduced attachment of GAPDH to vesicles and consequent decrease in transport efficiency (Zala et al. 2013b). The specific vesicular localization of a glycolytic enzyme producing ATP may constantly provide the energy required by the molecular motors to drive fast axonal transport over long distances.

Besides being a facilitator of vesicular trafficking, HTT also regulates the directionality of axonal transport based on its phosphorylation status. HTT phosphorylation at serine 421 (S421) promotes anterograde transport by recruiting kinesin-1 to the microtubule-associated motor machinery and vesicles; conversely, unphosphorylated HTT favours kinesin-1 detachment and retrograde movement of vesicles (Colin et al. 2008).

1.1.3 Molecular mechanisms of Huntington's Disease pathogenesis

The expansion of CAG repeats located in coding regions is commonly thought to confer a deleterious gain-of-function to the mutant protein. Accordingly, experimental analyses in animal and *in vitro* models as well as in HD patients' tissues provide considerable evidence that the polyQ expansion in HTT results primarily in a toxic gain-of-function phenotype. This is also suggested by the autosomal dominant inheritance pattern of HD. However, deletion or depletion of wild-type HTT also leads to neurodegeneration (O'Kusky et al. 1999; Dragatsis, Levine, and Zeitlin 2000) and several studies indicate that the expansion of the polyQ tract can also cause HTT loss-of-function. Therefore, a combination of gain-of-function mechanisms and loss of normal HTT function might contribute to the pathogenesis of HD. Moreover, considering the widespread subcellular localization of HTT and the broad range of cellular processes in which it is involved, mutant HTT protein is likely to cause neurodegeneration through a variety of mechanisms. These pathogenic mechanisms are probably not exclusive, but rather highly interconnected.

1.1.3.1 Gain of toxic function

Multiple neurodegenerative pathways which are indicative of a toxic gain-of-function of expanded HTT have been implicated in the pathogenesis of HD, including misfolding and aggregation of mutant HTT, proteolytic cleavage of expanded HTT, impairment of the proteostasis network, abnormal protein-protein interactions, mitochondrial dysfunctions, early transcriptional dysregulation, axonal transport defects, altered synaptic dysfunctions (**Figure 8**) (Bates et al. 2015).

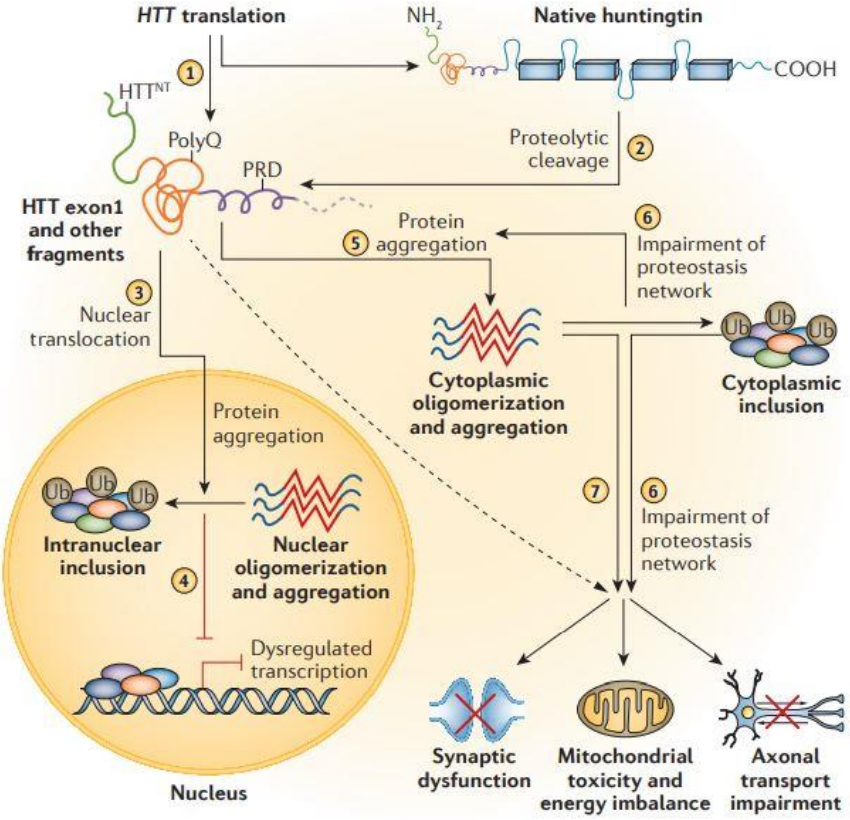

Figure 8: Pathogenetic cellular mechanisms in Huntington's Disease.
(Bates et al. 2015)

The accumulation of protein aggregates in the brain is a common pathogenic hallmark of neurodegenerative disorders and particularly of polyglutamine diseases. Initially, aggregates were considered to play a crucial role in HD pathogenesis. The expansion of the polyQ tract in HTT causes a conformational change that triggers the aggregation process, which is thought to proceed with the nucleated growth polymerization mechanism proposed by Perutz and colleagues (Perutz and Windle 2001). In

particular, polyglutamine repeats form β-sheets held together by hydrogen bonds, leading to the generation of amyloid fibrils (Perutz et al. 1994). However, the mechanism by which mutant HTT aggregates is complex and not completely understood. In addition, although the presence of insoluble aggregates is a hallmark of HD, their role in disease pathogenesis remains controversial. HTT aggregates are both intranuclear and cytoplasmatic and they are also found in neuronal processes (DiFiglia et al. 2007). Intracellular aggregates are thought to exert toxicity mainly through sequestration and consequent depletion of several proteins, including other polyQ-containing proteins, thereby causing alterations or loss of their canonical function. On the other hand, a number of studies reported inverse correlation between the presence of aggregates and cell death, supporting the idea that large inclusion bodies containing aggregated HTT might be neuroprotective because they reduce the levels of the soluble mutant protein (Saudou et al. 1998; Arrasate et al. 2004). In agreement with this, many reports indicate that the most toxic species are intermediate soluble HTT oligomers that precede the formation of amyloid fibrils and inclusions (Ross et al. 2017).

Moreover, there is substantial evidence that the accumulation of N-terminal polyQ-containing HTT fragments is a key early pathogenic step in HD (Jimenez-Sanchez et al. 2017). The importance of small HTT fragments has been highlighted by their detection in several HD mouse models and human post-mortem brains (Bates et al. 2015). They are generated through proteolysis of HTT by several proteases, including caspases and calpains, which recognize PEST domains mostly located in disordered regions of the protein (Warby et al. 2008). Furthermore, a highly pathogenic HTT exon1 protein is produced by an aberrant splicing event (Sathasivam et al. 2013). Both wild-type and mutant HTT are good substrates for cleavage; however, an increase of the activity of proteases has been observed in the brain of HD patients (Saudou and Humbert 2016). N-terminal fragments of HTT containing an expanded polyQ stretch eventually drive toxicity in the cell because of their higher propensity to form nuclear toxic aggregates (Jimenez-Sanchez et al. 2017).

Once these various cytotoxic species of HTT are produced, they cause dysregulation of many downstream cellular processes, leading to an extremely complex molecular pathogenesis. For instance, N-terminal fragments that translocate to the nucleus form intranuclear aggregates and cause widespread transcriptional abnormalities. Importantly, transcriptional dysregulation is a key and early event in the pathogenesis

of HD, often occurring before the onset of symptoms (Sharma and Taliyan 2015), and it mainly arises from abnormal interaction of expanded HTT with several transcription factors, transcriptional co-regulators and chromatin-remodeling proteins, and their sequestration into nuclear and/or cytoplasmic aggregates. Disruption of the activity of gene expression regulators results in both depletion and ectopic activation of numerous gene products that eventually affect neuronal functions and survival. Some critical pathways are in fact dysregulated in HD, such as the CRE/CREB-mediated and the Sp1-dependent pathways. In particular, mutant HTT interferes with the transcriptional activity of CREB/CBP and TFIID, preventing their binding to the CRE sequence in the promoter region of several genes, including *PGC1-α* (Peroxisome proliferator-activated receptor gamma coactivator 1-alpha), leading to reduced activation of this master regulator of mitochondrial function and biogenesis. Misregulation of the vast number of genes controlled by PGC1-α is likely to underlie the mitochondrial dysfunctions observed in HD (Zuccato, Valenza, and Cattaneo 2010). Expanded HTT also inhibits the binding of Sp1 and its co-activator TAFII130 to DNA, thereby affecting the transcription of the D2 dopamine receptor gene, among many others (Dunah et al. 2002). In addition, interaction of the polyQ-polyP region of mutant HTT with the glutamine-rich C-terminal of CBP causes its sequestration in cytoplasmic aggregates (Steffan et al. 2000; Nucifora et al. 2001). This results in reduction of CBP-mediated histone acetyltransferase (HAT) activity and consequent imbalance between HATs and histone deacetylases (HDACs), causing general transcriptional repression. Accordingly, studies in invertebrate and mouse models of HD have shown that HDAC inhibitors can ameliorate the neurodegeneration phenotype (Steffan et al. 2001; Ferrante et al. 2003; Hockly et al. 2003).

The expression and accumulation of misfolded polyQ-expanded HTT leads also to an impairment of the two major cellular processes responsible for degradation and clearance of misfolded proteins: the ubiquitin-proteasome system (UPS) and autophagy (Jimenez-Sanchez et al. 2017). The collapse of the proteostasis network might be explained by the sequestration of components of the UPS machinery into aggregates and/or the poisoning of the proteasome by degradation-resistant HTT species (Jimenez-Sanchez et al. 2017). Remarkably, as disease progresses, the protein quality control system becomes progressively compromised, and the failure of clearance mechanisms is expected to further exacerbate HD pathogenesis.

Finally, synaptic dysfunctions and alterations of the neuronal circuitry at the cortico-striatal connection significantly contribute to disease pathogenesis. Neurotransmission abnormalities are thought to arise from both excitotoxicity and deficient delivery of synaptic vesicles and synaptic receptors at dendrites and axon terminals. Molecular mechanisms underlying excitotoxicity comprise aberrant distribution and activity of glutamatergic NMDA (N-methyl-D-aspartate) receptors (NMDAR) and dysregulated release and uptake of glutamate at the cortico-striatal synapse (Zuccato, Valenza, and Cattaneo 2010). Axonal transport defects might derive from mutant HTT-mediated sequestration of wild-type HTT and components of the molecular motor machinery into aggregates (Gunawardena et al. 2003; Trushina et al. 2004). An example is the disruption of HAP1-KIF5C complex by mutant HTT, with consequent deficits of trafficking and delivery of GABA(A) receptors to synapses (Twelvetrees et al. 2010). However, other observations suggest that defective axonal trafficking might be caused by loss-of-function of wild-type HTT, and they will be outlined in the following section.

Given the wide range of gain-of-function mechanisms through which mutant HTT causes neuronal dysfunction and degeneration, in the last years several HTT lowering therapeutic strategies aimed at mitigating all downstream pathogenic effects exerted by polyQ-expanded HTT have been developed and are currently being tested in clinical trials. These potential therapies as well as possible issues and future challenges have been recently reviewed by Tabrizi and collaborators (Tabrizi, Ghosh, and Leavitt 2019).

1.1.3.2 Loss of normal Huntingtin function

Abnormal expansions of the polyQ repeats can also abrogate or modify the normal function of wild-type HTT. As previously described, not only HTT favours the transcription of *BDNF* gene (Zuccato et al. 2001), but it also facilitates the axonal trafficking of BDNF-containing vesicles and its delivery to the cortico-striatal synapse (Gauthier et al. 2004). Importantly, expanded HTT loses the ability to exert both functions. First, mutant HTT fails to interact with REST/NRSF in the cytoplasm, leading to increased translocation of REST/NRSF to the nucleus (Zuccato et al. 2003). Enhanced REST/NRSF binding to promoter regions drives the recruitment of Sin3A-HDACs complexes, thereby triggering chromatin remodeling into a closed architecture

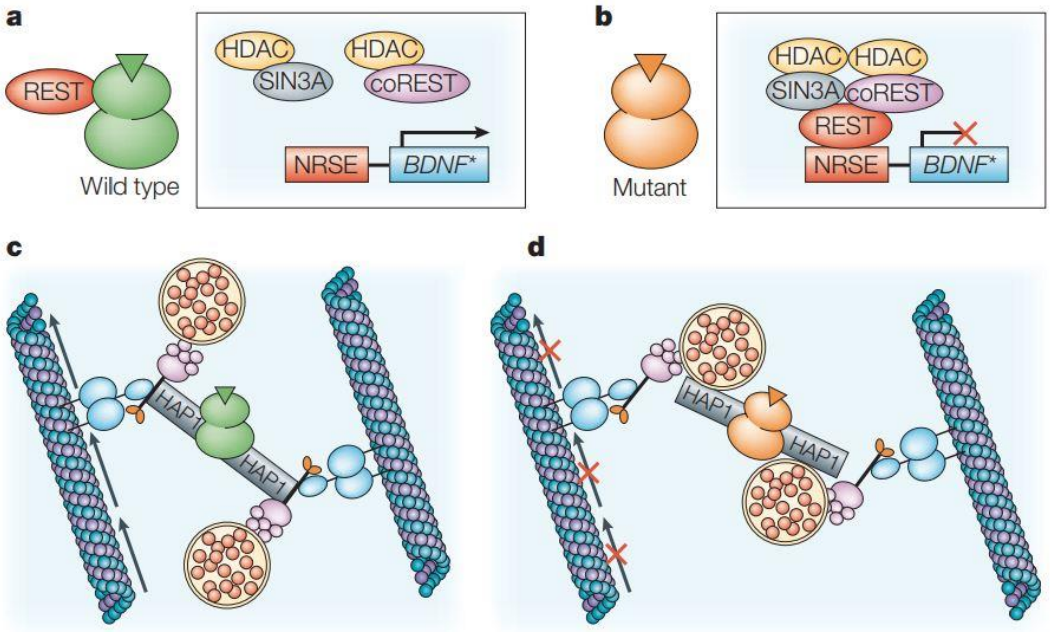

Figure 9: Loss of HTT normal function in the regulation of BDNF production and transport. a) Wild-type HTT sequesters REST/NRSF in the cytoplasm, leading to *BDNF* transcription. b) Mutant HTT fails to interact with REST/NRSF, which translocates to the nucleus and represses *BDNF* expression. c) Wild-type HTT controls BDNF transport along microtubules by assembling p150^{Glued} (grey) with the dynein (blue) and dynactin complexes (pink) through its interaction with HAP1. d) Mutant HTT binds more tightly to HAP1 and interferes with the transport of BDNF vesicles along microtubules by wild-type HTT (Cattaneo, Zuccato, and Tartari 2005).

and suppression of the transcription of numerous genes, including *BDNF* (**Figure 9**) (Zuccato et al. 2003). Second, polyQ-expanded HTT binds with higher affinity to HAP1 and interferes with the ability of wild-type HTT to interact with HAP1, resulting in reduced binding of normal HTT and p150^{Glued} dynactin to microtubules and compromised assembly of the motor machinery (**Figure 9**); these mutant HTT-induced BDNF transport deficits cause a loss of neurotrophic support to striatal neurons (Gauthier et al. 2004). Moreover, trafficking defects in HD are not restricted to BDNF transport in cortical neurons but also affect the retrograde transport of its receptor TrkB in striatal neurons (Liot et al. 2013). Considering the strict dependence of the striatum on the production and transport of BDNF from the cortex, loss of normal HTT function in the regulation of these interconnected processes might explain the selective striatal vulnerability observed in the early stages of HD.

An additional axonal transport defect associated with HTT loss-of-function is the trafficking of autophagosomes. It has been reported that HTT and HAP1 regulate autophagosome dynamics by promoting their transport on microtubules (Wong and Holzbaur 2014). The polyQ expansion impairs axonal transport of autophagosomes, leading to inefficient autophagosome-lysosome fusion and reduced cargo degradation (Wong and Holzbaur 2014). Impairment of the autophagic flux in HD might also be linked to the proposed role of HTT as a scaffold for the recruitment of the autophagic machinery during selective autophagy, a function that may be lost upon expansion of the polyQ repeats (Ochaba et al. 2014). As a result, defective clearance due to loss of wild-type HTT function might contribute to neurotoxicity in HD.

1.2 Post-translational modifications in neurodegeneration

Post-translational modifications (PTMs) dramatically increase the size and complexity of the proteome, and are essential for the fine-tuning of the function, activity, stability, localization and interaction of proteins with their binding partners. In the context of neurodegenerative diseases, PTMs play a central role as modulators of protein homeostasis. PTMs such as phosphorylation, arginine methylation, palmitoylation, acetylation, SUMOylation, ubiquitination, and proteolytic cleavage can affect for instance the subcellular localization, turnover, degradation, aggregation propensity and clearance of proteins linked to neurodegeneration. In this way, PTMs can either enhance or suppress the toxicity of the disease-causing proteins, which are typically prone to accumulate into insoluble aggregates and elicit toxicity through gain-of-function mechanisms. A high degree of crosstalk between different PTMs is also observed; this implies that changes in one PTM may influence other PTMs of the same protein, with major impact on its function, degradation and toxicity. Remarkably, several intrinsic and extrinsic signaling cascades regulate PTMs in the cell and pharmacologic or genetic modulation of these signaling pathways offers valuable therapeutic opportunities, in addition to specific targeting of the enzymes directly responsible for the catalysis of each PTM.

This thesis focuses specifically on protein arginine methylation and its emerging role in neurodegeneration, with a particular focus on its impact for the native function of HTT and HD pathogenesis. Despite being a highly abundant PTM in mammalian cells, arginine methylation of HTT has not been described yet. In the following paragraph, an overview of identified PTMs of HTT and their effect on wild-type and mutant HTT is presented.

1.2.1 Post-translational modifications of Huntingtin

HTT is subjected to numerous PTMs, including phosphorylation, acetylation, ubiquitylation, sumoylation and palmitoylation (**Figure 5**) (Saudou and Humbert 2016). Most PTMs of HTT are clustered in the proteolytic domains (PEST domains) within unstructured regions between HEAT repeats (Ratovitski et al. 2017). Importantly, significant stoichiometric differences between wild-type and HD mouse brain were detected for several PTMs (Ratovitski et al. 2017). PTMs play a critical role

in the regulation of HTT function and activity but they also modulate the toxicity of polyQ-expanded HTT. Indeed, the therapeutic relevance of several HTT PTMs has been demonstrated. Some examples are described hereafter.

HTT is phosphorylated at S13 and S16 by inflammatory kinase IKK and this modification regulates HTT nuclear localization and promotes proteasomal and lysosomal degradation of both wild-type and mutant HTT, thereby reducing toxicity (Thompson et al. 2009). Phosphorylation of HTT at S421 is mediated by Akt and the serum- and glucocorticoid kinase SGK (Humbert et al. 2002; Rangone et al. 2004), whereas its dephosphorylation is mediated by calcineurin (Pardo et al. 2006). As previously mentioned, S421 phosphorylation regulates the directionality of axonal transport by promoting anterograde trafficking (Colin et al. 2008). Furthermore, it abrogates mutant HTT-induced toxicity eliciting a neuroprotective effect in cultured striatal neurons and in a rat model of HD (Humbert et al. 2002; Pardo et al. 2006). Activation of Akt (also known as Protein Kinase B, PKB) by the insulin-like growth factor 1 (IGF-1) signaling pathways or inhibition of calcineurin-dependent S421 dephosphorylation might represent therefore effective therapeutic strategies (Humbert et al. 2002; Pardo et al. 2006). HTT is also phosphorylated by cyclin-dependent kinase 5 (Cdk5) at S1181 and S1201 and these PTMs regulate neuronal cell death: absence of Cdk5-mediated phosphorylation renders wild-type HTT toxic whereas phosphorylation at S1181 and S1201 protects from polyQ-induced toxicity (Anne, Saudou, and Humbert 2007). Moreover, phosphorylation of mutant HTT at S434 or S536 reduces proteolysis of HTT by caspase-3 and calpain, thereby lowering expanded HTT-mediated toxicity. Acetylation of expanded HTT at K444 by CREB-binding protein (CBP) improves clearance of mutant HTT aggregates by the autophagic-lysosomal pathway and leads to neuroprotection in primary striatal and cortical neurons and in a *C. elegans* model of HD, suggesting that stimulation of HTT acetylation may represent a mechanism for removing accumulated mutant HTT (Jeong et al. 2009). Conversely, SUMOylation stabilizes the pathogenic exon 1 fragment of HTT, reduces aggregation of polyQ-expanded HTT and promotes its ability to repress transcription in cultured cells; moreover, SUMOylated mutant HTT exacerbates neurotoxicity in a *Drosophila* model of HD (Steffan et al. 2004). Finally, palmitoylation of HTT by the palmitoyl transferase huntingtin interacting protein 14 (HIP14) at C214 is crucial for HTT function and trafficking; in contrast, expansion of the polyQ tract

results in reduced interaction between mutant HTT and HIP14, decreased HTT palmitoylation and enhanced neuronal death (Yanai et al. 2006).

1.2.2 Arginine methylation

1.2.2.1 Protein Arginine Methyltransferases

Arginine methylation is one of the most abundant post-translational modifications (PTMs) in mammalian cells; indeed, the occurrence of this modification is comparable to phosphorylation and ubiquitylation (Larsen et al. 2016). Arginine methylation is catalyzed by a family of enzymes called protein arginine methyltransferases (PRMTs). The mammalian PRMT family comprises nine conserved members (PRMT1-9) with established enzymatic activity, although other two putative PRMTs gene transcripts (PRMT10 and PRMT11) have been identified in humans (Wolf

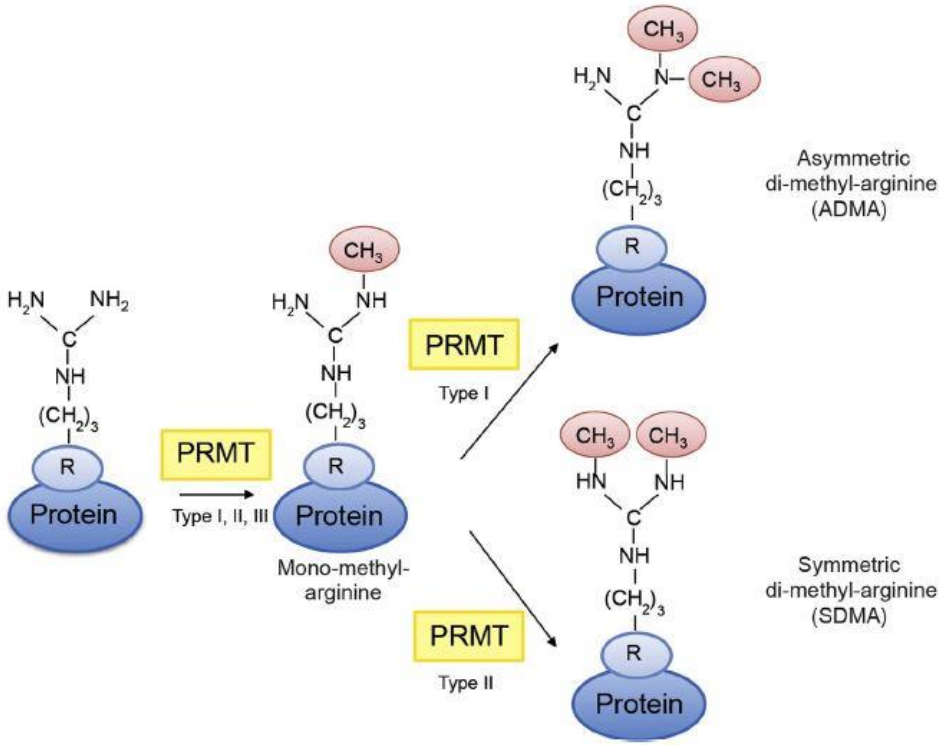

Figure 10: Arginine methylation by protein arginine methyltransferases. PRMTs catalyze the transfer of a methyl groups to the side chain of arginine, thereby generating monomethylarginine or dimethylarginine. Type I PRMTs form asymmetric dimethylarginine and type II PRMTs generate symmetric dimethylarginine, whereas type III PRMTs catalyze only the formation of monomethylarginine (Basso and Pennuto 2015).

2009; Bedford and Clarke 2009). PRMTs catalyze the transfer of methyl groups from S-adenosylmethionine (SAM) to the terminal nitrogen atom of the guanidinium side chain of arginine residues, generating methylarginine and S-adenosylhomocysteine (SAH). Three distinct types of methylated arginine residues occur in mammalian cells, i.e. ω-N^G-monomethylarginine (MMA), ω-N^G,N'^G-symmetric dimethylarginine (SDMA) and ω-N^G,N^G-asymmetric dimethylarginine (ADMA), the latter being the most prevalent in cells (Bedford and Clarke 2009). PRMTs are classified into three categories according to their catalytic activity: type I (PRMT1, PRMT2, PRMT3, PRMT4 also known as CARM1, PRMT6, and PRMT8) and type II (PRMT5 and PRMT9) PRMTs generate MMA as an intermediate before the formation of ADMA and SDMA, respectively, whereas PRMT7 is the only type III enzyme which catalyzes uniquely the formation of MMA (**Figure 10**) (Blanc and Richard 2017). Most MMA modifications are presumably precursors for the subsequent methylation by Type I and II PRMTs, but some proteins also exist in a monomethylated state (Gayatri and Bedford 2014). PRMTs mainly target arginine residues within arginine- and glycine-rich motifs, termed RGG/RG motifs, such as GAR, RXR, and RGG sequences, which are often involved in nucleic acid binding and protein-protein interactions (Thandapani et al. 2013). PRMT family members share a conserved seven-β-strand catalytic domain containing the SAM binding pocket, as well as additional 'double E' and 'THW' sequence motifs that are particular to the PRMT subfamily of methyltransferases. PRMTs differ in their substrate specificity as well as in their subcellular localization (except for PRMT8 which is membrane-bound), although their distribution in specific cellular compartments may vary in different cell types (Basso and Pennuto 2015). PRMTs appear to interact both transiently or permanently with their binding partners and it is still not clear whether PRMTs require the presence of other regulatory subunits to form an active enzymatic complex *in vivo*. Of note, it seems that PRMTs have non-redundant functions and mouse full knockouts display generally clear and distinct phenotypes (Bedford and Clarke 2009). Arginine methylation is enriched in RNA-binding proteins and histones (Gayatri and Bedford 2014); however PRMTs catalyze arginine methylation of a large fraction of the proteome and the major role of this PTM in modulating protein function has gained increasing evidence in the last years.

1.2.2.2 Biological role of arginine methylation

The covalent modification of arginine with methyl groups can directly regulate the physiological function of proteins by modifying their binding properties. Indeed, arginine is unique among amino acids as each guanidino group of arginine residues contains five potential hydrogen bond donors which can interact with hydrogen bond acceptors found on DNA, RNA and proteins. Each methyl group added to an arginine residue changes its shape without altering its charge and removes one hydrogen bond donor, thereby modifying the interaction of the methylated protein with its native binding partners; moreover, the methylation of arginine residues can also increase their affinity to aromatic rings in cation–pi interactions, thus promoting additional interactions (Bedford and Clarke 2009; Blanc and Richard 2017). Consequently, arginine methylation is emerging as a potent regulator of a wide spectrum of cellular processes, including regulation of gene expression, signal transduction, DNA repair, maturation and nucleocytoplasmic transport of RNA, protein stability, and ribosomal assembly (Basso and Pennuto, 2015). Arginine methylation plays a major role in both transcriptional and epigenetic regulation: PRMTs methylate and modulate the activity of transcription factors, co-activators and histone proteins, acting both as co-activators and co-repressors (Bedford and Clarke, 2009). Specifically, PRMTs deposit important activating (H4R3me2a, H3R2me2s, H3R17me2a, H3R26me2a, H3R8me2a) as well as repressive (H3R2me2a, H3R8me2a, H3R8me2s, H4R3me2s) histone marks (Blanc and Richard 2017).

Besides modulating protein-protein interactions, the methylation of arginines in polypeptides creates binding sites for recognition by methylarginine-binding domains. The primary “readers” of methylarginine marks are Tudor domain-containing proteins. The complete family of Tudor domain-containing proteins contains thirty-six proteins that are not fully characterized yet and can be divided largely into a methyllysine-binding group and a methylarginine-binding group (Gayatri and Bedford 2014; Chen et al. 2011). To date, only three mammalian proteins containing Tudor domains have been demonstrated to bind methylated arginine motifs, namely SMN, SPF30 and TDRD3 (Bedford and Clarke, 2009). For many PTMs a highly dynamic ‘writer-reader-eraser’ system has been identified, comprising proteins that can recognize and bind specific PTMs and others that can remove the modification. On the contrary, the existence of erasers able to remove arginine methylation is still

controversial. It has been reported that arginine demethylation *in vitro* can be catalyzed by some lysine demethylases, such as the Jumonji-domain containing protein 6 (JMJD6 (B. Chang et al. 2007), KDM3A, KDM4E and KDM5C; nonetheless, further *in vivo* investigation is required (Blanc and Richard 2017). Due to their ubiquitous expression and to the wide range of substrates they can methylate, PRMTs are involved in a number of different diseases, including cancer, cardiovascular disease, viral pathogenesis, multiple sclerosis, spinal muscular atrophy (Wolf 2009; Bedford and Clarke 2009). Over the last few years, PRMTs have also been directly implicated in aging, metabolic diseases and several neurodegenerative diseases (Blanc and Richard 2017).

1.2.2.3 Arginine methylation in neurodegeneration

Arginine methylation has been recently shown to have a major impact in the pathogenesis of neurodegenerative diseases, including amyotrophic lateral sclerosis (ALS), Alzheimer's disease (AD) and polyglutamine diseases such as spinal and bulbar muscular atrophy (SBMA) and HD. Mutations in the gene coding for Fused in Sarcoma (FUS) have been associated with both familial and sporadic forms of ALS, a fatal late-onset motor neuron disease. Wild-type FUS interacts with PRMT1 and PRMT8 and undergoes extensive arginine methylation at several RXR and RGG motifs (Tradewell et al. 2012; Scaramuzzino et al. 2013). ALS-linked FUS mutants mislocalize to the cytosol where they form insoluble stress granule-like inclusions. Arginine methylation has a key role in nuclear-cytoplasmic shuttling of FUS and global pharmacologic inhibition of PRMTs as well as depletion of PRMT1 reduced the mislocalization and cytoplasmic accumulation of FUS mutants in cell lines and motor neurons (Tradewell et al. 2012; Scaramuzzino et al. 2013). Thus, arginine methylation regulates the toxicity of ALS-related FUS and contributes to the toxic gain-of-function conferred by the disease-causing mutations.

SBMA (also known as Kennedy's disease) is caused by the expansion of a polyglutamine tract in the androgen receptor (AR) and leads to selective loss of lower motor neurons. A recent study carried out by Maria Pennuto and colleagues in collaboration with our laboratory has demonstrated that AR physically and functionally interacts with PRMT6 and that this interaction is enhanced by polyQ expansion in mutant AR (Scaramuzzino et al. 2015). PRMT6 acts as a specific co-activator of wild-type and polyQ-expanded AR

and mutant AR transactivation by PRMT6 is increased compared to that of normal AR. In addition, AR transactivation requires the catalytic activity of PRMT6 and occurs through arginine methylation at two Akt consensus site motifs (RXRXXS, where R is arginine, S serine and X any amino acid) present in AR. AR was previously shown to be phosphorylated by Akt at the serines located in the same two Akt consensus sites (Palazzolo et al. 2007). Remarkably, phosphorylation by Akt at these sites suppresses polyQ AR-induced toxicity (Palazzolo et al. 2007) and stimulation of Akt by IGF-1 is protective in SBMA transgenic mice (Palazzolo et al. 2009). Moreover, serine phosphorylation and arginine methylation at Akt consensus site motifs are mutually exclusive and while Akt-mediated phosphorylation diminishes toxicity, arginine methylation by PRMT6 enhances expanded AR-elicited cell death and leads to neurodegeneration in fly models of SBMA (Scaramuzzino et al. 2015). These findings indicate that PRMT6 is a modifier of mutant AR toxicity *in vitro* and *in vivo* and demonstrate a direct role for arginine methylation in the pathogenesis of polyglutamine disorders. Importantly, the regulation of Akt-mediated phosphorylation by arginine methylation may apply to several Akt consensus site-containing proteins involved in the pathogenesis of neurodegenerative disorders (Basso and Pennuto 2015).

It has been recently reported by Ratovitski and collaborators that HTT interacts with PRMT5 in transfected neurons and HD brain. Interestingly, wild-type HTT stimulates symmetric arginine dimethylation (SDMA) of histones by PRMT5/MEP50 complex *in vitro*, a function which is partially lost upon polyQ expansion of HTT (Ratovitski et al. 2015). Accordingly, SDMA histone marks are reduced in human HD brains, suggesting that a loss of normal HTT ability to facilitate PRMT5 activity and consequent PRMT5 deficiency could contribute, at least in part, to HD pathogenesis (Ratovitski et al. 2015). In addition, PRMT5 was identified as a regulator of Aβ-induced toxicity in human cells and *C. elegans* models of AD, suggesting that stimulation of neuronal PRMT5 activity may represent a potential therapeutic strategy for the prevention of AD (Quan et al. 2015).

1.3 Aim of the thesis

Recent evidence supports a key role for arginine methylation in neurodegeneration and particularly in polyglutamine diseases, such as SBMA and HD. However, whether HTT is methylated at arginine residues has not been investigated yet, and the role of arginine methylation in the pathogenesis of HD remains to be fully elucidated. Maria Pennuto's group demonstrated that PRMT6-mediated arginine methylation of polyQ-expanded androgen receptor (AR) is a modifier of SBMA pathogenesis (Scaramuzzino et al. 2015). AR is methylated by PRMT6 at arginine residues within two Akt consensus sites (RXRXX[S/T]), and this PTM enhances both the transcriptional activity of wild-type AR and the toxicity of mutant AR. The Akt consensus site motif is shared between several proteins associated with neurodegeneration, including HTT which contains two Akt consensus sites (^{416}**R**S**R**SGS^{421}; ^{2063}**R**F**R**LST^{2068}) (Basso and Pennuto 2015). This raises the intriguing possibility that HTT could be methylated at arginine residues as well, with a possible impact on the function of normal HTT and the toxicity of polyQ-expanded HTT. In this work, we focused our attention on one of the most thoroughly characterized functions of HTT, i.e. the role of HTT in axonal trafficking.

The objective of this work is to elucidate the role of PRMT-mediated arginine methylation in the pathogenesis of HD. I tested the central hypothesis that arginine methylation of HTT is a modifier of HD pathogenesis, by pursuing the following specific aims:

1) To determine whether HTT is methylated at arginine residues *in vivo*.
   To address this, by mass spectrometry we analyzed the PTMs of vesicle-associated HTT purified from mouse brain and we subsequently identified which PRMTs interact with HTT and catalyze its arginine methylation.
2) To unravel the role of arginine methylation in the regulation of wild-type HTT function. We tested the hypothesis that arginine methylation modulates HTT-mediated axonal transport by studying vesicular trafficking dynamics in neurons expressing methylation-defective HTT.
3) To assess whether arginine methylation modulates mutant-HTT induced toxicity.
   The role of arginine methylation in HD pathogenesis was investigated through a gain- and loss-of-function approach.

2. Materials and methods

2.1 Animals

Animal care and experimental procedures were conducted in accordance with the Ethical Committee of the University of Trento and were approved by the Italian Ministry of Health (D. Lgs no. 2014/26, implementation of the 2010/63/UE). Animals were maintained with access to food and water ad libitum and kept at a constant temperature (19–22°C) on a 12:12 h light/dark cycle. Primary mouse cortical neurons were obtained from wild-type C57BL/6J mice (Charles River Laboratories, ITALIA) mated to generate male and female embryos.

As HD mouse model, we used $Hdh^{CAG140/+}$ heterozygous knock-in mice generated on a C57BL/6J background, which express human HTT exon 1 sequence with 140 CAG repeats, as previously described (Virlogeux et al. 2018). All experimental procedures were performed in an authorized establishment (Institut des Neurosciences de Grenoble (GIN), U1216, license #B3851610008) in strict accordance with the local animal welfare committee (Comité Local Grenoble Institut Neurosciences, C2EA-04) and the EU guidelines (directive 63/2010/EU) on the protection of animals used for experimental research.

2.2 Purification of vesicle-associated HTT for mass spectrometry analysis

The subcellular fractionation was performed as previously described (Hinckelmann et al., 2016). Briefly, mouse brains were collected and mechanically homogenized in lysis buffer (HEPES 4 mM, sucrose 320 mM pH 7.4) containing protease inhibitor (Sigma Aldrich-P8340) and phosphatase inhibitor (Sigma Aldrich-P5726) cocktails. The homogenate was subjected to sequential centrifugation steps (Figure 1A) to isolate the small vesicles-rich fraction (P3), which was resuspended in lysis buffer. To select vesicle-associated HTT, the P3 fraction (1 mg) was pre-cleared for 1 hour at 4°C with Protein A Sepharose beads (Sigma Aldrich-P9424) and subjected to immunoprecipitation on a rotating wheel for 3 hours at 4°C with agarose beads pre-incubated with 2,5 µg anti-HTT D7F7 antibody (Cell Signaling-5656). The beads were washed three times in lysis buffer and proteins were eluted with Laemmli buffer and

boiled at 95°C for 10 min. After SDS-PAGE, the band corresponding to HTT was cut and analysed by LC-MS/MS to identify HTT post-translational modifications (PTMs). MS was performed with an LTQ Orbitrap XL mass spectrometer (Thermo Scientific), equipped with a nanoESI source (Proxeon). The top eight peaks in the mass spectra (Orbitrap; resolution, 60,000) were selected for fragmentation (CID; normalized collision energy, 35%; activation time, 30 ms, q-value, 0.25). Dynamic exclusion was enabled (repeat count, 2; repeat duration, 10 s; exclusion duration, 20 s). MS/MS spectra were acquired in the LTQ in centroid mode. Proteins were identified using the MaxQuant software package version 1.2.2.5 (MPI for Biochemistry, Germany) and UniProt database version 04/2013.

2.3 Purification of HTT from transfected HEK293 cells and mass spectrometry analysis

HEK293 cells were transfected with full-length human expanded (82Q) HTT constructs (described in Arbez et al. 2017) using Lipofectamine 2000 reagent (ThermoFisher). 24h post transfection cells were lysed by the Dounce homogenization in Triton lysis buffer containing 50 mM Tris, pH 7.0, 150 mM NaCl, 5 mM EDTA, 50 mM $MgCl_2$, 0.5% Triton X100, 0.5% Na deoxycholate, Protease Inhibitor Cocktail III (Calbiochem), and Halt Phosphatase Inhibitor Cocktail (ThermoFisher), followed by centrifugation at 13,000 g. Lysates were pre-cleared by incubating with Protein G-Sepharose beads (GE Healthcare) for 1 h at 4°C, followed by incubation overnight at 4°C with MW1 polyQ-specific antibody (Hybridoma Bank, University of Iowa) to IP expanded HTT. These were then incubated with Protein G-Sepharose for 1 h at 4°C. The IPs were washed 3 times with the lysis buffer, and HTT protein was eluted from the beads with heating (80°C) in 2xSDS Laemmli sample buffer (BioRad), followed by fractionation on NuPAGE 4-12% Bis-Tris polyacrylamide gels (ThermoFisher). HTT protein bands were visualized with SimplyBlue Safe Stain (ThermoFisher). Aliquots (about 10% of the sample) were analyzed by western blotting with antibodies to HTT (MAB2166) and polyQ-specific antibody MW1. PolyQ-expanded HTT protein bands were cut out of the gel, subjected to in-gel digestion with LysC and analyzed by tandem mass spectrometry (MS) on the Q-Exactive mass spectrometer as described previously (Ratovitski et al. 2017).

2.4 Plasmids

The vector for the expression of wild-type human N-terminal HTT (pCAG 17Q HTT-N548) was obtained from E. Cattaneo (University of Milan, Italy). pCAG 73Q HTT-N548 and pCAG 145Q HTT-N548 were obtained by cloning of the fragment containing the polyCAG tract from vectors expressing full-length human HTT (Coriell Institute #CH00023 and #CH00024, respectively). To generate HTT-N548-mCherry constructs, HTT-N548 sequence was amplified by PCR with primers containing KpnI and BamHI restriction sites at the 5' and 3', respectively (Fwd: CAGAGGTACCCCACCATGGCGACCCTG; Rev: CCATCTGACCCTGCCGGGATCCCAGA), and cloned upstream of mCherry sequence in pCDNA3.1-mCherry vector (the stop codon was substituted by a glycine residue). For toxicity experiments in primary neurons, HTT-N548-mCherry sequences were then cloned into HpaI and EcoRI restriction sites of the LentiLox 3.7 backbone under the control of the neuron-specific synapsin I promoter (Tripathy et al., 2017), using the following primers for the PCR: Fwd CAGAGTTAACCACCATGGCGACC; Rev TCTGGAATTCTTACTTGTACAGCTC. HTT methylation-defective arginine-to-lysine mutants were obtained by site-directed mutagenesis PCR using the following forward (F) and reverse (R) primers: R101K-F, 5'-TCAGCTACCAAGAAAGACAAGGTGA-3'; R101K-R, 5'-TGTCAGACAATGATTCACCTTGTCTTTC -3'; R118K-F, 5'-ATAGTGGCACAGTCTGTCAAGAATTC -3'; R118K-R, 5'-CTGAAATTCTGGAGAATTCTTGACA-3'; R416K,R418K-F, 5'-AGGAGTCTGGTGGCAAAAGCAAGAGT-3'; R416K,R418K-R, 5'-TTCCACAATACTCCCACTCTTGCTTTTG -3'. All constructs were confirmed by sequencing. For the expression of EGFP-PRMT6 in primary neurons, EGFP-PRMT6 sequence was cloned downstream of synapsin I promoter in the LentiLox 3.7 backbone described above using primers containing HpaI and EcorI restriction sites at the 5' and 3', respectively (Fwd: CAGAGTTAACCACCATGGTGAGCAA; Rev: TCTGGAATTCTCAGTCCTCCAT). PRMT2 shRNA constructs (in pGFP-C-shLenti vector) were purchased from Origene (cat. No. TL500997), whereas lentiviral constructs (pLKO.1-puro) for shRNA against PRMT6 and the corresponding scrambled were kindly provided by Ernesto Guccione (Phalke et al. 2012). Both contain a puromycin resistance cassette. The most efficient knock-down was observed with PRMT2 shRNA

TL500997D and shPRMT6 #1 (CACCGGCATTCTGAGCATCTT). STHdh clones expressing these shRNAs were used for the assessment of toxicity.

2.5 Cell lines and transfection

HEK293T cells were maintained in DMEM supplemented with 10% fetal bovine serum, L-Glutamine (2mM) and PenStrep (1%) and grown at 37°C with 5% CO_2. Immortalized striatal cells (STHdh, Trettel et al., 2000) were maintained in DMEM supplemented with 10% fetal bovine serum, L-Glutamine (2mM), sodium pyruvate (1mM), G418 (0,4 mg/ml) and grown at 33°C with 5% CO_2. HEK293T cells were transfected with polyethylenimine (PEI), whereas STHdh cells were electroporated using Amaxa Nucleofector™ (Lonza) before plating.

Generation of stable STHdh single-cell clones was carried out by transduction at multiplicity of infection (MOI) 10 or 20 with lentiviruses expressing either scrambled or shRNA against mouse PRMT2 or PRMT6, followed by selection with puromycin (1,5 µg/ml for STHdh Q7/Q7 and 2,5 µg/ml for STHdh Q111/Q111, respectively) and dilution cloning in 96-well tissue culture plates to isolate individual cells.

2.6 Co-immunoprecipitation assays

All immunoprecipitation procedures were carried out at 4°C. HEK293T and STHdh cells were washed with ice-cold PBS and lysed in IP buffer (50 mM HEPES, 250 mM NaCl, 5 mM EDTA, 0.1% NP-40) plus protease inhibitors. Lysates were homogenized and cleared through 22G and 25G needles and kept on ice for 45 min. After 30 min centrifugation at 13200 rpm, the protein concentration was assessed and equal amounts of proteins for each sample were incubated overnight with the indicated antibody (anti-HTT: Merck-Millipore #MAB2166; anti-GFP: Roche #11814460001; anti-mono- and dimethylarginine: Abcam #ab412) on a rotating wheel. The samples were then incubated with 30 µl of Protein A/G Plus Agarose beads (Santa Cruz, sc-2003) for 2h.

Rat neurons transduced with HTT-mCherry lentiviral constructs were lysed in IP buffer (50 mM Tris-HCl pH 7.5, 137 mM NaCl, 10 mM $MgCl_2$, 10% Glycerol, 1% Triton X-100) containing protease inhibitor cocktail (Sigma-Aldrich). Mouse brain and testis were lysed in IP buffer (50 mM Tris-HCl pH 8.0, 1% NP-40) using a Dounce

homogenizer, triturated with the pipette and finally homogenized by several passages through a 2.5G syringe needle. Rat neuron and tissues lysates were pre-cleared with Sepharose 4B Fast Flow beads (Sigma-Aldrich) or Protein A/G Plus Agarose beads (Santa Cruz, sc-2003), respectively, for 3h under rotation. The primary antibody (anti-HTT: Merck-Millipore #MAB2166; anti-mCherry: Institute Curie Cat#A-P-R#13; anti-mono- and dimethylarginine: Abcam #ab412; anti-PRMT6: Bethyl Laboratories #A300-928A) was incubated with Sepharose beads for 3h and then the pre-cleared lysates were added and incubated overnight under rotation.
For all co-immunoprecipitation assays, after incubation with the primary antibodies and the beads, the samples were washed three times in cold IP buffer, resuspended in 2X SDS sample buffer, boiled for 5 min at 95°C and subjected to SDS–PAGE.

2.7 Western blotting

For western blotting, cells were lysed 24-48 hours post-transfection using 1% Triton lysis buffer (25 mM Tris–HCl pH 7.4, 100 mM NaCl, 1 mM EGTA, 1% Triton X-100) or RIPA buffer (50 mM Tris-HCl pH 8.0, 150mM NaCl, 1% NP-40, 0,5% Na-deoxycholate, 2% SDS) plus protease inhibitors. For the analysis of PRMT6 expression in WT and $Hdh^{CAG140/+}$ mice, whole brain or dissected cortex and striatum were lysed immediately after dissection in HEPES/sucrose buffer (320mM sucrose, 4mM HEPES pH 7.4), using a Dounce homogenizer, triturated with the pipette and finally homogenized by several passages through a 2.5G syringe needle. Protein extracts were denatured at 95°C for 5 minutes and then subjected to SDS-PAGE. Proteins were transferred onto nitrocellulose membranes and blocked in 5% non-fat milk or BSA in TBS buffer, 0.1% Tween. Primary antibodies were incubated for 1h at RT or alternatively overnight at 4°C. InfraRed dye-conjugated (LI-COR Biosciences) or HRP-conjugated secondary antibodies were incubated for 1h at RT (1:10000 dilution in blocking solution) and signals were detected with an Odyssey infrared imaging system (LI-COR Biosciences) or Chemidoc™ (Bio-Rad), respectively. The following primary antibodies were used anti-HTT (Merck-Millipore #MAB2166, 1:1000), anti-GFP (Life Technologies #A10262, 1:1000), anti-tubulin (Sigma #T7816, 1:10000), anti-mCherry (Life Technologies #PA5-34974, 1:2500), anti-PRMT6 (Bethyl Laboratories #A300-929A, 1:1000; Proteintech #15395-1-AP, 1:1000; Abcam #ab47244, 1:1000), anti-asymmetric dimethylarginine (Millipore #07-414, 1:250), anti-mono and

dimethylarginine (Abcam #ab412, 1:500), anti-p150 (BD Transduction Laboratories #610474, 1:1000), anti-KHC (Covance #MMS-188P, SUK4, 1:1000), anti-GM130 (Abcam #ab52649, 1:1000; BD Transduction Laboratories #610822, 1:1000), anti-Lamin B1 (Abcam #16048, 1:1000; Abcam #133741, 1:1000), anti-calnexin (Enzo #ADI-SPA-860F, 1:1000; Sigma #C4731, 1:1000). Quantifications were performed using ImageJ 1.52 software.

2.8 Immunocytochemistry

STHdh cells and primary cortical neurons were grown on poly-D-Lysine coated coverslips. Cells were fixed with 4% paraformaldehyde for 15–20 min at room temperature (RT). Cells were permeabilized with 0.1% Triton X-100 in phosphate buffered saline (PBS), and blocked with PBS containing 10% FBS and 0.05% Triton X-100 for 1h at RT. Primary antibodies were incubated overnight at 4°C in blocking solution with the following dilutions: HTT (Merck-Millipore #MAB2166, 1:100), PRMT2 (Abcam #ab66763, 1:100), PRMT6 (Abcam #ab47244, 1:100), mCherry (Life Technologies #PA5-34974, 1:600), MAP2 (Abcam #ab11267, 1:500 or Merck-Millipore #AB15452, 1:100), GFP (Merck-Millipore #MAB2510, 1:1000). The next day, after three washes with PBS, Alexa Fluor conjugated secondary antibodies (1:1000) were incubated for 1h at RT in the dark. The coverslips were then washed three times with PBS, incubated with Hoechst (Sigma #B2261) diluted in PBS for 10 min and mounted on glass slides with ProLong™ Diamond Antifade Mountant (Life technologies #P36961). Primary neurons and STHdh slides were imaged with a 63x oil-immersion objective using the Zeiss Axio Observer Z1 inverted microscope or an inverted confocal microscope (LSM 710, Zeiss) coupled to an Airyscan detector, respectively.

2.9 In situ PLA

The Duolink starter kit (Sigma-Aldrich; DUO92101) was used to study the interaction of endogenous HTT with endogenous PRMT2/PRMT6 in STHdh cells. The assay was performed following manufacturer's instructions. Primary antibodies were incubated with the same dilutions used for immunocytochemistry experiments. Slides were imaged with a 63x oil-immersion objective using the Zeiss Axio Observer Z1 inverted microscope.

2.10 *In vitro* methylation assay

The peptides for in vitro methylation assays were obtained from United Biosystems Inc. In vitro methylation reactions were carried out at 37°C for 1.30h in phosphate-buffered saline with 20 µg of human HTT peptides (R101: ELSATKKDRVNHCLTW; R118: NIVAQSVRNSPEFQKW; R416/R418: KEESGGRSRSGSIVEW), 400 ng of human recombinant PRMTs (PRMT2: Active Motif #31392; PRMT6: Active Motif #31394) and 5 µCi of S-adenosyl-L-[methyl-3H] methionine (PerkinElmer). Samples were subjected to 16% SDS-PAGE and Coomassie Brilliant Blue (CBB) staining. After overnight destaining, the gel was incubated for 45 min with En3Hance™ (PerkinElmer), washed in cold water for 30 min and dried for 2h at 55°C. The dried gel was exposed to film at -80°C for at least one week.

2.11 Primary cortical neurons

For viability assays, primary cortical neurons were cultured from E15.5 C57BL/6J mouse embryos as previously described (Basso et al. 2012). Briefly, the cortices were dissected out of the embryos, digested in papain solution (20U papain, 500µM EDTA and 100µM cystine in 1X Eagles' Balanced Salt Solution (EBSS)) for 20 min. This was followed by DNase I treatment for 3 min. The dissociated cells were centrifuged at 2800 rpm for 5 min. The supernatant was discarded and the digestion was blocked with a solution containing Trypsin inhibitor (Sigma T9253) and bovine serum albumin (Sigma A7030) in 1X EBSS. After a centrifugation at 2800 rpm for 10 min, the cells were seeded in poly-D-lysine-coated plates in Minimum Essential Media (MEM) supplemented with 10% fetal bovine serum, L-Glutamine (2mM) and PenStrep (1%). Neurons were transduced at days *in vitro* (DIV) 0-2 at MOI 3. The day after, the medium was replaced with Neurobasal medium supplemented with B27, sodium pyruvate (1mM), PenStrep (1%), L-Glutamine (2 mM) and AraC (100 mM, Sigma C1768). Half of the media was replaced with fresh media every 7 days. For immunoprecipitation and subcellular fractionation experiments, primary cortical neurons from E17.5 rat embryos were prepared as previously described (Virlogeux et al, 2018).

2.12 Viral production and titration

HTT-mCherry, VAMP2-mCherry or EGFP-PRMT6 lentiviral vectors together with pCMV-dR8.91 (Delta 8.9) plasmid containing *gag*, *pol* and *rev* genes and VSV-G envelope plasmid were expressed in HEK293T cells by calcium phosphate transfection. 16h post-transfection the medium was discarded and replaced with fresh medium. 24h later the medium was collected, centrifuged at 2500 rpm for 10 min (to pellet down any cellular debris), filtered (0.45µm pore size filters) and stored at -80°C in aliquots, until use. Before infection, the viruses were quantified using the SG-PERT reverse transcription assay (Vermeire et al. 2012). In brief, viral particles were lysed for 10 min at RT by adding an equal volume of 2X lysis buffer [0.25% Triton X-100, 50 mM KCl, 100 mM Tris–HCl pH 7.4, 40% glycerol and 0.8 U/µL RNase inhibitor (RiboLock, Fermentas)]. Lysates were then added to a single-step, RT-PCR assay with 3,5 nM MS2 RNA (Roche) as template, 500 nM of each primer (5'-TCCTGCTCAACTTCCTGTCGAG-3' and 5'-CACAGGTCAAACCTCCTAGGAATG-3'), and hot-start Taq (Truestart Hotstart Taq, Fermentas), all in 20 mM Tris–Cl pH 8.3, 5 mM $(NH4)_2SO_4$, 20 mM KCl, 5 mM $MgCl_2$, 0.1 mg/ml BSA, 1/20 000 SYBR Green I (Invitrogen, #S7563), and 200 µM dNTPs. The reaction was carried out according to the following program: 42°C for 20 min for RT reaction, 95°C for 2 min for enzyme activation, followed by 40 cycles of denaturation at 95°C for 5 s, annealing at 60°C for 5 s, extension at 72°C for 15 s and acquisition at 80°C for 5 s. A standard curve was obtained using known concentrations of high-titer viral supernatants (kindly provided by Dr. Massimo Pizzato). Lentiviral particles used to express HTT-mCherry and EGFP-PRMT6 in cortical neurons for the analysis of axonal trafficking were kindly produced by Aurelie Genoux.

2.13 Microfluidic devices

Microfluidic devices were prepared as recently described (Virlogeux et al 2018). Briefly, using an epoxy resin-based V1 500 master mold (Taylor et al. 2010) we imprinted the microfluidic chamber on a mixture of silicon elastomer (PDMS) and its curing agent. Air bubbles were removed by incubation in a desiccator under vacuum for 1 h, and polymerization was performed by incubating the PDMS for 3 h at 60°C. Finalized PDMS microchambers were cut and washed with 100% ethanol followed by a quick passage through an ultrasonic bath and then washed with distilled water. Cut

PDMS and glass-bottom, 0.17 µm-thick, 35 mm-diameter Petri dishes (FluoroDish, WPI) were placed into plasma cleaner under vacuum for 30 s for surface activation. After a rapid passage in an oven at 60°C, PDMS pieces were attached on Petri dishes to form an irreversible tight seal. The microfluidic devices were then coated with poly-D-lysine (0.1 mg/ml) in the upper and synaptic chambers, and with a mix of poly-D-lysine (0.1 mg/ml) + laminin (10 µg/ml) in the lower chamber overnight at 4°C. Microchambers were finally washed 3 times with growing medium (Neurobasal medium supplemented with 2% B27, 2 mM Glutamax, and 1% penicillin/streptomycin) and placed at 37°C before neuron plating.

2.14 Primary neuronal cultures in microfluidic devices

For trafficking analyses, primary cortical and striatal neurons were prepared by dissecting the cortex and the striatum from E15.5 wild-type (C57/BL6J) mouse embryos. The structures were digested with a papain/cysteine solution, followed by two incubations in trypsin inhibitor solution, and finally dissociated mechanically. Dissociated neurons were re-suspended in Neurobasal (NB) medium supplemented with B27 (2%), L-Glutamine (2mM) and PenStrep (1%) and plated in the chamber with a final density of ~7000 cells/mm^2. Cortical neurons were plated first on the upper chamber after the addition of growing medium in the synaptic chamber. Striatal neurons were subsequently added in the lower chamber. Neurons were left in the incubator for at least 3 hours, then all compartments were gently filled with growing medium. Neurons in microchambers were transduced at DIV1 and the medium was changed the day after. Acquisitions were done at DIV 12-14.

2.15 Live-cell imaging

Live-cell recordings were performed using an inverted microscope (Axio Observer, Zeiss) coupled to a spinning-disk confocal system (CSU-W1-T3, Yokogawa) connected to wide field electron-multiplying CCD camera (ProEM+1024, Princeton Instrument) and maintained at 37°C and 5% CO2. For HTT-mCherry trafficking, images were taken every 200 ms for 30 s (63x oil-immersion objective, 1.46 NA). Kymographs were generated using KymoToolBox plugin for ImageJ (Zala et al. 2013) to extract the following kinetics parameters (previously described in Virlogeux et al. 2018):

anterograde/retrograde velocity, number of anterograde/retrograde vesicles per 100 µm, linear flow rate, directional flux. In detail:

Anterograde velocity: $$V_a\ (\mu m/s) = \frac{Anterograde\ distance\ (\mu m)}{Time\ (s)}$$

Retrograde velocity: $$V_r\ (\mu m/s) = \frac{Retrograde\ distance\ (\mu m)}{Time\ (s)}$$

Number of anterograde vesicles per 100µm: $$N_a = \frac{n_a\ (Number\ of\ anterograde\ vesicles)}{Axon\ length\ (100\mu m)}$$

Number of retrograde vesicles per 100µm: $$N_r = \frac{n_r\ (Number\ of\ retrograde\ vesicles)}{Axon\ length\ (100\mu m)}$$

Linear flow rate: $$Q\ (\mu m/s) = |V_a| * n_a + |V_r| * n_r$$

Directional flux: $$D\ (\mu m/s) = V_a * n_a - V_r * n_r$$

For each experiment, at least 2-3 microchambers from 3 independent neuronal cultures were used, and a minimum number of 50-60 axons were analyzed.

2.16 Immunostaining in microchambers

Neurons in microchambers were fixed with a PFA (4%)/Sucrose (4%) solution in PBS for 20 min at room temperature (RT). The fixation buffer was rinsed three times with PBS and neurons were incubated for 1h at RT with a blocking solution (1% BSA, 2% normal goat serum, 0.1%Triton X-100). The compartments of interest were then incubated with primary antibodies diluted in blocking solution overnight at 4°C and appropriate Alexa Fluor conjugated secondary antibodies (1:1000) were incubated for 1h at RT. Immunostained chambers were maintained in PBS for a maximum of one week in the dark at 4°C. The following primary antibodies were used: HTT (Merck-Millipore #MAB2166, 1:100), PRMT6 (Abcam #ab47244, 1:100), mCherry (Novus Biologicals #NBP2-25158, 1:500). Images were acquired with a ×63 oil-immersion

objective (1.4 NA) using an inverted confocal microscope (LSM 710, Zeiss) coupled to an Airyscan detector to improve signal-to-noise ratio and to increase resolution.

2.17 Subcellular fractionation from whole mouse brain and primary rat neurons

Whole mouse brains were lysed in vesicle buffer (10 mM HEPES-KOH, 175 mM L-aspartic acid, 65 mM taurine, 85 mM betaine, 25 mM glycine, 6.5 mM MgCl2, 5 mM EGTA, 0.5 mM D-glucose, 1.5 mM CaCl2, 20 mM DTT, pH 7.2) containing protease inhibitors using a Dounce homogenizer. Rat neurons were lysed in IP buffer (50mM Tris-HCl pH 7.5, 137mM NaCl, 10mM MgCl2, 10% Glycerol, 1% Triton X-100) containing protease inhibitors. Both lysates were homogenized using a 2.5G syringe needle and subjected to sequential centrifugations at 4°C (10 min at 1200rpm, 40 min at 12000g, 90 min at 100000g) in order to purify a fraction enriched in nuclei (P1), a fraction containing mitochondria and large membranes such as Golgi and endoplasmic reticulum (P2), a fraction enriched in small vesicles (P3) and the corresponding cytoplasmic phases (S1, S2 and S3), as depicted in Figure 11A. Equal amounts of proteins for each fraction were loaded onto a 6% and a 10% SDS-polyacrylamide gel and examined by western blotting.

2.18 Immunogold labelling and Transmission Electron Microscopy (TEM)

For each experiment, the vesicle fraction (P3) purified from whole mouse brain was resuspended in 100-200µl PBS and 10µl were adsorbed to nickel formvar\carbon coated grids, fixed in 1% glutaraldehyde, washed twice with PBS, incubated with quenching solution (50mM glycine) three times for 3 min each and blocked 10 min at RT in blocking solution (PBS+1%BSA). The first primary antibody (e.g. anti-HTT D7F7 Cell Signaling #5656, 1:30 in PBS+1%BSA) was incubated for 1h at RT, washed in PBS+0,1%BSA and incubated with 5 nm gold anti rabbit antibody (1:50 in PBS+1%BSA) for 30 min at RT. The grids were then washed in PBS and the protocol was repeated starting from fixation in glutaraldehyde, using the second primary antibody (e.g. anti-PRMT6 Abcam #ab47244, 1:10) and the 15 nm gold anti rabbit antibody. Finally, the grids were fixed in 1% glutaraldehyde, washed in PBS and

distilled water, and finally stained and embedded by incubation in 2% methylcellulose/5% uranyl acetate for 10 min at RT in the dark. The samples were examined using JEOL 1200 EX transmission electron microscope equipped with a digital camera (Veleta).

2.19 Quantitative real-time PCR

Total RNA was extracted with TRIzol (Invitrogen). 1 μg of RNA was reverse transcribed using iScript Reverse Transcription Supermix (Bio-Rad) following manufacturer's instructions. Gene expression was measured by quantitative real-time PCR using the iTaq Universal SYBR Green Supermix (Bio-Rad) and C1000 Touch termocycler - CFX96 Real Time System (Biorad). The level of each transcript was measured with the threshold cycle (Ct) method using GAPDH (Glyceraldehyde-3-Phosphate Dehydrogenase) mRNA as endogenous control. Primers used: PRMT6 (NM_178891.5) Fwd: AGTCCATGCTGAGCTCCGT, Rev: TCCATGCAGCTCATATCCA; PRMT2 (NM_001077638) Fwd: TCTCTGAGCCATGCACAATC, Rev: CCAGCCTTCTGGATGTCAAA; GAPDH Fwd: AACCTGCCAAGTATGATGA, Rev: GGAGTTGCTGTTGAAGTC.

2.20 Toxicity assays in striatal cells

STHdh cells were seeded in triplicates into a 96-well tissue culture plate ($5*10^4$ cells/well) and treated with 5 μM Adenosine-2′,3′-dialdehyde (ADOX, Sigma #A7154) or 5 μM Methylthioadenosine (MTA, Sigma #D5011) for 24h in complete medium. For the toxicity assays with specific type I PRMTs inhibitors, STHdh cells ($2,5*10^4$ cells/well) were treated for 48h with 10 μM MS023 or the corresponding negative control MS094 in complete medium. These two compounds were kindly provided by Matthieu Schapira and Masoud Vedadi from the University of Toronto (Eram et al. 2016). Cell viability was assessed by MTT (Thiazolyl Blue Tetrazolium Bromide, Sigma #M5655) assay. Briefly, MTT (5 mg/ml in PBS) was diluted 1:10 into the medium and incubated for 1h at 37°C. After removing the medium, precipitates were dissolved in DMSO and absorbance at 570 nm was recorded with Infinite M200 Pro microplate reader (TECAN).

For the measurement of cell viability in STHdh single cell clones stably expressing shRNA against PRMT2 or PRMT6 and in STHdh cells electroporated with EGFP-PRMT6 construct, the cells were stressed for 24h with low-glucose DMEM (Gibco #11054020) without serum and stained with LIVE/DEAD® Fixable Near-IR dye (Invitrogen #L10119). The stained cells were then analysed by using a BD FACSCanto™ flow cytometer (Becton Dickinson). For shPRMT2 clones and STHdh overexpressing EGFP-PRMT6, only GFP-positive cells were considered for the calculation of the percentage of cell death.

2.21 Toxicity assay in neurons

Primary cortical neurons were seeded on 96-well tissue culture plates at a concentration of $2.5*10^4$ cells/well. At DIV0 the immature neurons were transduced at multiplicity of infection (MOI) 3 with viral particles expressing HTT-mCherry WT or R118K mutants along with EGFP or EGFP-PRMT6. At DIV11 the neurons were fixed and processed for immunocytochemistry for mCherry and MAP2/EGFP as described above. The plate was then imaged with Operetta High-Content Imaging System and analyzed for the total number of $mCherry^+/EGFP^+$ neurons in each condition. The experiments were carried out in triplicates and repeated at least three times independently.

2.22 Statistical analysis

All the experiments presented here were repeated at least three times. All data are presented as mean ± SEM. For multiple comparison, statistical analysis was conducted by one-way ANOVA followed by parametric or non-parametric post hoc test according to the distribution of the data. Significance of comparison between two groups was assessed either by the parametric Student-t test or the non-parametric Mann-Whitney test. The use of the specific tests has been reported in each figure legend. Statistically significant results were defined as follows: *P<0.05; **P<0.01; ***P<0.001 and ****P<0.0001.

3. Results

In this section of the thesis I present the results I obtained during my doctoral studies, that have been carried out at the Department of Cellular, Computational and Integrative Biology (CIBIO, University of Trento) in the *Laboratory of Transcriptional Neurobiology* led by Dr. Manuela Basso, in collaboration with Prof. Maria Pennuto (Department of Biomedical Sciences, University of Padua) and Prof. Frédéric Saudou, who leads the laboratory of *Intracellular Dynamics and Neurodegeneration* at the Grenoble Institute of Neuroscience (Université Grenoble Alpes), where I spent a research period abroad sponsored by an EMBO Short-Term Fellowship.

3.1 Huntingtin is methylated at arginine residues

3.1.1 Huntingtin is methylated at R101 and R118 in brain-derived vesicles

Several proteins involved in neurodegeneration are targets of Akt and contain one or more canonical Akt consensus sites (RXRXX[S/T]) (Basso and Pennuto 2015), that can be methylated at arginines with a possible impact on the native and toxic function of the disease protein, as shown by Scaramuzzino et al. (Scaramuzzino et al. 2015). HTT contains two Akt consensus sites, hence we wondered whether HTT is methylated at arginine residues.

HTT has a key role in the regulation of axonal trafficking and is highly associated with vesicles. To address whether HTT is arginine methylated *in vivo*, in collaboration with Frédéric Saudou's laboratory we immunopurified full-length HTT from vesicular fractions isolated from the brain of wild-type mice and analyzed HTT post-translational modifications by mass spectrometry (**Figure 11A**). Interestingly, we identified two arginine residues that are dimethylated *in vivo*, namely arginine 101 (R101) and

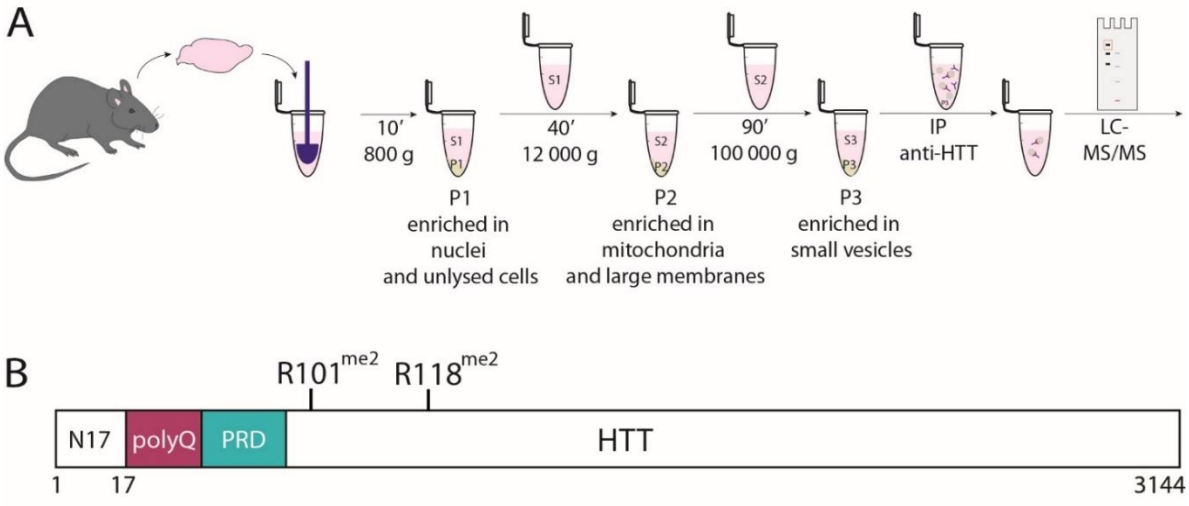

Figure 11: Vesicle-associated HTT is methylated at R101 and R118 *in vivo*. (A) Purification of vesicle-associated HTT from mouse brain for post-translational modifications (PTMs) analysis. Brain homogenates were subjected to sequential centrifugations to isolate the small vesicles-rich fraction (P3). HTT was immunoprecipitated from the P3 fraction and HTT PTMs were studied by LC-MS/MS. **(B)** Mass spectrometry analysis showed that vesicle-associated HTT purified from mouse brain is dimethylated at R101 and R118.

arginine 118 (R118) (**Figure 11B, Appendix Table 1 and Figure S1**). Surprisingly, with this experimental setup we did not detect methylation of HTT at the arginine residues contained in the Akt consensus sites.

We then asked whether the two methylated arginine residues are evolutionarily conserved. To answer this question, we compared HTT sequence in several metazoans that were previously examined in a comparative analysis published in 2008 by Elena Cattaneo and collaborators (Tartari et al. 2008). The phylogenetic analysis showed that R101 and R118 are very well conserved throughout evolution (**Figure 12**), suggesting an evolutionary conserved function for these residues. Notably, R101 and R118 are found in all the deuterostomes analyzed, except for R101 in the sea urchin (*S. purpuratus*). Although lost in protostomes, the two arginines are substituted by another positively charged amino acid, i.e. lysine (K), indicating a possible relevant role of this residue for the maintenance of HTT structure and/or function, with the only exception of R118 replacement by alanine (A) in *D. melanogaster* and *D. pseudoobscura* (**Figure 12**).

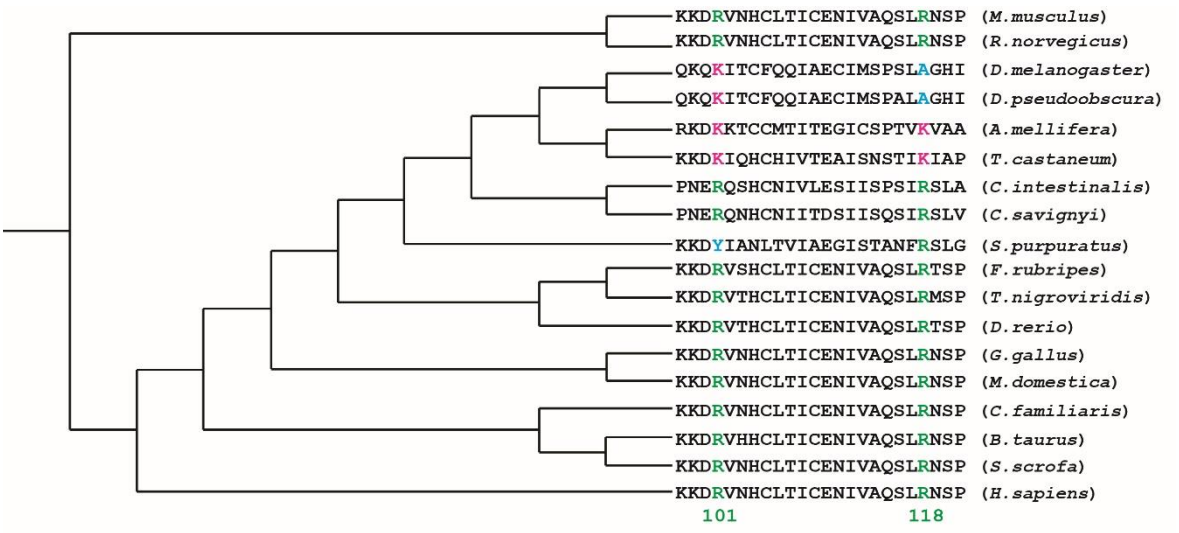

Figure 12: R101 and R118 in HTT are highly evolutionarily conserved. Cladogram showing high degree of conservation of R101 and R118 throughout evolution. The phylogenetic analysis was performed with CLC Sequence Viewer 8 software on the same dataset used by Tartari and colleagues (Tartari et al. 2008). Protostomes: *Drosophila melanogaster, Drosophila pseudoobscura, Apis mellifera, Tribolium castaneum*. Deuterostomes: *Ciona intestinalis, Ciona savignyi, Strongylocentrotus purpuratus, Fugu rubripes, Tetraodon nigroviridis, Danio rerio, Gallus gallus, Monodelphis domestica, Canis familiaris, Bos taurus, Sus scrofa, Mus musculus, Rattus norvegicus, Homo sapiens*.

3.1.2 Wild-type HTT interacts with PRMT2 and PRMT6

Based on these observations, I sought to identify the PRMTs responsible for HTT arginine methylation and to assess the biological relevance of this PTM for the native function of HTT and HD pathogenesis.

To determine whether HTT forms a complex with PRMTs, I co-expressed the N-terminal fragment of HTT corresponding to the first 548 amino acids bearing 17 glutamine residues (HTT 548-17Q) together with soluble enhanced green fluorescent protein (EGFP) or EGFP-tagged PRMT1-8 in HEK293T cells. By immunoprecipitating the EGFP-fused PRMTs, I found that HTT 548-17Q forms a complex predominantly with PRMT2 and PRMT6 and to a lower extent with PRMT1, PRMT5, and PRMT7 (**Figure 13A**).

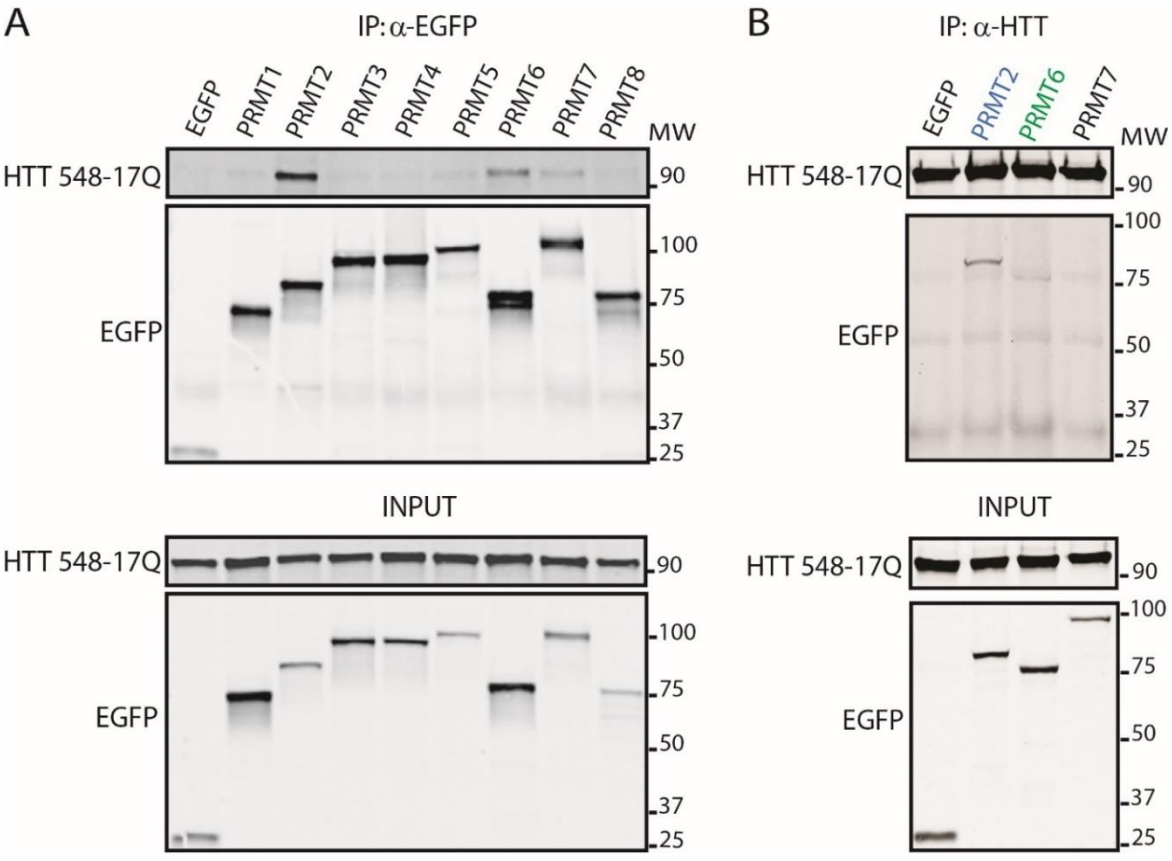

Figure 13: N-terminal HTT interacts with PRMT2 and PRMT6. (A) Co-Immunoprecipitation (Co-IP) assay in HEK293T cells overexpressing HTT N548-17Q together with soluble EGFP or EGFP-tagged PRMT1-8 showed that HTT primarily interacts with PRMT2 and PRMT6 and has lower affinity for PRMT1-5-7. Shown is one experiment out of four. **(B)** Reverse Co-IP assay in HEK293T cells overexpressing HTT N548-17Q together with soluble EGFP or EGFP-tagged PRMT2-6-7 showed that HTT primarily interacts with PRMT2 and PRMT6. Shown is one experiment out of two.

Similar results were obtained by the reverse immunoprecipitation performed with an antibody that recognizes HTT, confirming a stronger interaction of HTT with PRMT2 and PRMT6 compared to PRMT7 (**Figure 13B**).

To determine whether full-length HTT (FL-HTT) interacts with PRMT2 and PRMT6, I performed an immunoprecipitation assay in immortalized striatal cells obtained from knock-in mice expressing full-length HTT-7Q ($STHdh^{Q7/Q7}$) (Trettel et al. 2000). By immunoprecipitation of HTT, I demonstrated that endogenous FL-HTT interacts with overexpressed PRMT2 and PRMT6 in striatal cells (**Figure 14**). To show that endogenous HTT interacts with endogenous PRMTs, and to elucidate in which subcellular compartment they form a complex, we performed an *in situ* proximity ligation assay (PLA), which enables to detect protein-protein interactions in fixed cells. PLA signals confirmed that endogenous HTT associates with endogenous PRMT2 and PRMT6 in the nucleus as well as in the cytosol of $STHdh^{Q7/Q7}$ cells (**Figure 15A**). Significantly lower PLA signal was detected upon incubation with a single primary antibody, indicating that the red dots observed in Figure 15A specifically derive from PRMT2/PRMT6 and HTT interaction (**Figure 15B**).

Taken together, these results show that vesicle-associated HTT is methylated at arginine residues *in vivo*, specifically at R101 and R118, and that HTT forms a complex with PRMT2 and PRMT6 in non-neuronal cells and wild-type striatal cells.

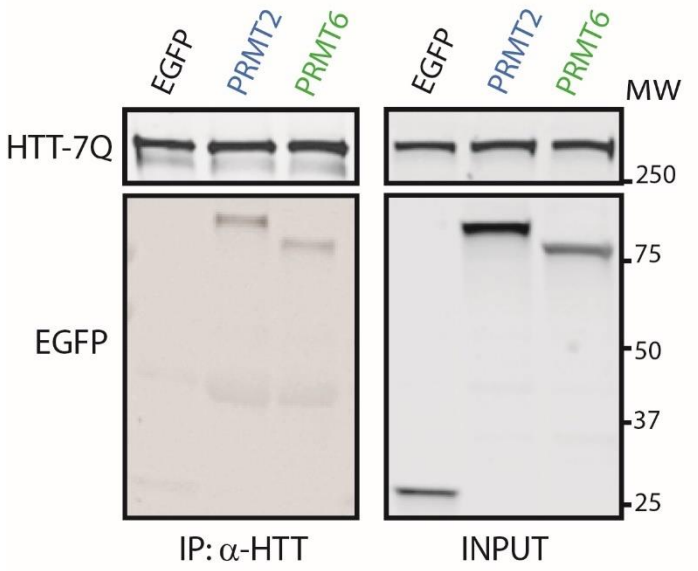

Figure 14: Full-length HTT interacts with overexpressed PRMT2 and PRMT6. Co-immunoprecipitation assay in $STHdh^{Q7/Q7}$ cells overexpressing EGFP-PRMT2 or EGFP-PRMT6 showed interaction of full-length endogenous HTT with PRMT2 and PRMT6. Shown is one experiment representative of four.

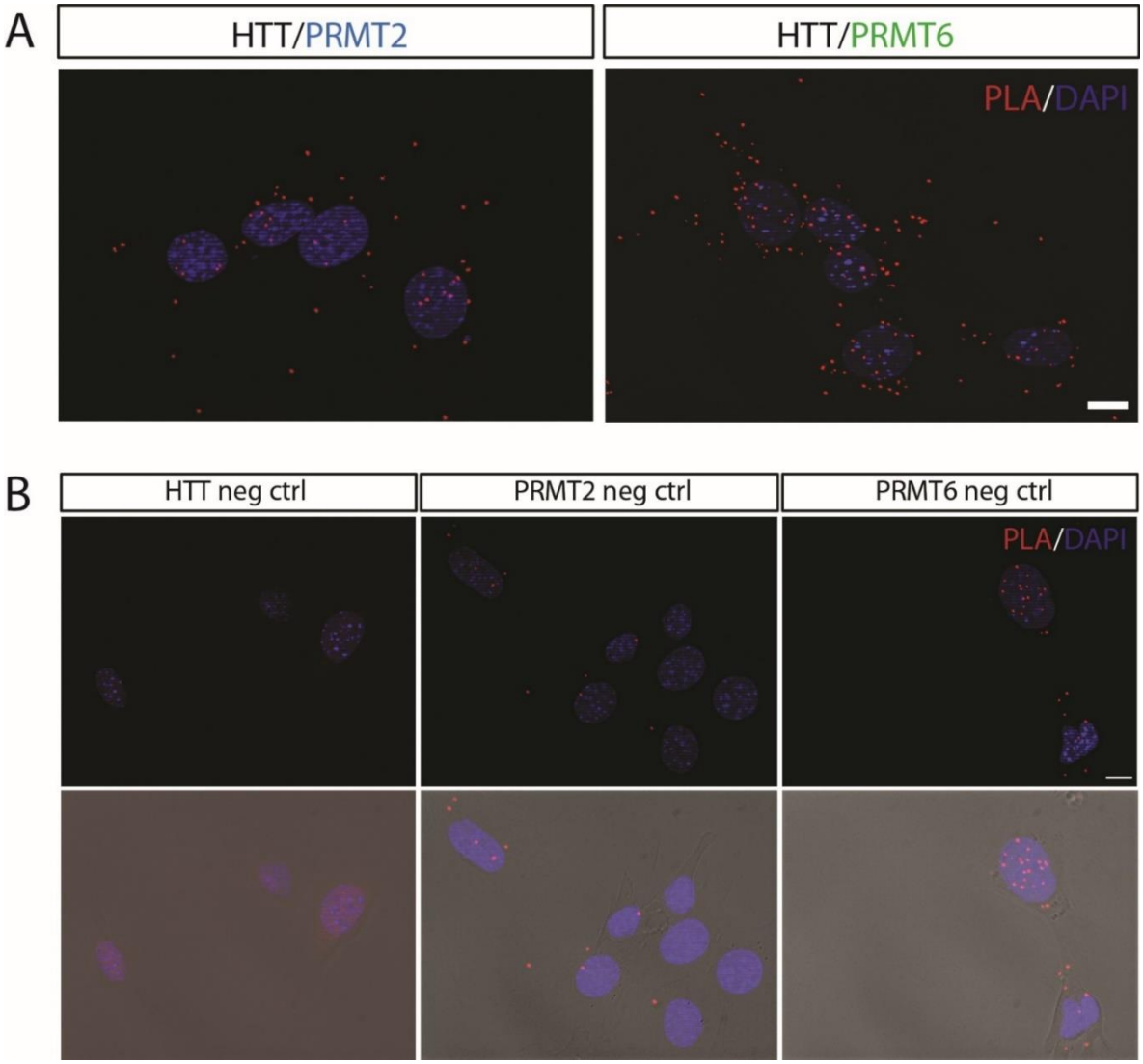

Figure 15: Full-length HTT interacts with endogenous PRMT2 and PRMT6 in striatal cells. **(A)** Proximity Ligation Assay (PLA) in STHdh$^{Q7/Q7}$ cells confirmed interaction between FL-HTT and endogenous PRMT2 (left panel) and PRMT6 (right panel). The red dots indicate close proximity of HTT and the two PRMTs. Nuclei were revealed with DAPI. Shown are representative images from three independent experiments. Bar, 10 µm. **(B)** Negative control assays showing background PLA-positive signals in STHdh$^{Q7/Q7}$ upon incubation with the indicated primary antibody. Bar, 10 µm.

3.1.3 PRMT6 methylates HTT at R118

PRMT2 and PRMT6 are type I PRMTs and catalyze the addition of one or two methyl groups to arginine to generate monomethylarginine (MMA) or asymmetric dimethylarginine (ADMA). To determine whether PRMT2 and PRMT6 are responsible for HTT methylation at R101 and R118 I performed an *in vitro* methylation assay by incubating peptides spanning either R101 or R118 with recombinant PRMT2 or PRMT6 and the radioactive methylation donor [^{3}H]-S-adenosylmethionine ([^{3}H]-SAM). I detected methylation of R118 by PRMT6, whereas PRMT2 did not modify these two arginine residues (**Figure 16**). These findings indicate that PRMT6 specifically methylates HTT at R118 *in vitro*. Considering that in our hands PRMT2 did not methylate peptides containing R101 and R118 *in vitro*, in this work I focused my attention on PRMT6-mediated HTT methylation at R118 and the role of this specific PTM for HTT function in both physiological and pathological conditions. Further investigation is needed to identify the enzyme responsible for HTT methylation at R101 and to determine the biological significance of HTT-PRMT2 interaction.

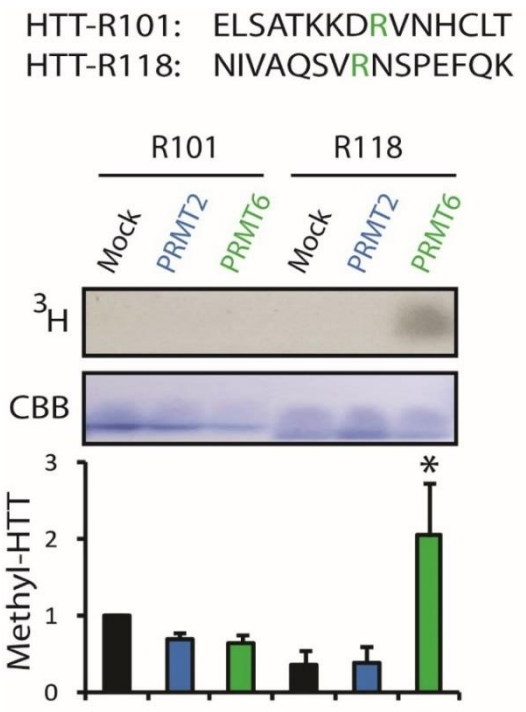

Figure 16: PRMT6 methylates HTT at R118 *in vitro*. *In vitro* methylation assay performed by incubating human HTT peptides and recombinant human PRMT2 or PRMT6 in the presence of [^{3}H]-SAM showed that PRMT6 methylates HTT at R118. Top: autoradiography. Bottom: Coomassie Brilliant Blue (CBB) staining. Graph: mean ± SEM, n=3. One-way ANOVA, Newman-Keuls post-hoc test, *p<0.05.

To assess whether PRMT6 methylates HTT in cells, I transfected HEK293T cells with HTT 548-17Q together with EGFP or EGFP-PRMT6, and I analyzed HTT arginine methylation by immunoprecipitation using either an antibody that specifically recognizes mono- and di-methylarginine (**Figure 17A**) or an anti-HTT antibody (**Figure 17B**) for the pull-down, as previously performed (Scaramuzzino et al. 2015). Overexpression of wild-type PRMT6 but not of its catalytically inactive form (PRMT6-V86K,D88A) enhanced the levels of methylated HTT by 1.3 and 1.8 fold in the two assays, respectively (**Figure 17A,B**).

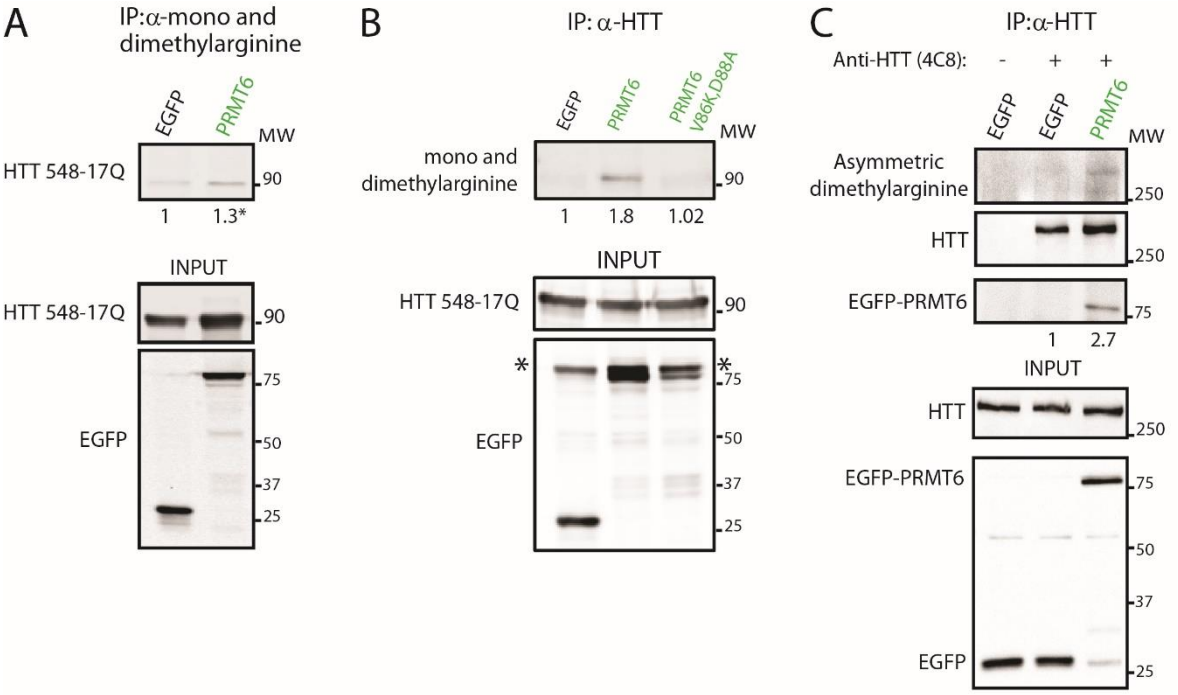

Figure 17: PRMT6 methylates HTT in non-neuronal cells and primary neurons. (A) Immunoprecipitation (IP) assay with an anti-mono- and di-methylarginine antibody in HEK293T cells overexpressing HTT N548-17Q together with EGFP-PRMT6 showed that PRMT6 methylates HTT in cells. Shown is a representative image from at least three independent experiments. Quantification (average) of HTT IP/HTT input ratio is shown at the bottom of the IP panel. Student's t-test, *p<0.05. **(B)** Reverse immunoprecipitation (IP) assay with anti-HTT antibody in HEK293T cells overexpressing HTT N548-17Q together with EGFP-PRMT6 or catalytically inactive EGFP-PRMT6 V86K,D88A confirmed that PRMT6 methylates HTT in cells. Shown is a representative image from at least three independent experiments. Quantification (average) of HTT IP/HTT input ratio is shown at the bottom of the IP panel. The asterisks indicate an upper non-specific band. **(C)** FL-HTT is methylated by PRMT6 in cortical neurons. IP assay in primary rat cortical neurons transduced with a lentiviral vector expressing EGFP or EGFP-PRMT6. Shown is one experiment representative of two. Quantification (average) of asymmetric dimethylarginine/HTT signal ratio is shown at the bottom of the IP panel.

To further validate methylation of HTT by PRMT6, I immunoprecipitated FL-HTT from rat primary neurons transduced with a lentiviral vector expressing EGFP-PRMT6. Revelation with an antibody that specifically recognizes ADMA showed that PRMT6 asymmetrically dimethylates HTT in neurons (**Figure 17C**). Moreover, this experiment confirmed interaction between FL-HTT and PRMT6 in neurons (**Figure 17C**). Finally, I performed *in vivo* immunoprecipitation assays with antibodies against methylarginine and PRMT6 in the brain and testis of wild-type mice. Although PRMT6 is expressed at very high levels in the testis, interestingly I detected HTT-PRMT6 interaction and arginine methylation of HTT in the brain but not in the testis of wild-type mice (**Figure 18**).

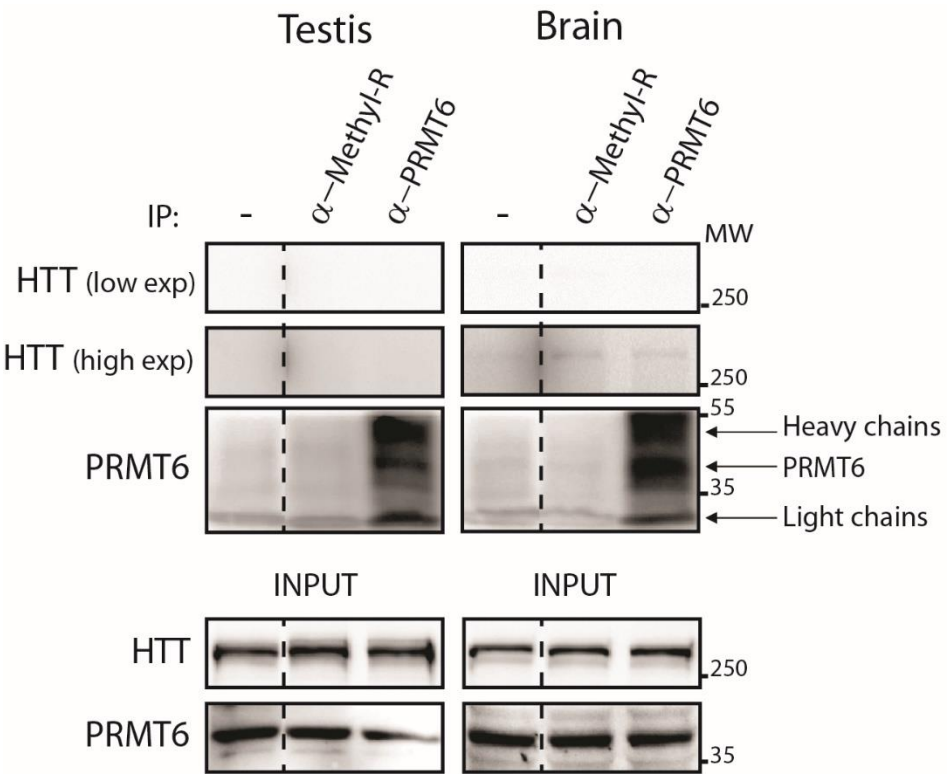

Figure 18: HTT interacts with PRMT6 and is methylated in the wild-type mouse brain.
IP assays with the indicated antibodies in wild-type mouse testis (left panel) and brain (right panel) showed HTT-PRMT6 interaction and HTT methylation in the mouse brain but not in the testis. Shown is one experiment representative of three. Dashed line: lanes were run on the same gel but were non-contiguous.

I then substituted R118 with lysine to generate a methylation-defective HTT mutant, HTT-R118K. HTT 548 17Q-R118K retained the ability to form a complex with PRMT6 (**Figure 19A**), and its global ADMA levels were similar in the presence of the mutation, suggesting that HTT is dimethylated at several other arginine residues by PRMT6 and/or possibly other type I PRMTs (**Figure 19B**). Altogether, these results indicate that PRMT6 methylates HTT at R118 in non-neuronal cells, primary neurons and brain of wild-type mice.

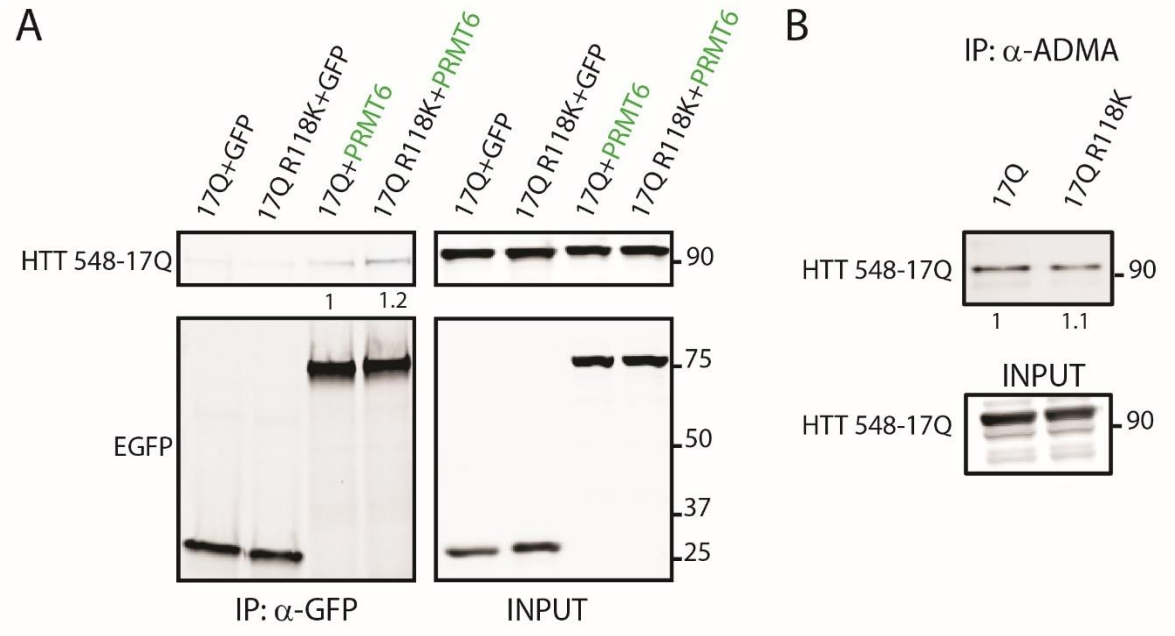

Figure 19: R118K mutation does not alter HTT-PRMT6 interaction and global asymmetric dimethylation of HTT. (A) Co-IP assay in HEK293T cells overexpressing either HTT N548-17Q or HTT N548-17Q R118K together with soluble EGFP or EGFP-tagged PRMT6 showed that methylation-defective HTT retains the ability to form a complex with PRMT6. Shown is one experiment out of four. Quantification (average) of HTT IP/HTT input ratio is shown at the bottom of the IP panel. **(B)** IP assay with an anti-ADMA antibody in HEK293T cells transfected with HTT N548-17Q or HTT N548-17Q R118K showed no difference in the levels of global ADMA in HTT R118K compared to wild type HTT. Shown is one experiment representative of four. Quantification (average) of HTT IP/HTT input ratio is shown at the bottom of the IP panel.

3.2 PRMT6 colocalizes with HTT in neurons and is recruited to vesicles in the brain

3.2.1 HTT and PRMT6 colocalize in neuronal cell bodies and axons

PRMT6 binds and methylates HTT at R118. Considering that we detected arginine methylation of HTT in the vesicular fraction purified from mouse brain and that HTT has a key role in axonal transport, I decided to check whether PRMT6 colocalizes with HTT in neuronal cells, specifically in the axon, and to test whether PRMT6 is recruited to vesicles.

To address the first question, I took advantage of a microfluidic device recently developed in Frédéric Saudou's lab (Virlogeux et al. 2018), in which cortical and striatal neurons are plated in two separate chambers and connect to each other through microchannels and an intermediate synaptic chamber, thus reconstructing a physiological corticostriatal network *in vitro* (**Figure 20A**). The microfluidic chamber has a peculiar architecture with long microchannels for cortical neurons (500 μM) and shorter microchannels for striatal neurons (75 μM) and a gradient of laminin from the cortical to the striatal compartment; this enables to build a functional and oriented corticostriatal circuit, where only cortical neurons can extend their axons to reach the synaptic chamber and form corticostriatal synapses (Virlogeux et al. 2018). Thanks to this device, I was able to contemporarily check HTT colocalization with PRMT6 in cortical neurons, striatal neurons and isolated axons. Primary cortical and striatal neurons derived from wild-type mouse embryos were plated in the corresponding fluidically isolated compartments and immunofluorescence analysis with primary antibodies targeting HTT and PRMT6 was performed in mature DIV14 neurons. I detected colocalization of endogenous HTT and PRMT6 in both cortical and striatal neurons, in the cell body as well as in neuronal processes (**Figure 20B,C**). Importantly, a high degree of colocalization of the two proteins of interest was observed in isolated cortical axons (**Figure 20C**), implying that vesicle-associated HTT could be methylated by PRMT6 in the axon.

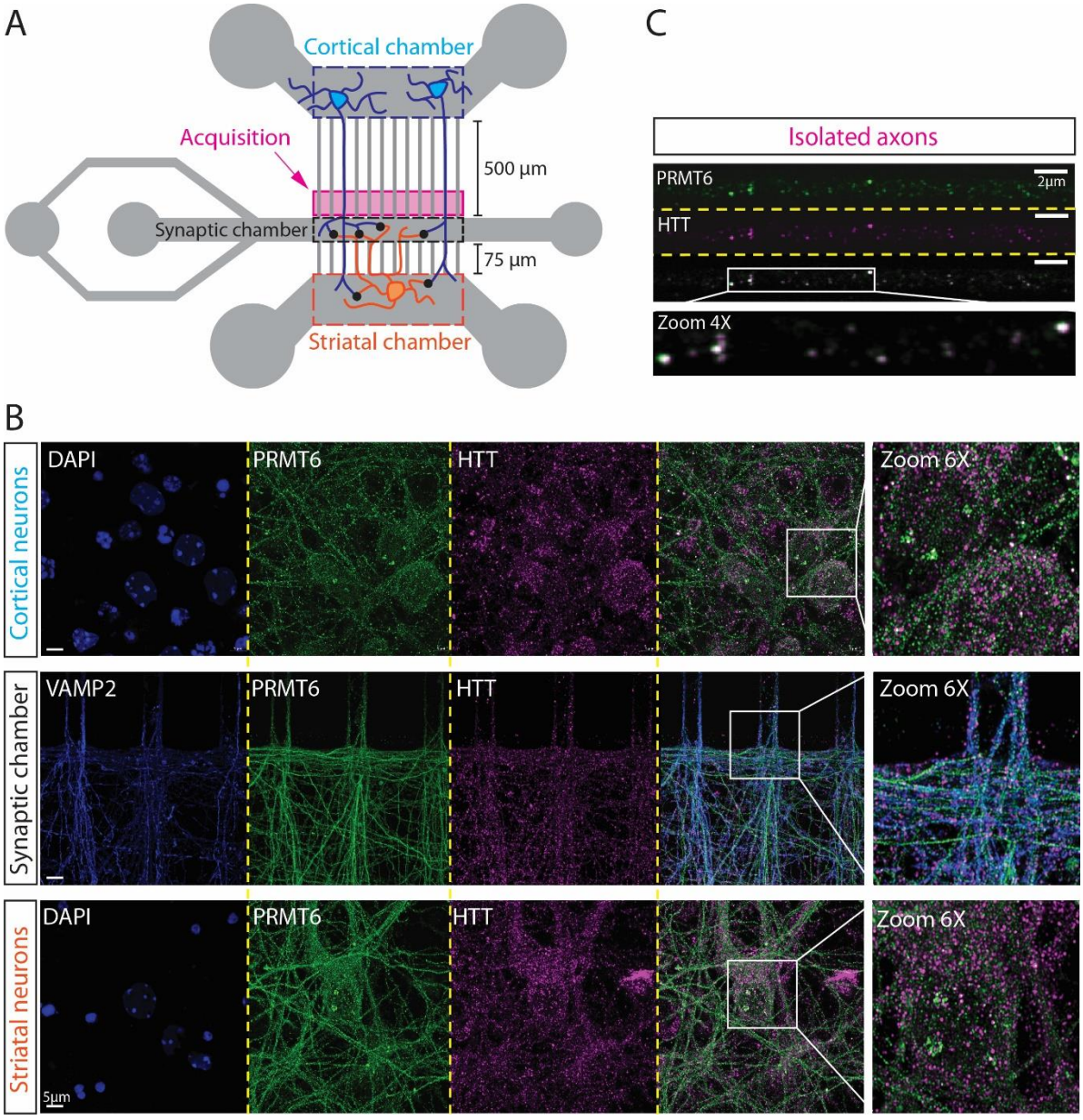

Figure 20: PRMT6 colocalizes with HTT in the soma and axons of neurons. A) Scheme depicting the microfluidic chamber reconstituting the corticostriatal network: cortical and striatal neurons are plated in two separate compartments and connect to each other in a synaptic chamber. **(B)** PRMT6 and HTT colocalize in mouse primary cortical (top panel) and striatal (bottom panel) neurons. Wild-type cortical and striatal neurons were plated in microfluidic chambers and immunocytochemical analysis was performed at DIV14. Cortical neurons were transduced with a lentiviral vector expressing VAMP2-mCherry, whose staining in the synaptic chamber (middle panel) was used as a marker of dendritic and axonal processes. Shown are representative images from three independent experiments. Bar, 5 µm. **(C)** PRMT6 colocalizes with HTT in axons. Mouse primary neurons were plated in microfluidic chambers as in (A). Immunostaining of PRMT6 and HTT was performed at DIV14 in isolated cortical axons (pink area highlighted in (A)). The 4X zoom shows axonal colocalization of PRMT6 and HTT. Shown are representative images from three independent experiments. Bar, 2 µm.

3.2.2 PRMT6 is recruited on vesicles in the brain

Next, in order to answer to the question of whether PRMT6 is recruited to small vesicles, I performed a subcellular fractionation of mouse brain extracts by successive centrifugation steps to eventually obtain a pellet fraction (P3) enriched in small vesicles and vesicle-associated proteins, as previously reported (Colin et al. 2008) and described in **Figure 11A**. I separated all the different fractions by SDS-PAGE and immunoblotted for HTT, PRMT6, and markers of the different subcellular fractions, such as the dynactin subunit p150^{glued} for the vesicular fraction (P3), GM130 as a marker of the Golgi apparatus (P2) and Lamin B1 as a marker of the nuclear compartment (P1). As shown in **Figure 21A**, HTT and PRMT6 are both present in the P3 fraction, suggesting that they are both recruited to small vesicles in the brain. To further prove the association of PRMT6 with vesicles, I performed transmission electron microscopy coupled to immunogold staining of brain-purified vesicles (P3 fraction) using anti-PRMT6 and anti-HTT primary antibodies. This experiment revealed PRMT6 and HTT co-presence on the surface of vesicles (**Figure 21B**). Taken together, these findings demonstrate that PRMT6 is recruited on vesicles together with

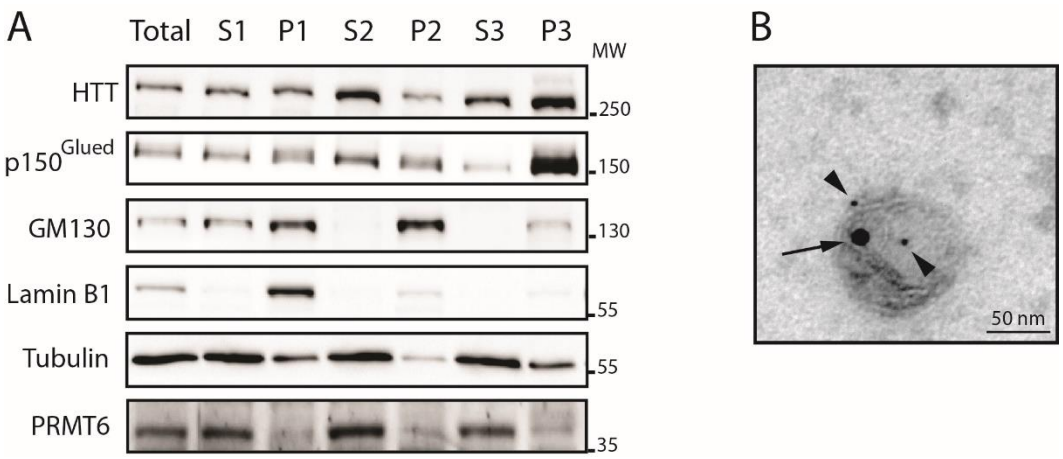

Figure 21: PRMT6 is present in brain-derived vesicles together with HTT. (A) Subcellular fractionation of mouse brain extracts showed that both HTT and PRMT6 are present in the small vesicles-rich fraction (P3). The fractions were analysed by immunoblotting for the presence of HTT, PRMT6, tubulin, laminB1 (nuclear marker, P1), GM130 (Golgi marker, P2) and p150^{Glued} (enriched in the P3 fraction). S1, S2 and S3 represent the corresponding cytosolic fractions. Shown is one experiment representative of three. **(B)** Immunogold transmission electron microscopy (TEM) analysis of the P3 fraction from (A) confirmed the presence of PRMT6 (15 nm Gold Nanoparticles, arrowhead) and HTT (5nm Gold Nanoparticles, arrow) in small vesicles isolated from mouse brains. Shown is one representative image from three independent experiments. Bar, 50 nm.

HTT, suggesting that PRMT6-mediated HTT methylation might influence vesicular transport along axons.

3.3 Arginine methylation of HTT regulates axonal trafficking

3.3.1 Loss of PRMT6-mediated R118 methylation impairs axonal trafficking of HTT-positive vesicles

HTT facilitates vesicular trafficking along axons by acting as a scaffold for key components of the molecular motor machinery, as described in the introduction (paragraph 1.1.2.2.1). Moreover, HTT phosphorylation at S421 modulates the directionality of axonal trafficking, favoring the anterograde movement of vesicles (Colin et al. 2008). Therefore, we wondered whether arginine methylation at R118 could also affect HTT-mediated vesicular transport. To test this hypothesis, we decided to monitor by live-cell imaging the axonal trafficking of HTT-positive vesicles in neurons expressing either wild-type HTT or the methylation-defective R118K HTT mutant.

For this purpose, I cloned HTT 548-17Q and the methylation-defective mutant in frame with mCherry in a lentiviral vector. HTT 548-17Q-mCherry and HTT 548-17Q R118K-mCherry are expressed at similar levels, as detected by immunoblotting, and displayed a similar subcellular localization in transduced cortical neurons (**Figure 22A,B**).

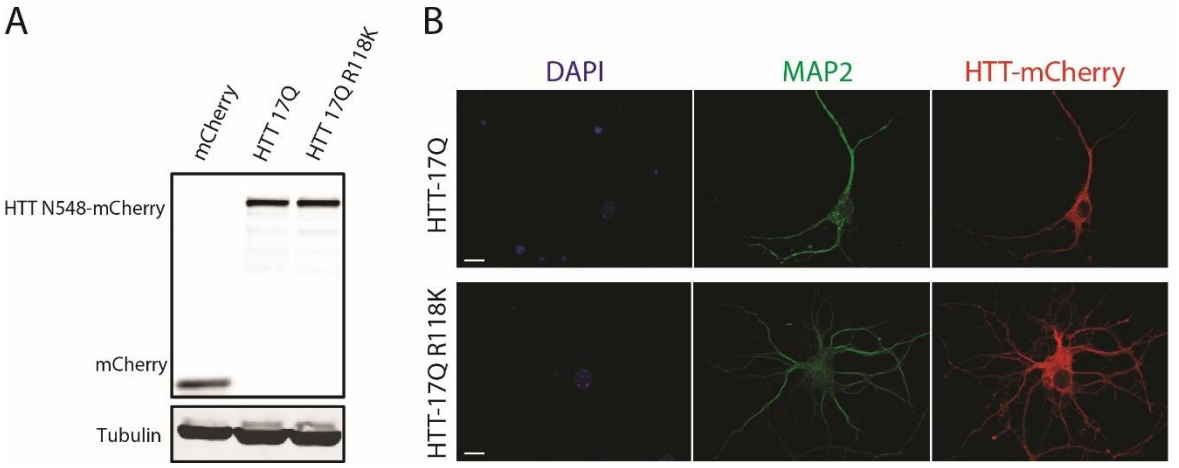

Figure 22: Expression of HTT 548-mCherry in primary cortical neurons. (A) Immunoblotting analysis showing similar levels of expression of mCherry-tagged HTT 548-17Q and HTT 548-17Q R118K in primary cortical neurons. **(B)** Immunocytochemical analysis of mCherry-tagged HTT 548-17Q and HTT 548-17Q R118K in DIV14 primary cortical neurons showed that the methylation-defective mutation does not change HTT subcellular localization. Bar, 10 µm.

Trafficking dynamics along the corticostriatal axis were analyzed using the microfluidic chamber described in Figure 19A, which is compatible with high-resolution videomicroscopy. I transduced cortical neurons plated in the microfluidic chambers with HTT 548-17Q-mCherry constructs and registered the trafficking of HTT-mCherry-positive vesicles in the distal part of axonal microchannels (pink area highlighted in **Figure 20A**) in order to avoid the contamination of both cortical and striatal dendrites, as depicted in **Figure 20A** and reported in Virlogeux et al 2018. Fast video acquisitions were performed at DIV14, when neurons in the microchambers are already organized in a mature network, with fully functional unilateral corticostriatal synapses (Virlogeux et al. 2018). These recordings showed reduced number of anterograde vesicles, decreased global linear flow rate and consequent abnormalities of the net directional flux (i.e. shift toward vesicular transport in the retrograde direction represented by negative values of directional flux) in neurons overexpressing the methylation-defective HTT-R118K mutant (**Figure 23A-C**).

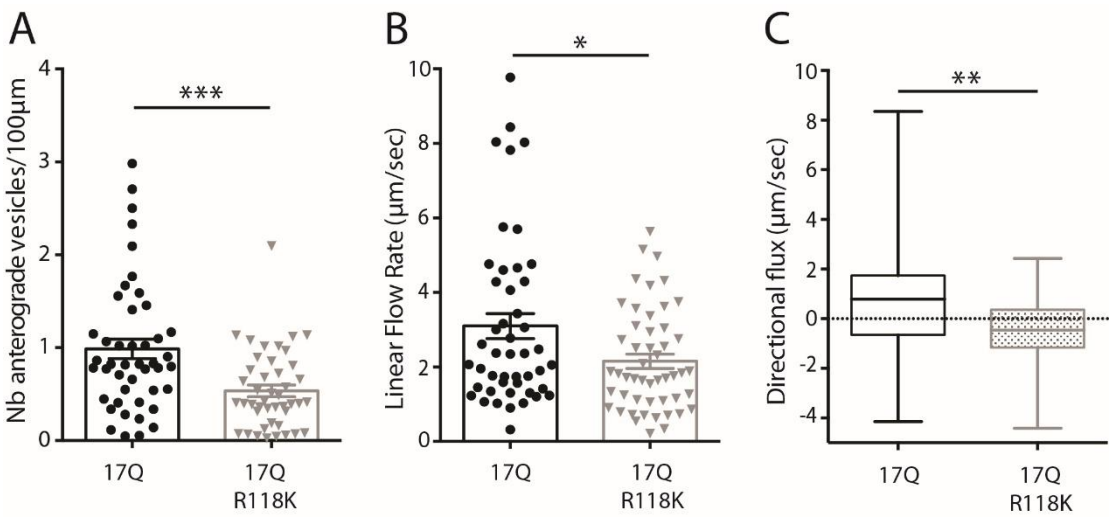

Figure 23: Loss of HTT methylation at R118 impairs axonal trafficking of HTT-positive vesicles. Analysis of the trafficking kinetics in DIV14 neurons transduced with lentiviral vectors expressing either wild-type HTT 548-17Q or HTT 548-17Q R118K fused to mCherry showed that loss of arginine methylation of HTT alters transport of vesicles along axons: **(A)** lowered number of anterograde vesicles, **(B)** decreased linear flow rate and **(C)** altered net directional flux. See paragraph 2.15 for the detailed description of trafficking parameters calculation. Graphs: mean ± SEM. Two-tailed non-parametric Mann-Whitney test, *p<0.05, ** p<0.01, *** p<0.001.

Representative kymographs showing the decrease in the number of anterograde vesicles in neurons expressing HTT 548-17Q R118K compared to control neurons transduced with HTT 548-17Q are reported in **Figure 24**. On the other hand, no significant variation was observed in the anterograde velocity, retrograde transport and in the cumulative distance travelled by vesicles (**Figure 25 and Figure 26**). These results suggest that HTT requires to be methylated at R118 to efficiently promote axonal transport in the anterograde direction.

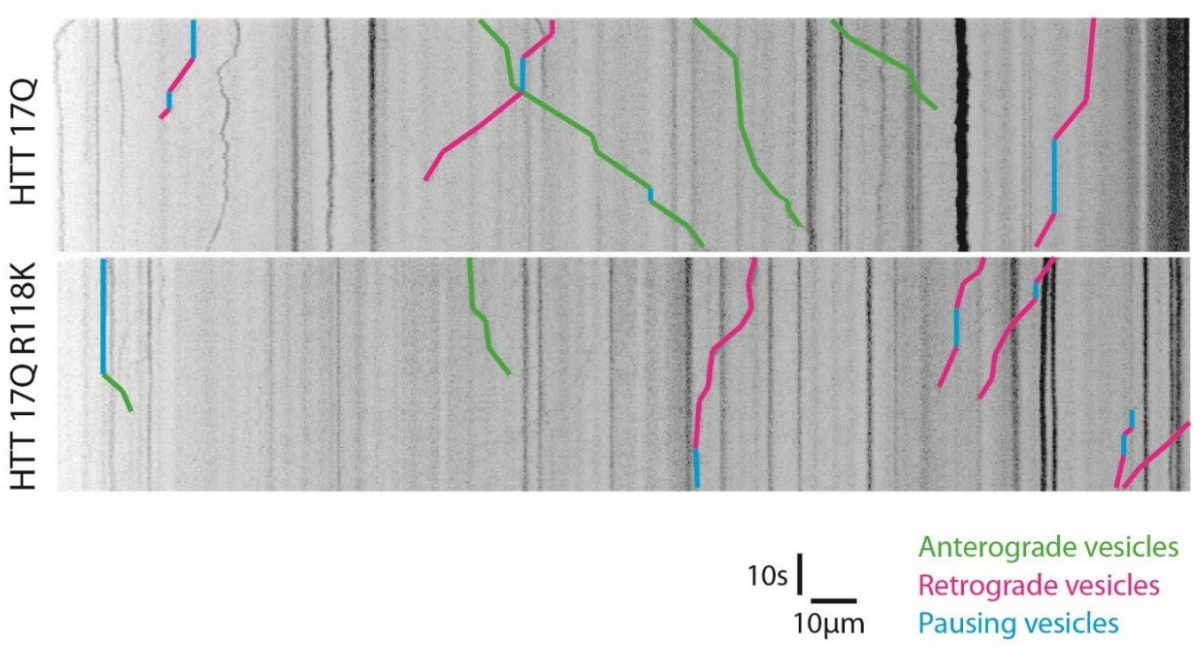

Figure 24: Kymographs depicting vesicle trafficking in neurons expressing wild-type HTT or HTT R118K. Representative kymographs showing decreased number of anterograde vesicles in neurons expressing HTT 548-17Q R118K compared to control neurons expressing HTT 548-17Q.

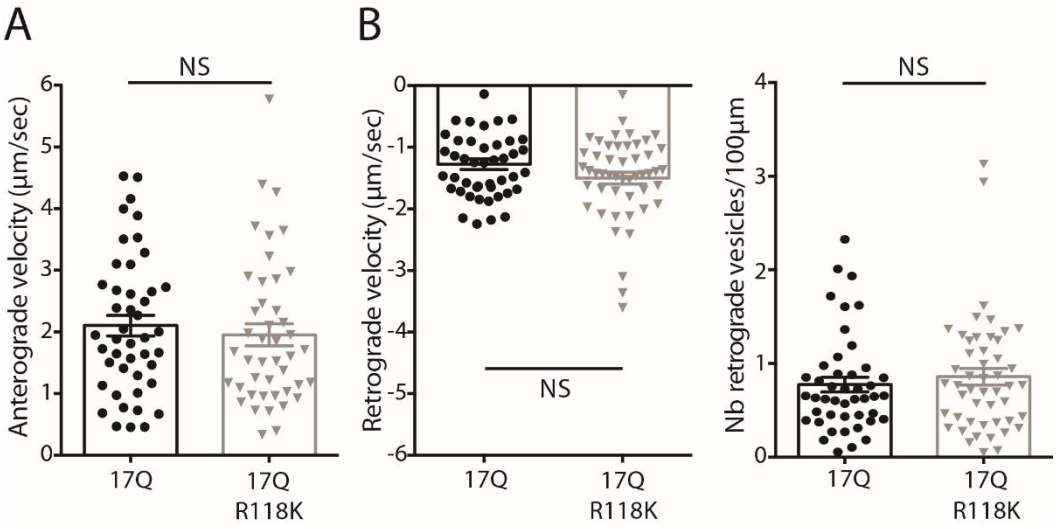

Figure 25: Loss of methylation at R118 does not affect anterograde velocity and retrograde trafficking. Analysis of the trafficking kinetics in DIV14 neurons transduced with lentiviral vectors expressing either wild-type HTT 548-17Q or HTT 548-17Q R118K fused to mCherry showed no significant alteration in anterograde velocity **(A)** and retrograde trafficking **(B)**. See paragraph 2.15 for the detailed description of trafficking parameters calculation. Graphs: mean ± SEM. Two-tailed non-parametric Mann-Whitney test, NS = not significant.

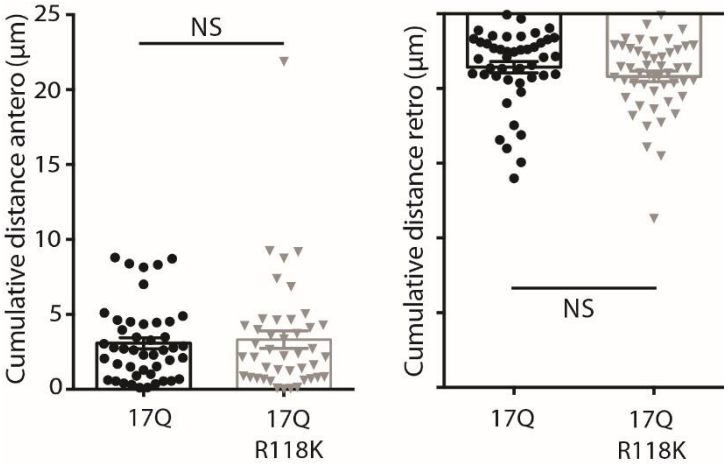

Figure 26: Loss of methylation at R118 does not modify the distance travelled by HTT-positive vesicles. Analysis of the trafficking kinetics in DIV14 neurons transduced with lentiviral vectors expressing either wild-type HTT 548-17Q or HTT 548-17Q R118K fused to mCherry showed no significant alteration in the cumulative distance travelled by HTT-positive vesicles. See paragraph 2.15 for the detailed description of trafficking parameters calculation. Graphs: mean ± SEM. Two-tailed non-parametric Mann-Whitney test, NS = not significant.

3.3.2 Loss of arginine methylation reduces the association of HTT with vesicles and causes toxicity in cortical neurons

Having shown that loss of HTT methylation at R118 impairs anterograde axonal transport, we hypothesized that the reduced efficiency of anterograde vesicular trafficking could be due to decreased interaction of HTT R118K with the motor proteins and consequent loss of HTT ability to coordinate the activity of the molecular motor machinery. To test this hypothesis, I transduced primary cortical neurons with lentiviral vectors expressing HTT 548-17Q-mCherry and HTT 548-17Q R118K-mCherry and analyzed the interaction of HTT with molecular motors by immunoprecipitation assay with an anti-mCherry antibody. As discussed in the introduction (paragraph 1.1.2.2.1), HTT interacts via HAP1 with kinesin-1 and the dynactin subunit $p150^{Glued}$, which are involved in anterograde and retrograde axonal transport, respectively. As expected, methylation-defective HTT interacts similarly to wild-type HTT with $p150^{Glued}$ (**Figure 27A**), consistently with the observation that the retrograde transport is not altered in neurons overexpressing HTT 548-17Q R118K (**Figure 25**). Surprisingly, despite the abnormalities observed in anterograde trafficking, I did not detect a defective interaction of HTT R118K with kinesin heavy chain (KHC) in the whole lysate nor in the vesicular fraction (**Figure 27A,B**). I then performed a subcellular fractionation of cortical neurons transduced with either HTT 548-17Q-mCherry or HTT 548-17Q R118K-mCherry followed by immunoblotting analysis and I observed that loss of arginine methylation at R118 reduced HTT recruitment to vesicles by 40% (**Figure 27C-D**). Taken together, these findings indicate that loss of arginine methylation does not alter the interaction of HTT with components of the molecular motor machinery, yet it reduces the presence of HTT in the vesicular fraction and causes a partial loss of normal HTT function in the regulation of axonal transport.

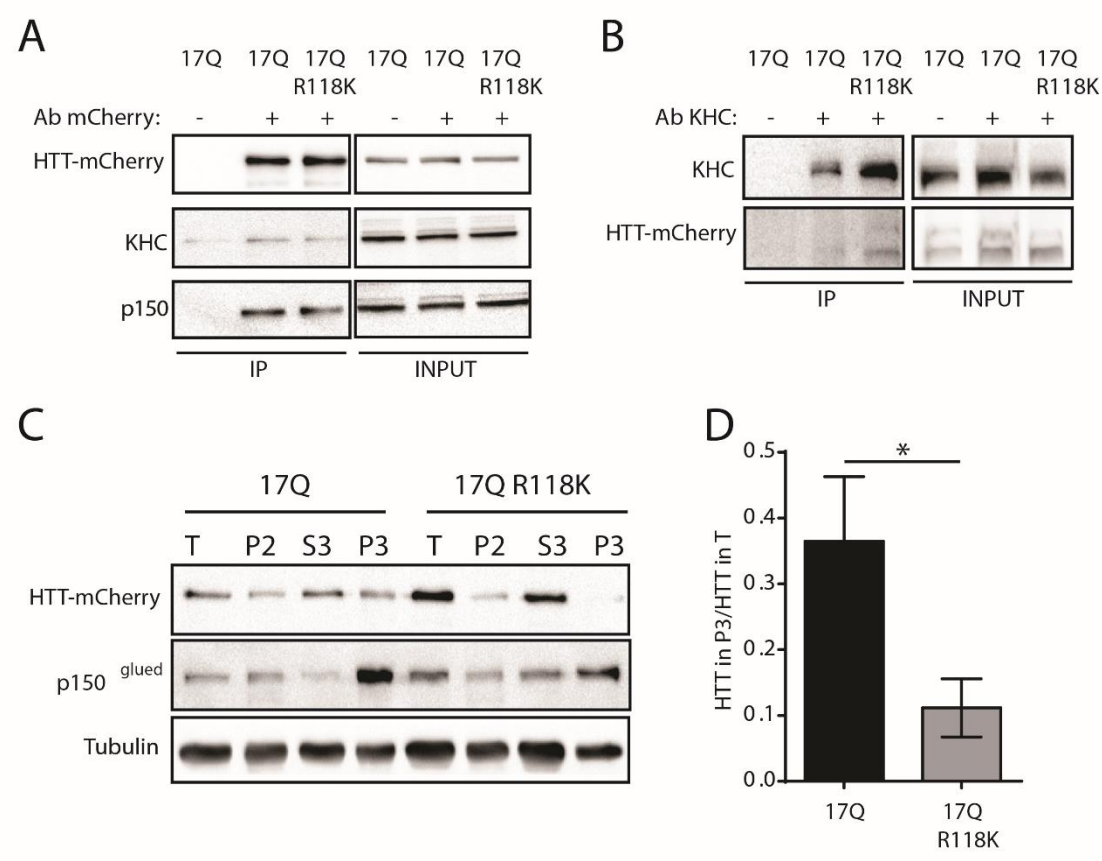

Figure 27: Loss of HTT methylation at R118 reduces the levels of vesicle-associated HTT.

(A) Immunoprecipitation (IP) assay in primary rat cortical neurons transduced with mCherry-tagged HTT N458-17Q or HTT 548-17Q R118K showed that methylation-defective R118K HTT preserves interaction with two components of the motor machinery, kinesin (KHC: Kinesin Heavy Chain) and $p150^{Glued}$. **(B)** IP assay in the small vesicle-rich fraction (P3) purified from cortical rat neurons transduced as in (A) showed that HTT R118K maintains the interaction with kinesin. **(C)** Immunoblotting analysis of subcellular fractionation of primary rat cortical neurons transduced as in (A) showed reduced presence of HTT-17Q R118K in the vesicular fraction (P3) compared to HTT-17Q. Shown is one experiment representative of three. **(D)** Quantification of HTT-548-mCherry signal in the P3 fraction over total fraction from (C). Graph: mean ± SEM, n=3. Student's t-test, *$p<0.05$.

Considering the central role played by axonal trafficking for the function and survival of neurons, we asked whether defects in vesicular trafficking correlated with neuronal toxicity. To address this question, I transduced primary cortical neurons with lentiviruses expressing either HTT 548-17Q-mCherry or HTT 548-17Q R118K-mCherry and measured cell viability. I quantified the number of mCherry-positive viable neurons at DIV11 with the Operetta High Content Imaging System (Tripathy et al. 2017). Interestingly, overexpression of HTT 548-17Q R118K reduced neuronal viability by almost 50% compared to control neurons, indicating that dysregulated trafficking of HTT-positive vesicles dramatically impacts neuronal survival (**Figure 28**). Of note, overexpression of PRMT6 together with the methylation-defective HTT mutant did not rescue cell death, proving that increased neuronal toxicity is specifically mediated by the loss of methylation at R118 (**Figure 28**).

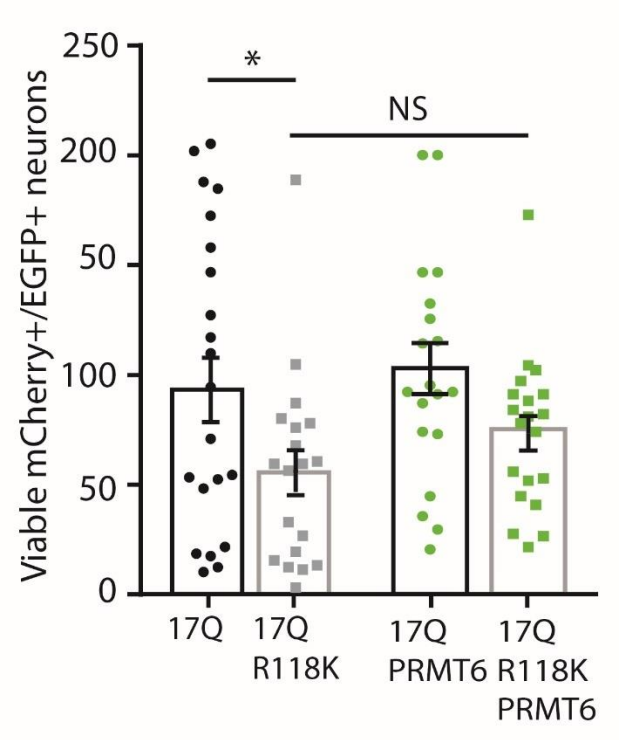

Figure 28: Loss of R118 methylation in HTT results in increased neuronal death. Analysis of cell viability in DIV11 mouse primary cortical neurons expressing HTT 548-17Q-mCherry or HTT 548-17Q R118K-mCherry showed that overexpression of the methylation defective HTT mutant results in increased cell death and that PRMT6 overexpression does not rescue the toxicity induced by HTT-17Q R118K. The total number of viable mCherry$^+$ neurons in each condition was calculated using the Operetta High-Content Imaging system. Graph: mean ± SEM, n=3. One-way ANOVA, Tukey's post hoc test, *p<0.05, NS = not significant.

3.4 HTT-PRMT6 interaction and R118 methylation are preserved upon polyglutamine expansion

3.4.1 PolyQ-expanded HTT interacts with PRMT6 and is methylated at R118

Expansion of polyglutamine tracts in proteins often causes aberrant protein-protein interactions as well as loss of interaction with native partners. We asked whether expansion of the polyQ stretch in HTT affects its interaction with PRMTs and HTT methylation at R118. To address this, first I co-expressed HTT 548 with 145 glutamine residues (HTT 548-145Q) together with EGFP or EGFP-tagged PRMT1-8 in HEK293T cells and analyzed HTT-PRMTs interaction by co-immunoprecipitation (co-IP) assay, as previously tested for wild-type HTT 548-17Q in **Figure 13A**. This experiment showed that also mutant N-terminal HTT interacts with PRMT2 and PRMT6 (**Figure 29**).

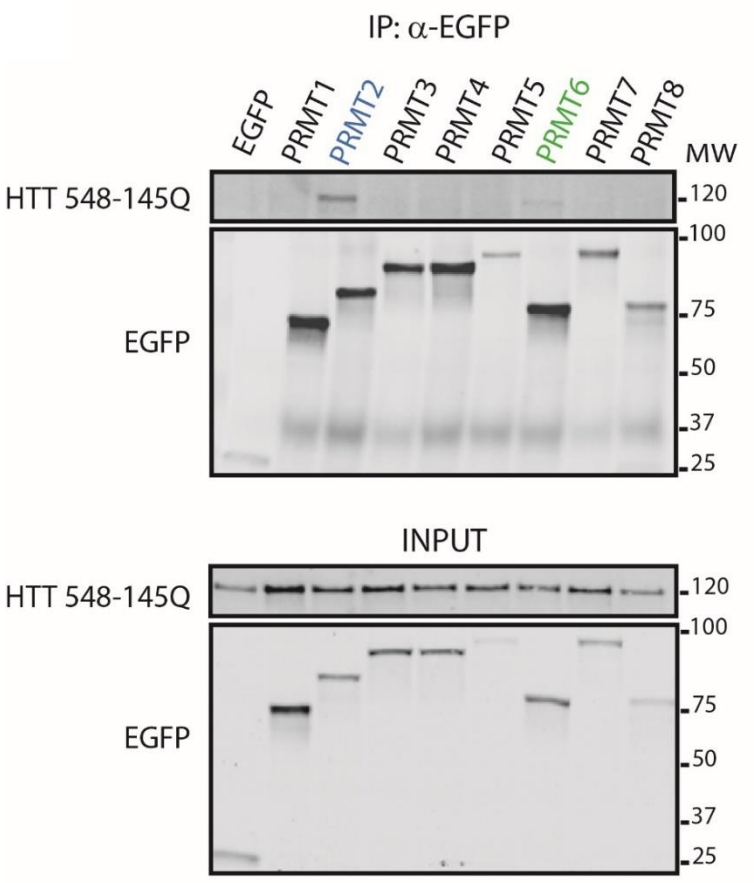

Figure 29: PolyQ-expanded N-terminal HTT interacts with PRMT2 and PRMT6. Co-IP assay in HEK293T cells overexpressing HTT 548-145Q together with soluble EGFP or EGFP-tagged PRMT1-8 showed that polyQ-expanded HTT interacts with PRMT2 and PRMT6. Shown is one experiment representative of three.

Similarly, full-length (FL) polyQ-expanded HTT retains the ability to bind PRMT2 and PRMT6, as shown by co-IP assay in striatal cells expressing HTT-111Q (STHdh$^{Q111/Q111}$) transfected with EGFP-tagged PRMTs (**Figure 30A**). These data were further validated by performing a PLA in STHdh$^{Q111/Q111}$ cells, which showed that the interaction of FL-HTT with PRMT2 and PRMT6 is maintained upon polyQ expansion (**Figure 30B**).

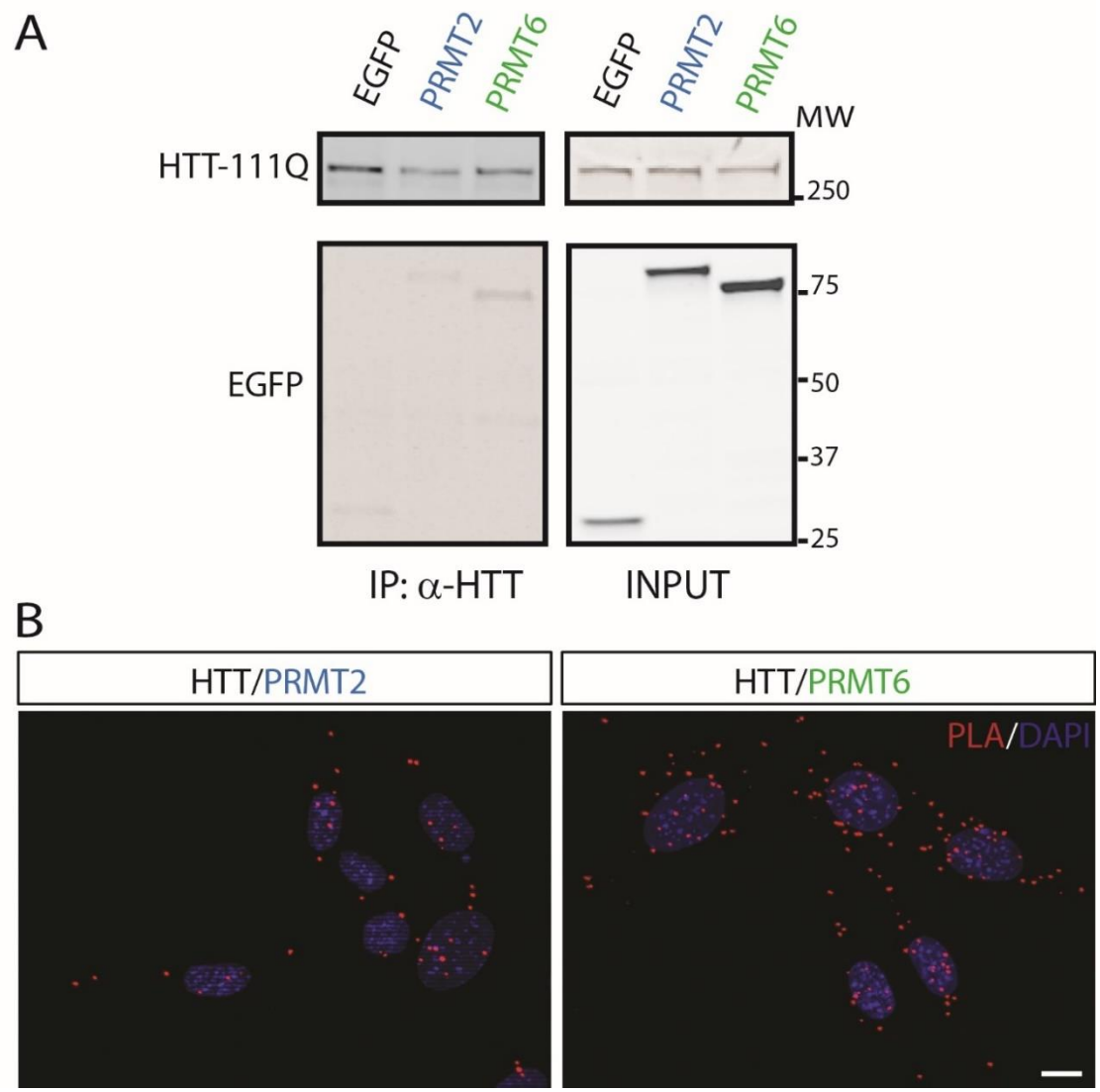

Figure 30: Full-length mutant HTT interacts with PRMT2 and PRMT6. (A) Co-IP assay in STHdh$^{Q111/Q111}$ cells overexpressing EGFP-PRMT2 or EGFP-PRMT6 showed interaction of FL polyQ-expanded HTT with PRMT2 and PRMT6. Shown is one experiment out of four**. (B)** PLA in STHdh$^{Q111/Q111}$ cells confirmed interaction between mutant FL-HTT and endogenous PRMT2 (left panel) and PRMT6 (right panel). The red dots indicate close proximity of HTT and the two PRMTs. Nuclei were revealed with DAPI. Shown are representative images from three independent experiments. Bar, 10 μm.

Next, to understand whether an expanded polyQ tract in HTT reduces its interaction with PRMTs with respect to a non-pathogenic polyQ tract, I compared the interaction between HTT 548-17Q, HTT 548-73Q and HTT 548-145Q with PRMT2 and PRMT6 by co-IP assay in HEK293T cells. Upon expansion of the polyQ tract to 73 glutamine residues, the ability of HTT to form a complex with PRMT2 and PRMT6 was decreased by 10 and 20%, respectively; further expansion to 145 glutamine residues decreased the interaction of HTT with PRMT2 and PRMT6 by 40 and 50%, respectively (**Figure 31**). This experiment indicates that, though not significant, a tendency to reduced HTT-PRMTs interaction is observed when HTT contains an expanded polyQ stretch, implying that a partial loss of PRMT6-mediated arginine methylation of HTT might be observed in the brain of HD mouse models and HD patients.

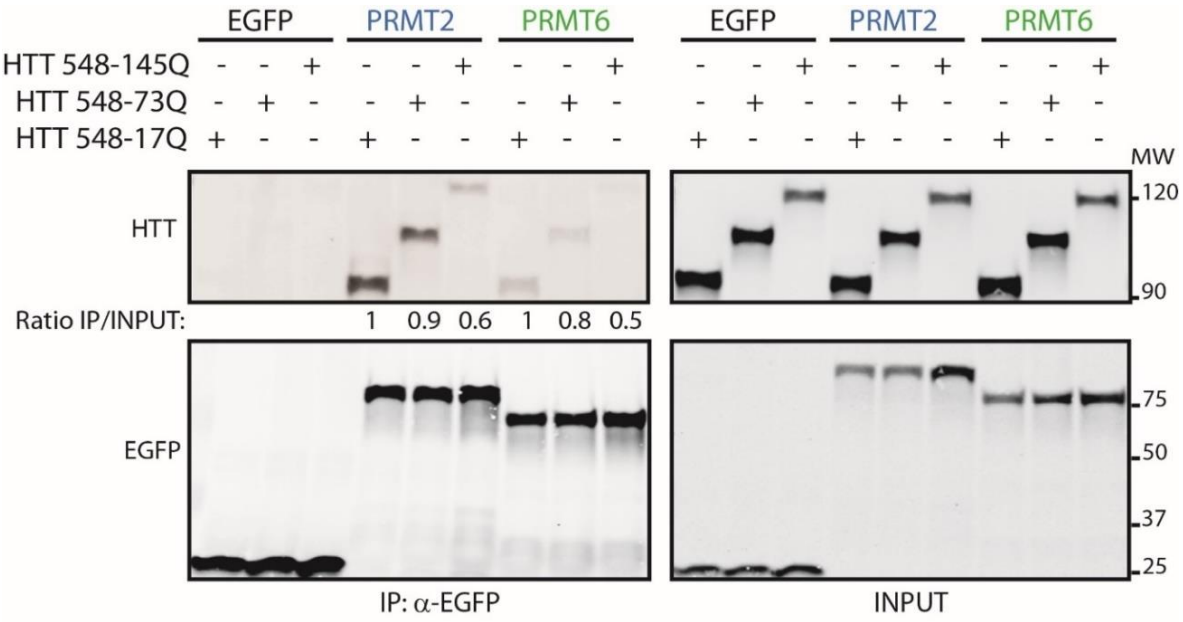

Figure 31: The polyQ expansion partially interferes with HTT-PRMTs interaction.
Co-IP assay in HEK293T cells overexpressing wild-type (HTT 548-17Q) or polyQ-expanded N-terminal HTT (HTT 548-73Q or HTT 548-145Q) together with soluble EGFP and EGFP-tagged PRMT2 or PRMT6 showed a tendency to decreased HTT-PRMTs interaction upon expansion of the polyQ tract. Shown is one experiment out of four. Quantification (average) of HTT IP/HTT input ratio is shown at the bottom of the IP panel.

After assessing that polyQ-expanded HTT retains the capacity of binding PRMT6, we wondered whether we could still detect dimethylation of R118 in mutant HTT. To test this, in collaboration with the laboratory of Christopher Ross we overexpressed full-length HTT-82Q in HEK293 cells and after HTT immunoprecipitation we performed mass spectrometry analysis. As shown in **Figure 32**, we found that polyQ-expanded HTT is dimethylated at R118, indicating that PRMT6 catalyzes methylation of both wild-type and mutant HTT.

Considering that I observed a tendency to decreased HTT-PRMTs interaction upon polyQ expansion, I decided to investigate whether there is a difference in the levels of R118 methylation in wild-type and polyQ-expanded HTT. To this aim, I obtained a specific antibody recognizing asymmetric dimethylation of R118 (R118me2a) from Biomatik and I performed immunoprecipitation experiments in HEK293T cells overexpressing N-terminal wild-type (HTT-548 17Q) or polyQ-expanded (HTT 548-73Q) HTT, using both anti-HTT and anti-R118me2a antibodies. Unfortunately, despite several attempts and troubleshooting steps, I did not manage to get a proper signal for specific R118 ADMA of HTT through immunoprecipitation and western blotting (data not shown in this thesis). Probably, the most suitable option to address whether arginine methylation of HTT is reduced upon polyglutamine expansion would be a quantitative mass spectrometry analysis of R118 methylation of wild-type and polyQ-expanded HTT, possibly immunopurified from the brain of healthy individuals and HD patients.

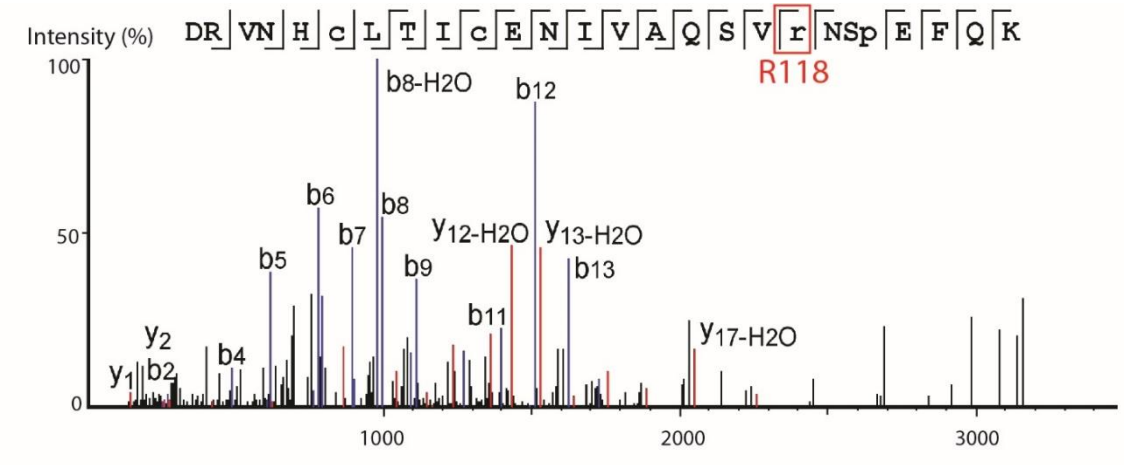

#	b	b-H2O	b-NH3	b (2+)	Seq	y	y-H2O	y-NH3	y (2+)	#
1	116.03	98.02	99.01	58.52	D					26
2	272.14	254.13	255.11	136.57	R	3059.51	3041.50	3042.49	1530.26	25
3	371.20	353.19	354.18	186.10	V	2903.41	2885.40	2886.39	1452.21	24
4	485.25	467.24	468.22	243.12	N	2804.35	2786.33	2787.32	1402.67	23
5	622.31	604.30	605.28	311.65	H	2690.30	2672.29	2673.28	1345.65	22
6	782.34	764.33	765.31	391.67	C(+57.02)	2553.24	2535.23	2536.22	1277.12	21
7	895.42	877.41	878.39	448.21	L	2393.21	2375.20	2376.19	1197.11	20
8	996.47	978.46	979.44	498.73	T	2280.13	2262.12	2263.10	1140.56	19
9	1109.55	1091.54	1092.53	555.28	I	2179.08	2161.07	2162.05	1090.04	18
10	1269.59	1251.57	1252.56	635.29	C(+57.02)	2066.00	2047.99	2048.97	1033.50	17
11	1398.63	1380.62	1381.60	699.81	E	1905.97	1887.97	1888.94	953.48	16
12	1512.67	1494.66	1495.65	756.83	N	1776.92	1758.92	1759.92	888.96	15
13	1625.76	1607.74	1608.73	813.38	I	1662.88	1644.88	1645.87	831.94	14
14	1724.82	1706.81	1707.79	862.91	V	1549.80	1531.79	1532.77	775.40	13
15	1795.86	1777.85	1778.83	898.44	A	1450.73	1432.72	1433.70	725.86	12
16	1923.92	1905.91	1906.89	962.46	Q	1379.69	1361.68	1362.68	690.35	11
17	2010.95	1992.94	1993.92	1005.97	S	1251.63	1233.62	1234.63	626.29	10
18	2110.02	2092.01	2092.99	1055.51	V	1164.59	1146.59	1147.57	582.80	9
19	2294.15	2276.14	2277.12	1147.57	R(+28.03)	1065.53	1047.52	1048.51	533.27	8
20	2408.19	2390.18	2391.17	1204.60	N	881.40	863.42	864.37	441.20	7
21	2495.22	2477.21	2478.20	1248.11	S	767.36	749.35	750.33	384.18	6
22	2624.27	2606.26	2607.24	1312.63	P(+31.99)	680.32	662.31	663.30	340.66	5
23	2753.31	2735.30	2736.28	1377.15	E	551.28	533.27	534.26	276.13	4
24	2900.38	2882.37	2883.35	1450.69	F	422.24	404.23	405.21	211.62	3
25	3028.44	3010.43	3011.41	1514.72	Q	275.17	257.16	258.14	138.09	2
26					K	147.11	129.10	130.09	74.06	1

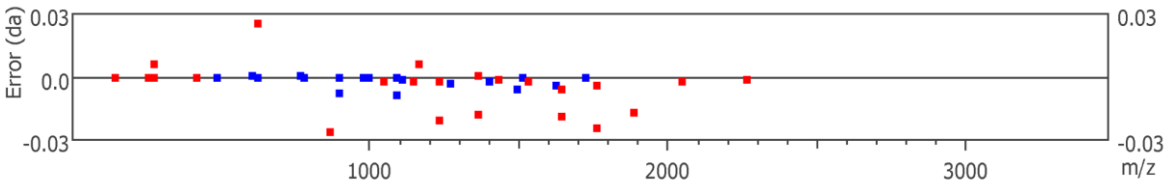

Figure 32: PolyQ-expanded HTT is dimethylated at R118 in cells. ESI-MS/MS tandem mass spectra of indicated dimethylated peptide produced by LysC in-gel digestion of full-length HTT-82Q purified from transfected HEK293 cells, followed by MS/MS. The tables of predicted fragmentation ions show blue and red highlighted masses present in the spectra within 0.03 Da, as shown in the lower panels below the table.

3.4.2 PRMT6 is equally expressed in the brain of wild-type and HD mice

We found that loss of HTT arginine methylation leads to axonal transport defects and increased susceptibility to neuronal death. We then wondered whether the expression of PRMT6 is altered in HD. Indeed, reduced PRMT6 expression would lead to decreased methylation of HTT at R118 and vesicular trafficking defects that might contribute to HD pathogenesis and neurodegeneration. To address this, first I measured PRMT6 mRNA transcript and protein levels in STHdh$^{Q111/Q111}$ cells compared to STHdh$^{Q7/Q7}$ and found that both PRMT6 transcript and protein levels were similar in STHdh$^{Q7/Q7}$ and STHdh$^{Q111/Q111}$ striatal cells (**Figure 33A, B**). Second, I validated this data by analyzing PRMT6 protein expression in the whole brain and cortex of Hdh$^{CAG140/+}$ mice compared to wild-type age-matched mice by western blotting. Hdh$^{CAG140/+}$ knockin mice heterozigously express full-length *HTT* with a humanized exon 1 bearing 140 CAG repeats (Menalled et al. 2002). Consistently with the results obtained in striatal cells, PRMT6 was equally expressed in 2 months- and 6 months-old mutant and control mice (**Figure 34A-F**). These results indicate that PRMT6 expression is not dysregulated in cells and murine tissues expressing polyQ-expanded HTT. Ongoing experiments in post-mortem human brain samples will assess whether PRMT6 is differentially expressed in HD patients compared to healthy individuals.

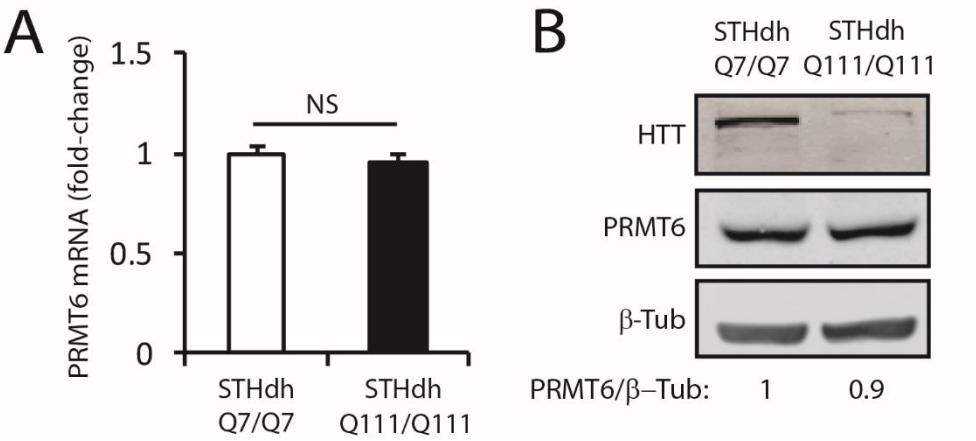

Figure 33: Analysis of PRMT6 expression in striatal cells. PRMT6 is equally expressed in STHdh$^{Q7/Q7}$ and STHdh$^{Q111/Q111}$ cells as shown by RT-PCR analysis **(A)** and western blotting **(B)**. Student's t-test, NS = not significant.

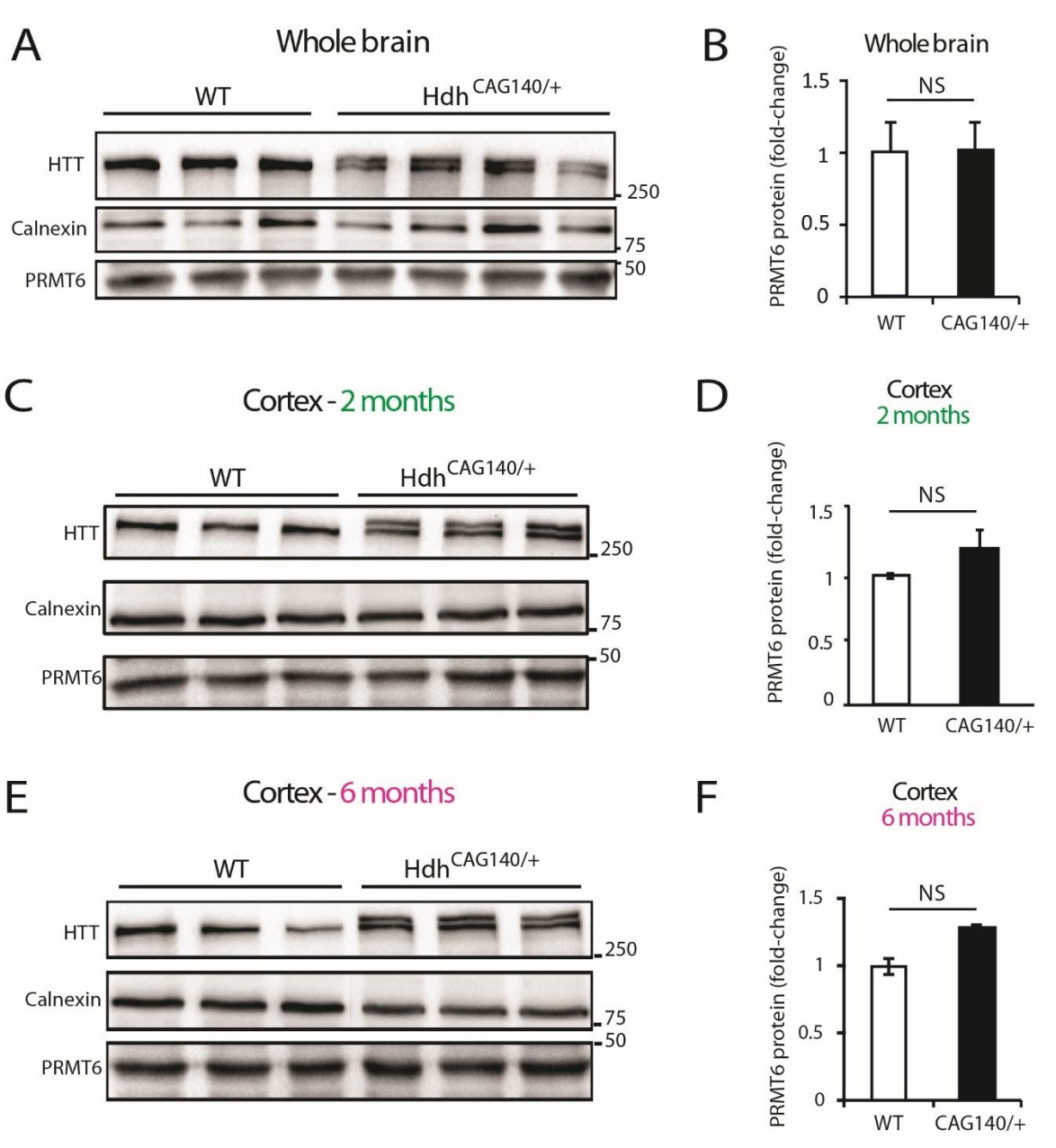

Figure 34: PRMT6 is equally expressed in the brain of WT and HD mice. Immunoblot analysis of PRMT6 expression in the whole brain **(A)** of 2 months old mice and in the cortex of 2 months **(C)** and 6 months **(E)** old mice showed no difference in PRMT6 expression levels between WT and $CAG^{140/+}$ mice. (**B**) (**D**) and (**F**) Quantification of A) (C) and (E), respectively. Graphs: mean ± SEM. Student's t-test, NS = not significant.

3.5. PRMT6 is a novel modifier of mutant-HTT induced toxicity

3.5.1 Inhibition of arginine methylation enhances polyQ-expanded HTT toxicity

We found that HTT is methylated at R118 by PRMT6 in the brain and that loss of arginine methylation of wild-type HTT results in impaired anterograde axonal trafficking and neuronal toxicity. Next, I sought to assess the biological relevance of arginine methylation in HD pathogenesis. First, I tested whether loss of PRMT function modifies polyQ-expanded HTT-induced toxicity. As expected, in normal conditions STHdh$^{Q111/Q111}$ cells showed a 27% decrease in cell viability compared to STHdh$^{Q7/Q7}$ cells (**Figure 35A**). Treatment with the two pan PRMT inhibitors adenosine-2′,3′-dialdehyde (Adox) and methylthioadenosine (MTA), further decreased the viability of STHdh$^{Q111/Q111}$ cells by 17% and 13%, respectively (**Figure 35B**). Both PRMT2 and PRMT6 are class I PRMTs that catalyze the formation of monomethylarginine and asymmetric dimethylarginine. Notably, treatment of the cells with a class I PRMT selective inhibitor, namely MS023 (Eram et al. 2016), reduced STHdh$^{Q111/Q111}$ viability by 39% compared to cells treated with the negative control compound MS094 (vehicle) (**Figure 35B**).

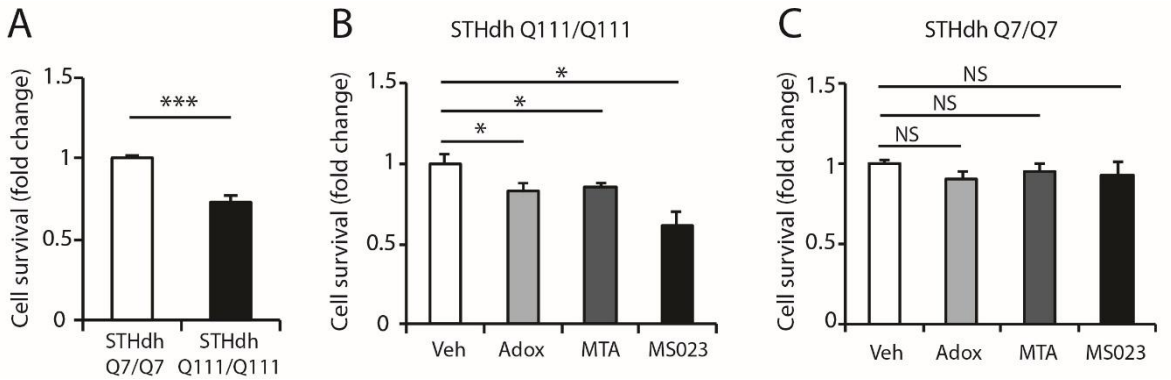

Figure 35: Inhibition of arginine methylation decreases survival in mutant HTT-expressing cells. **(A)** Cell survival analysis of untreated STHdh$^{Q7/Q7}$ and STHdh$^{Q111/Q111}$ cells. **(B)** Cell survival analysis in STHdh$^{Q111/Q111}$ cells treated with general inhibitors of methyltransferase activity (MTA and Adox) or a specific type I PRMTs inhibitor (MS023) showed exacerbation of mutant HTT-induced toxicity upon downregulation of arginine methylation. **(C)** Cell survival analysis in STHdh$^{Q7/Q7}$ cells showed no significant change in cell survival upon treatment with arginine methylation inhibitors. Graphs: mean ± SEM, n=3. One-way ANOVA, Newman-Keuls post-hoc test, *p<0.05, ***p<0.001, NS = not significant.

Neither Adox, MTA, nor MS023 treatment modified the viability of STHdh$^{Q7/Q7}$ cells (**Figure 35C**). These results indicate that loss of arginine methyltransferase function does not *per se* modify the viability of striatal cells expressing wild-type HTT, yet it exacerbates toxicity in striatal cells expressing polyQ-expanded HTT.

3.5.2 PRMT6 downregulation reduces the survival of striatal cells expressing polyQ-expanded HTT

To determine whether specific modulation of PRMT6 function impacts the toxicity of polyQ-expanded HTT, I undertook both a loss-of-function and a gain-of-function approach in striatal cells expressing wild-type and polyQ-expanded HTT. To silence PRMT6 expression in striatal cells, I transduced the cells with lentiviral vectors expressing either a scramble shRNA or an shRNA against PRMT6 and established single-cell clones by serial dilutions and antibiotic selection. By RT-PCR and western blotting I verified that the shRNA against PRMT6 decreased mRNA transcript levels by about 45-to-80% and the protein level of about 50% in both cell lines (**Figure 36A,B**). Knock-down of PRMT6 reduced cell survival by 47% in STHdh$^{Q111/Q111}$ cells, and to a lower extent (27%) in STHdh$^{Q7/Q7}$ cells (**Figure 36C**). The reduced cell viability observed in STHdh$^{Q7/Q7}$ cells upon targeted silencing of PRMT6 is consistent with the increased neuronal toxicity caused by the methylation-defective R118K mutation in wild-type HTT (**Figure 28**). HTT also interacts with PRMT2, though I didn't detect methylation of HTT by PRMT2 at R101 nor at R118. Interestingly, specific PRMT2 silencing did not modify cell survival in striatal cells (**Figure 37**), suggesting that the PRMT6-mediated modulation of mutant HTT-induced toxicity involves direct methylation of HTT at R118.

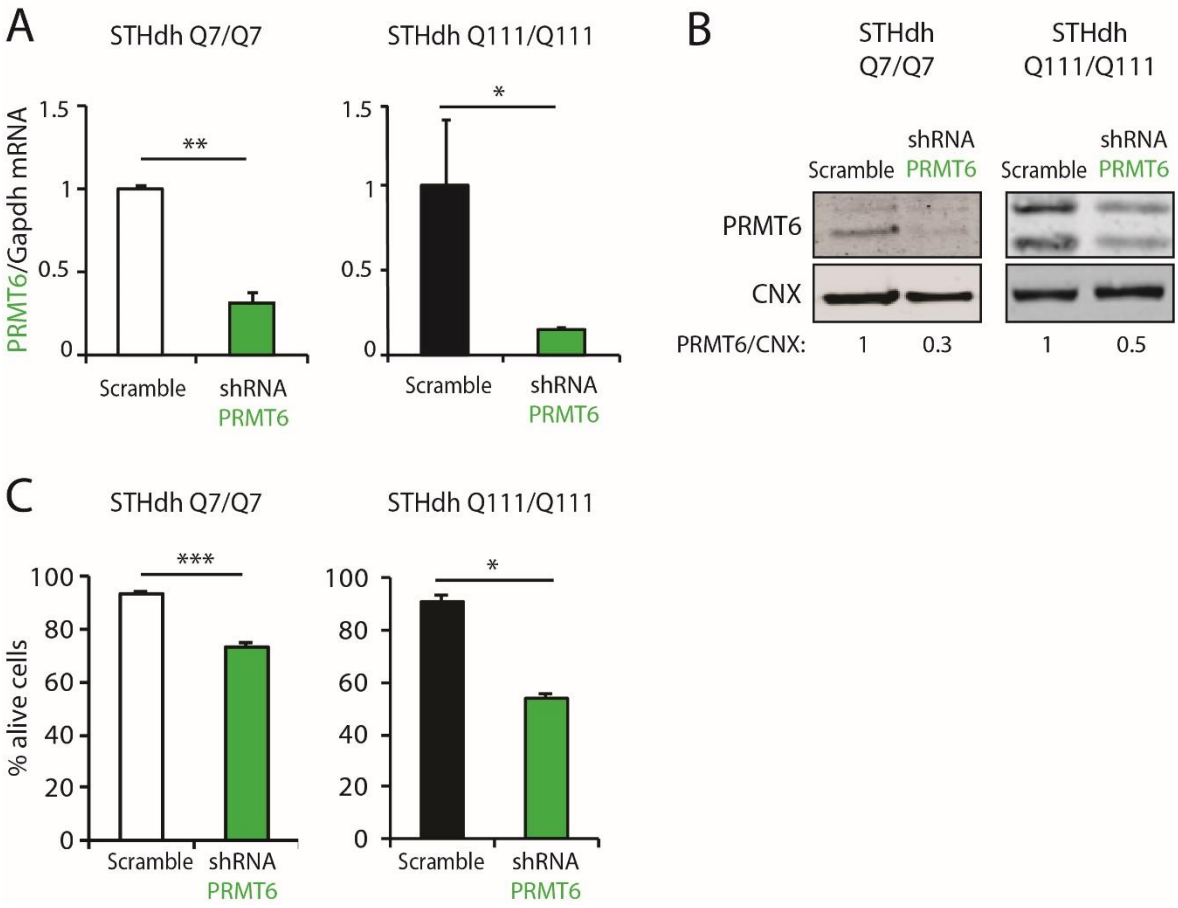

Figure 36: PRMT6 silencing enhances cell death in striatal cells. (A) RT-PCR analysis of PRMT6 transcript levels in single cell clones expressing an shRNA against PRMT6. Graph: mean ± SEM, n=3. **(B)** Immunoblotting analysis of PRMT6 protein levels in single cell clones stably expressing a scramble shRNA or an shRNA against PRMT6. **(C)** Live/dead assay in STHdh$^{Q7/Q7}$ and STHdh$^{Q111/Q111}$ single cell clones stably expressing a scramble shRNA or an shRNA against PRMT6 showed reduced percentage of alive cells upon specific PRMT6 silencing. Graph: mean ± SEM, n=3. Student's t-test, *p<0.05, **p<0.01, ***p<0.001.

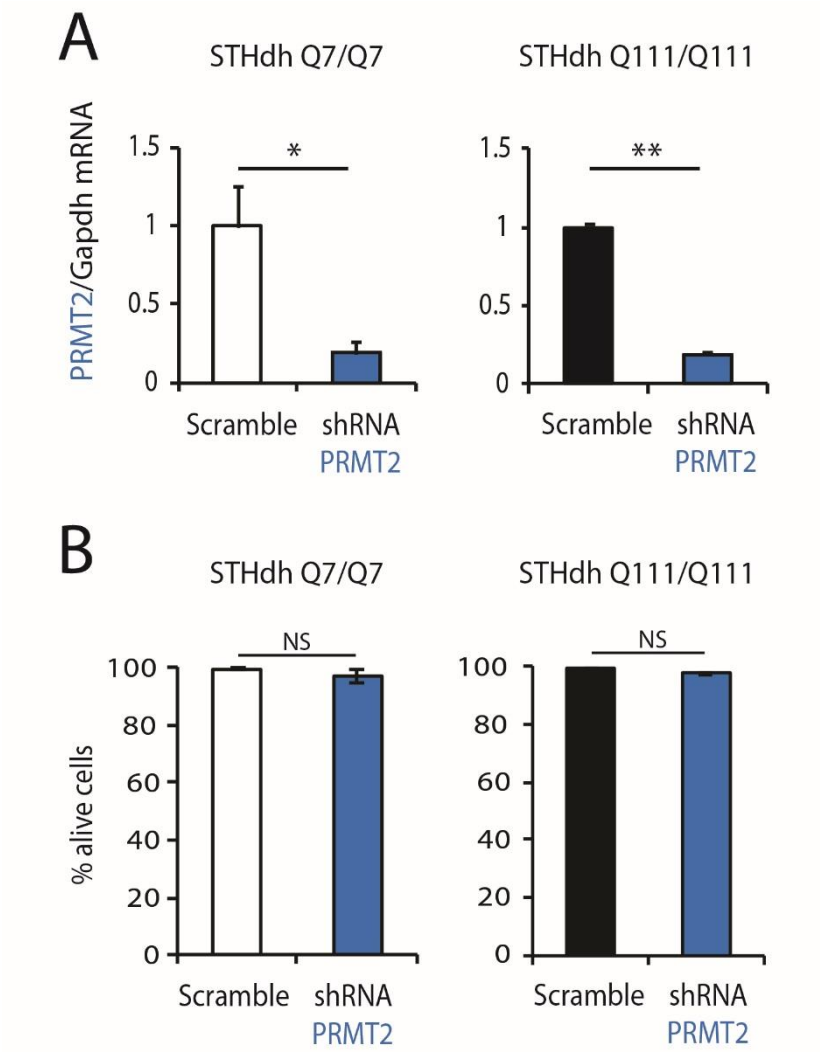

Figure 37: PRMT2 downregulation does not affect cell survival of striatal cells. (A) RT-PCR analysis of PRMT2 transcript levels in single cell clones expressing a scramble shRNA or an shRNA against PRMT2. Graph: mean ± SEM, n=3. **(B)** Live/dead assay in STHdh$^{Q7/Q7}$ and STHdh$^{Q111/Q111}$ single cell clones stably expressing a scramble shRNA or an shRNA against PRMT2 showed no significant change in cell survival upon specific PRMT2 silencing. Graph: mean ± SEM, n=3. Student's t-test, *p<0.05, **p<0.01, NS = not significant.

On the other hand, overexpression of PRMT6 in striatal cells had the opposite effect, leading to a modest increase in cell survival in both STHdh$^{Q7/Q7}$ and STHdh$^{Q111/Q111}$ cells (**Figure 38A,B**). Taken together, these results indicate that PRMT6 modifies the toxicity of polyQ-expanded HTT in striatal cells.

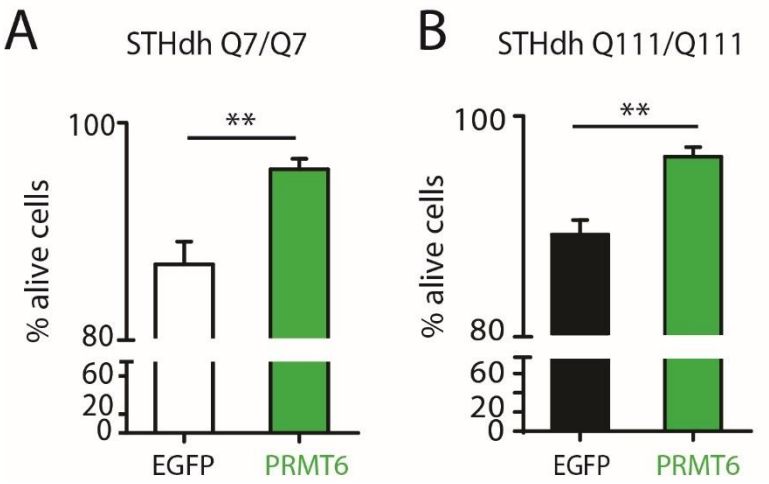

Figure 38: PRMT6 overexpression promotes cell survival in striatal cells. Live/dead assay in STHdh$^{Q7/Q7}$ **(A)** or STHdh$^{Q111/Q111}$ **(B)** cells transfected with EGFP or EGFP-PRMT6 showed that PRMT6 overexpression increases viability in wild-type and mutant HTT-expressing cells. Graph: mean ± SEM, n=6. Student's t-test, **p<0.01.

3.5.3 PRMT6 overexpression rescues expanded HTT-induced toxicity in neurons

To test whether PRMT6 overexpression reduces toxicity in HD, I cultured primary cortical neurons and co-transduced them with lentiviruses expressing mCherry-tagged polyQ-expanded HTT with 73 glutamine residues (HTT 548-73Q-mCherry) (**Figure 39A**) and lentiviral vectors expressing EGFP or EGFP-PRMT6 (not shown). I fixed the cells at DIV11 and I quantified the number of mCherry-positive alive neurons, as previously described (Figure 26). As expected, the expression of HTT 548-73Q reduced neuronal viability of almost 40% compared to HTT 548-17Q (represented by the dotted line in the graph) and most importantly, the overexpression of PRMT6 rescued neuronal death (**Figure 39B**). I also tested the effect of the expression of methylation-defective polyQ-expanded HTT (HTT 548-73Q R118K-mCherry) on neuronal viability (**Figure 39A**). As shown in **Figure 39B**, the expression of HTT 548-73Q R118K induced toxicity similarly to HTT 548-73Q, but importantly the overexpression of PRMT6 failed to rescue neuronal death, suggesting that methylation of HTT at R118 is necessary to mediate neuronal survival. Altogether, these findings

pose arginine methylation as a novel PTM that modulates mutant-HTT induced neurotoxicity and suggest that promoting PRMT6-mediated arginine methylation of HTT could be of therapeutic interest for the treatment of HD.

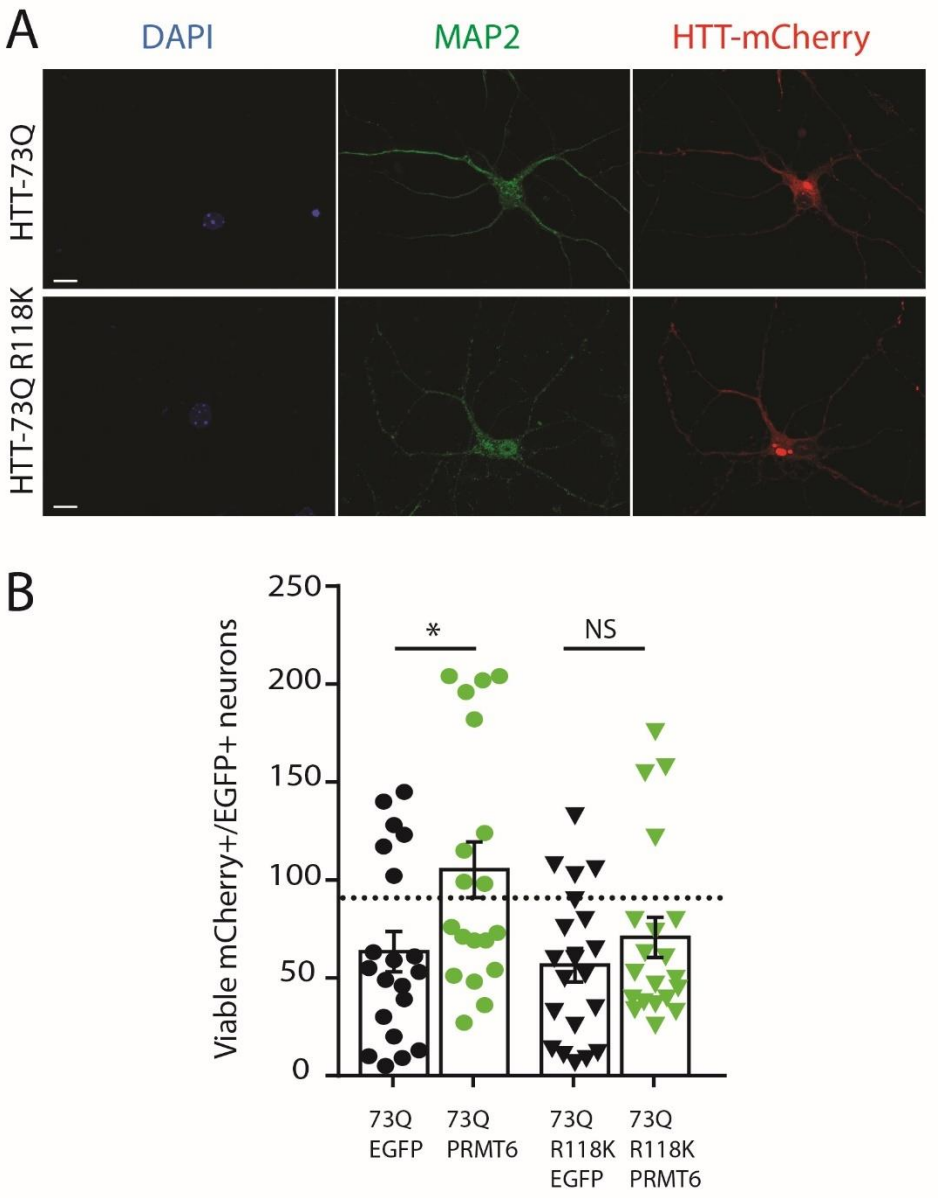

Figure 39: PRMT6 overexpression rescues cell death in mutant HTT-expressing neurons. (A) Immunocytochemical analysis showing expression and subcellular localization of mCherry-tagged HTT 548-73Q and HTT 548-73Q R118K in DIV14 primary cortical neurons. Bar, 10 µm. **(B)** Analysis of cell viability in mouse primary cortical neurons expressing mCherry-tagged HTT 548-73Q or HTT 548-73Q R118K together with EGFP or EGFP-PRMT6 showed that PRMT6 overexpression rescues toxicity caused by HTT-73Q but not methylation-defective HTT-73Q R118K. The total number of viable $mCherry^+/EGFP^+$ neurons in each condition was calculated using the Operetta High-Content Imaging system. The dotted line indicates the number of viable control neurons overexpressing HTT 548-17Q reported in the graph in Figure 28. Graph: mean ± SEM, n=4. Two-way ANOVA, Tukey's post hoc test *$p<0.05$, NS = not significant.

3.5.4 PRMT6 upregulation increases axonal trafficking efficiency in neurons expressing polyQ-expanded HTT

The results described above show that PRMT6 silencing exacerbates mutant HTT-induced toxicity, whereas PRMT6 overexpression rescues toxicity in neurons expressing polyQ-expanded HTT. Moreover, the beneficial effect of PRMT6 overexpression seems to be specifically mediated by HTT methylation at R118, since PRMT6 fails to rescue cell death in neurons expressing the methylation-defective HTT R118K mutant. This led us to hypothesize that an improvement of vesicular trafficking along axons could underlie the decreased susceptibility to neuronal death.

To test this hypothesis, I plated primary cortical and striatal neurons in microfluidic chambers and transduced them as described for the viability assay in Figure 37. At DIV14 axonal trafficking dynamics of mCherry-positive vesicles were analyzed through live-cell recordings as previously described in paragraph 3.3.1. PRMT6 overexpression in neurons transduced with HTT 548-73Q-mCherry significantly improved the efficiency of axonal trafficking in the anterograde direction, represented by the shift toward positive values of the net directional flux (**Figure 40A**). On the contrary, no significant change in the net flux of mCherry-positive vesicles was observed in neurons expressing HTT 548-73Q R118K-mCherry upon PRMT6 overexpression. This result correlates with the observation that PRMT6 does not rescue polyQ-expanded HTT-induced neuronal death when R118 is substituted by a lysine (**Figure 39B**). Of note, subcellular fractionation of cortical neurons overexpressing HTT 548-73Q-mCherry together with EGFP-tagged PRMT6 showed that in our experimental conditions EGFP-PRMT6 accumulated in the small vesicle-rich fraction (P3) (**Figure 40B**), suggesting that the rescue in neuronal viability and the improved efficiency of anterograde axonal transport is mediated by an enrichment of PRMT6 in the vesicular fraction and direct methylation of HTT at R118, which may happen *in situ* in the axoplasm or on the surface of vesicles.

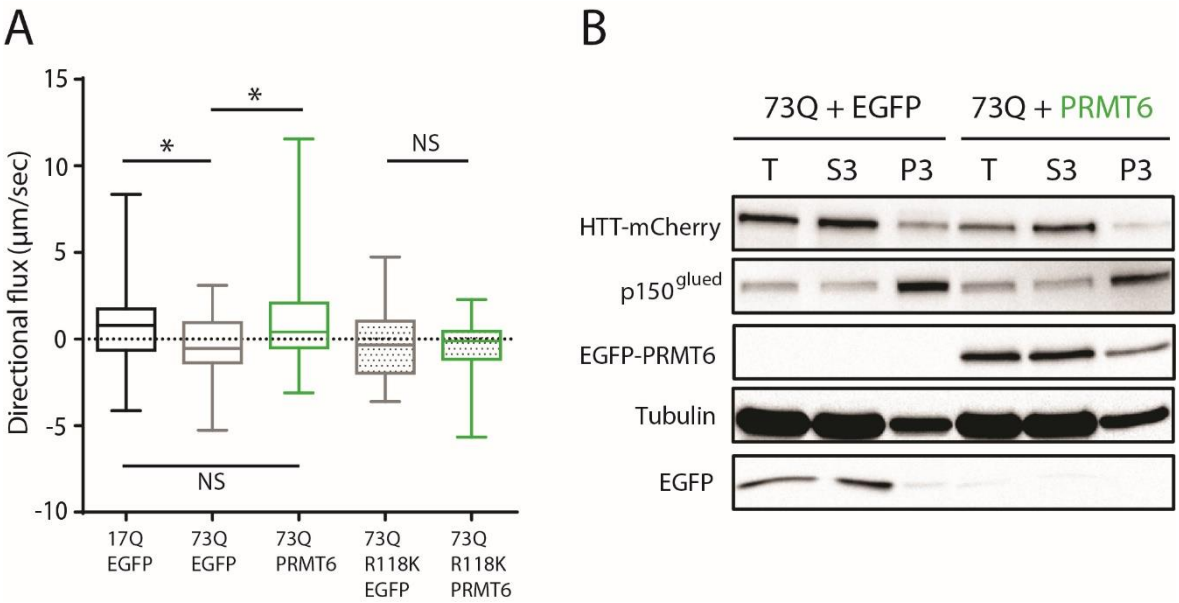

Figure 40: PRMT6 overexpression promotes anterograde axonal trafficking in neurons expressing polyQ-expanded HTT. (A) Analysis of the trafficking kinetics in DIV14 neurons transduced with lentiviral vectors expressing mCherry-tagged HTT 548-73Q or HTT 548-73Q R118K together with EGFP or EGFP-PRMT6 showed that upregulation of PRMT6 promotes anterograde vesicular trafficking. See paragraph 2.15 for the detailed description of directional flux calculation. Graph: mean ± SEM, n=3. Kruskal-Wallis test, Dunn's post hoc, *p<0,05, NS = not significant. **(B)** Immunoblotting analysis of subcellular fractionation of primary rat cortical neurons transduced with polyQ-expanded HTT (HTT 548-73Q-mCherry) together with EGFP or EGFP-PRMT6 showed that, in our experimental conditions, overexpressed EGFP-tagged PRMT6 is found in the vesicular fraction (P3). Shown is one representative experiment out of three.

4. Discussion

Arginine methylation of proteins involved in neurodegeneration has been recently identified as a critical modifier of disease pathogenesis, yet its role in HD is still unexplored. This work provides the first evidence that HTT is methylated at arginine residues and that this PTM modulates the native function of wild-type HTT and the toxicity elicited by mutant HTT. I showed that vesicle-associated HTT is methylated *in vivo* at two evolutionarily conserved residues, R101 and R118, and that methylation of R118 is catalyzed by PRMT6. PRMT6 colocalizes with HTT in the axon of cortical neurons and is recruited on vesicles. Interestingly, loss of R118 methylation impairs HTT-mediated anterograde axonal trafficking and exacerbates polyQ-expanded HTT toxicity. Conversely, PRMT6 overexpression improves the global efficiency of anterograde axonal transport and rescues cell death in neurons expressing polyQ-expanded HTT. These findings establish a role for arginine methylation as a novel modifier of HD pathogenesis and suggest that stimulation of HTT methylation might represent a new therapeutic strategy for HD.

4.1 Huntingtin is methylated at arginines

HTT is highly post-translationally modified and several PTMs are crucial for their impact on the activity of both normal and mutant HTT. Arginine methylation is one of the most abundant PTMs in mammalian cells; however, arginine methylation of HTT has not been described yet. Interaction of HTT with PRMT5 has been reported by Ratovitski and colleagues (Ratovitski et al. 2015), but it remains unclear whether HTT is itself a substrate for PRMTs. Recently, arginine methylation at the Akt consensus site (RXRXX[S/T]) of another polyglutamine protein, androgen receptor (AR), has been described as a key PTM that modulates SBMA pathogenesis (Scaramuzzino et al. 2015). The presence of two Akt consensus sites in HTT (^{416}**R**S**R**SGS^{421}; ^{2063}**R**F**R**LST^{2068}) prompted us to investigate whether HTT is methylated at these and/or other arginine residues.

We show for the first time that HTT is dimethylated *in vivo* at two arginines, R101 and R118, located in the N-terminal region. This is consistent with the observation that most of the known HTT interactors bind the N-terminus region of the protein, owing

to the peculiar three-dimensional structure of HTT (Guo et al. 2018). Surprisingly, we did not detect methylation at the Akt consensus sites of HTT. This could be due to technical issues (e.g. resolution) of the mass spectrometry analysis and also to our specific experimental setup. We chose to analyze arginine methylation of vesicle-associated HTT because of its critical role in the regulation of axonal trafficking and its high abundance in the brain vesicular fraction. HTT could be methylated at the arginines contained in the Akt consensus sites by PRMTs that do not localize in the axon or on vesicles, and methylation of those arginines might not be detectable by mass spectrometry analysis of HTT immunopurified from the vesicular fraction. Therefore, we cannot exclude arginine methylation of HTT at the Akt consensus sites or other arginine residues, and further analyses of HTT PTMs in whole cell lysates are required to address this.

I found that wild-type HTT interacts with several PRMTs. The strongest affinity has been observed for two class I PRMTs, namely PRMT2 and PRMT6, but it is noteworthy that HTT also forms a complex with PRMT1, PRMT5 (as already reported) and PRMT7, reinforcing the idea that HTT might be methylated at other sites and supporting the concept that the interaction of HTT with PRMTs is relevant for HTT biology and possibly HD pathogenesis. In an *in vitro* methylation assay, PRMT6 selectively methylated a human HTT peptide spanning R118, and PRMT6-mediated arginine methylation of N-terminal and full-length HTT was confirmed in HEK293T cells and primary cortical neurons, respectively. On the other hand, recombinant PRMT2 did not methylate HTT peptides spanning R101 and R118 *in vitro*. However, we cannot rule out that PRMT2 requires the presence of additional cofactors that are normally recruited in the cell in order to catalyze the transfer of methyl groups and PRMT2 may also methylate other arginines in HTT. Moreover, the other PRMTs interacting with HTT may target R101 and R118 as well. Given that by mass spectrometry we only identified the presence of two methyl groups on both these two arginines, it is unlikely that modification of these residues is mediated by PRMT7, the only type III enzyme catalyzing exclusively monomethylarginine (Blanc and Richard, 2017).

Considering that PRMT2 in our hands did not methylate the two selected arginines, I decided to focus on PRMT6 and the role of R118 methylation in the regulation of HTT

native function and HD pathogenesis, which are discussed in the following paragraphs. Nevertheless, the physiological significance of HTT-PRMT2 interaction remains to be established. Of note, PRMT2 was previously reported to interact with HTT in a large-scale screening performed using the yeast-two hybrid system (Tourette et al. 2014). PRMT2 interacts with the polyproline tract at the N-terminus of HTT through its Src Homology 3 (SH3) domain (Tourette et al. 2014), a small protein domain of about 60 amino acids that binds proline-rich sequences and is involved in the formation of numerous protein complexes in the cell. PRMTs target a multitude of cytoplasmic and nuclear proteins, including histones. PRMT2 is responsible for the asymmetric dimethylation of Histone 3 Arginine 8 (H3R8me2a), a histone mark whose enrichment at promoters and enhancers correlates with the presence of active histone marks (Blythe et al. 2010; Dong et al. 2018). As described in the introduction (paragraph 1.1.2.2), HTT regulates transcription in multiple ways, for example by interacting with transcription factors and scaffolding transcriptional complexes. Therefore, I speculate that HTT might facilitate PRMT2-mediated H3R8 dimethylation by connecting PRMT2 to other transcriptional regulators and chromatin remodeling enzymes in a macromolecular complex. Similarly, PRMT6 acts as a histone methyltransferase catalyzing several post-translational modifications on histone tails, including H3R2me2a, H3R42me2a, H2AR29me2a (Guccione et al. 2007; Casadio et al. 2013; Waldmann et al. 2011), leading either to transcriptional repression or activation. Interestingly, by co-immunoprecipitation assay I observed that PRMT2 and PRMT6 are part of the same complex (data not shown in this thesis), therefore it is not surprising that both these two enzymes interact not only with AR (Scaramuzzino et al. 2015), but also with HTT. HTT may thus serve as a scaffold coordinating the assembly of a large protein complex containing multiple transcriptional co-factors, including several 'writers' such as PRMT2 and PRMT6 that catalyze the deposition of specific histone marks on chromatin.

Most importantly, PRMT6 and HTT both interact with subunits of the epigenetic silencing complex PRC2 (Stein et al. 2016; Seong et al. 2010): HTT increases PRC2-mediated deposition of H3K27me3 histone mark and the genomic occurrence of H3R2me2a coincides with that of H3K27me3. Moreover, PRMT6 downregulation and HTT knockout both result in reduced H3K27me3 occupancy. These observations strongly support an *in vivo* interaction between HTT and PRMT6 and suggest that these

two proteins cooperate together with PRC2 to achieve an efficient epigenetic regulation of gene expression.

In conclusion, we can envision that HTT-PRMTs interaction results in regulation of HTT function and toxicity by direct arginine methylation of HTT, which is further discussed in the next sections, but it also leads to the modulation of PRMT function in other cellular processes, as it was already described by Ratovitski et al. for HTT-PRMT5 interaction (Ratovitski et al. 2015).

4.2 Methylation of Huntingtin at R118 regulates axonal trafficking

HTT has a well-established role in the regulation of axonal transport, which is conserved across evolution (Gunawardena et al. 2003; Zala et al. 2013a). We found that HTT immunopurified from the brain vesicular fraction is methylated at R118 and that PRMT6 is the enzyme responsible for this modification. Hence, we hypothesized that arginine methylation of HTT could influence HTT-mediated vesicular trafficking along neuronal axons. Interestingly, as opposed to previous reports describing an exclusive nuclear localization of PRMT6 (Herrmann et al. 2009), I observed HTT-PRMT6 colocalization in the cytoplasm as well as in the axon of cortical neurons. In addition, for the first time to my knowledge I detected the presence of PRMT6 on small vesicles purified from mouse brain. These observations suggest that HTT methylation at R118 by PRMT6 might occur both in the cell body and in the axoplasm, as well as on vesicles themselves. Although the existence of arginine demethylases able to remove methyl groups from methylated arginines is still controversial, it is possible that arginine methylation is reversible. The ability of PRMT6 to locally methylate vesicle-associated HTT would be fundamental in a scenario in which arginine methylation is a reversible PTM, as it would allow a constant and tight regulation of R118 methylation levels.

In order to explore the role of HTT methylation in fast axonal transport, I decided to mimic the loss of arginine methylation by transducing cortical neurons with lentiviruses expressing the methylation-defective HTT R118K tagged with mCherry, and to follow the movement of mCherry-positive vesicles along cortical axons. In previous studies, the role of HTT in axonal transport has been mainly investigated by examining the trafficking of specific organelles or cargoes, such as BDNF-containing

vesicles. Here, I decided to monitor the movement of vesicles associated to exogenously expressed HTT, in order to decipher the direct effect of changes in HTT PTMs on the ability of the protein to exert its function. I took advantage of a physiologically relevant customized microfluidic chip that reproduces an oriented corticostriatal circuit *in vitro* and allows the study of trafficking dynamics through high-resolution live-cell imaging, recently developed in the laboratory of Frédéric Saudou (Virlogeux et al. 2018). Notably, the expression of HTT R118K mutant in cortical neurons resulted in impaired axonal trafficking, with decreased number of vesicles moving anterogradely and consequent abnormalities in the global vesicular flux with respect to neurons expressing wild-type HTT. On the contrary, the retrograde transport did not show any overt phenotype. Importantly, the defect in axonal transport caused by loss of HTT methylation correlated with a 50% reduction in neuronal survival, suggesting that an impairment of HTT-dependent vesicle trafficking triggers neuronal death. However, considering the wide variety of cellular functions regulated by HTT, we cannot exclude that the increase in neuronal death is to be attributed also to dysfunctions in other cellular processes.

A failure in R118 methylation seems to lead to a loss-of-function of HTT, which is no longer able to facilitate anterograde vesicular trafficking. Methylation-defective HTT preserves its interaction with key components of the molecular motor machinery involved in both retrograde and anterograde transport, such as $p150^{Glued}$ and kinesin-1, respectively. As previously described, the interaction of HTT with kinesin-1 and $p150^{Glued}$ is mediated by HAP1, indicating that loss of R118 methylation does not affect the binding of HAP1 either. Nevertheless, HTT R118K is substantially less recruited to small vesicles compared to wild-type HTT, as demonstrated by the measurement of HTT levels in the vesicular fraction of cortical neurons, although further analyses are needed to confirm this result. This observation is consistent with the reduced number of HTT-positive vesicles travelling anterogradely, yet it does not explain the fact that retrograde transport is not affected by the overexpression of HTT R118K. It will be important to investigate how HTT methylation at R118 promotes the association of HTT with vesicles, thereby promoting anterograde axonal trafficking. The interaction of HTT with molecular motors, particularly kinesin-1, might be favoured by additional unknown factors that associate with HTT; the loss of methylation might cause a critical conformational change or the alteration of HTT binding properties, ultimately resulting

in the abrogation of key protein-protein interactions that normally determine the indirect association of HTT with vesicles. Moreover, although axonal translation of HTT has been reported (Shigeoka et al. 2016), HTT is mainly synthetized in the cell body and transported anterogradely along the axon. Therefore, a defect in axonal transport of HTT may also underlie the reduced availability of HTT in the axoplasm and the consequent loss of normal HTT function in the modulation of vesicular trafficking. We can hypothesize that unidentified Tudor domain-containing proteins recognizing methylated R118 on HTT in some way regulate a key step in one of these two processes. However, once again a dysfunctional axonal transport of HTT would not explicate the impairment of vesicle movement in a single direction. An interesting possibility is that arginine methylation of HTT could selectively facilitate the transport of vesicles in the anterograde direction, similarly to phosphorylation of S421 (Colin et al.2008).

HTT controls the transport of many different cargoes, such as BDNF-containing vesicles, synaptic precursor vesicles, endosomes and lysosomes, autophagosomes, etc., as previously mentioned in the introduction. Therefore, it is plausible to assume that a complete or partial loss of R118 methylation would lead to abnormalities in the trafficking of several organelles, with a huge negative impact on global neuronal homeostasis. Moreover, it is worth to notice that in the brain PRMT6 is expressed at higher levels in the hippocampus, olfactory bulb and cerebellum, but it is also expressed in the cortex and striatum, as reported in Allen Mouse Brain Atlas. This implies that dysregulation of PRMT6-mediated HTT methylation could cause a defect in fast axonal transport in both cortical and striatal neurons and contribute to the dysfunction of the corticostriatal axis observed in HD.

4.3 Arginine methylation is a novel modifier of Huntington's Disease

PTMs that either suppress or enhance neurotoxicity are druggable and valuable therapeutic targets in neurodegenerative diseases (Sambataro and Pennuto 2017). In order to understand whether arginine methylation is a modifier of mutant HTT-induced toxicity, I used both a loss-of-function and a gain-of-function approach. I found that pharmacologic inhibition of arginine methyltransferase activity and, most importantly, specific PRMT6 silencing enhance toxicity in striatal cells expressing polyQ-expanded HTT, whereas PRMT6 overexpression rescued neuronal death in

cortical neurons through an improvement of anterograde trafficking efficiency. Interestingly, I observed that PRMT6 did not rescue cell death in neurons expressing the methylation-defective polyQ-expanded HTT, demonstrating that methylation of HTT at R118 is required for the enhancement of neuronal survival. These findings support the idea that a loss of PRMT6 function might contribute to HD pathogenesis and that promoting arginine methylation of HTT could be a potential therapeutic strategy.

PRMT6 protein levels are unaltered in the whole brain and cortex of an HD mouse model ($Hdh^{CAG140/+}$ knockin mice) and HTT-PRMT6 interaction as well as R118 methylation are preserved upon expansion of the polyQ tract. However, a tendency towards a reduced interaction between HTT and PRMT6 has been observed in cell lines by immunoprecipitation experiments (**Figure 31**). This result is not unexpected, given that polyglutamine expansions in proteins often hamper the interaction with their native partners. A decreased HTT-PRMT6 interaction in HD would lead to lowered levels of HTT methylation, anterograde axonal transport impairment and increased susceptibility to neuronal death. Moreover, an interesting observation is that the gene coding for S-adenosylhomocysteine hydrolase (SAHH), *ACHY*, is downregulated in peripheral leukocytes of HD patients (Chang et al. 2012). SAHH is the enzyme that catalyzes the hydrolysis of S-adenosylhomocysteine (SAH) to adenosine and homocysteine (**Figure 41**). SAH strongly inhibits S-adenosylmethionine (SAM)-

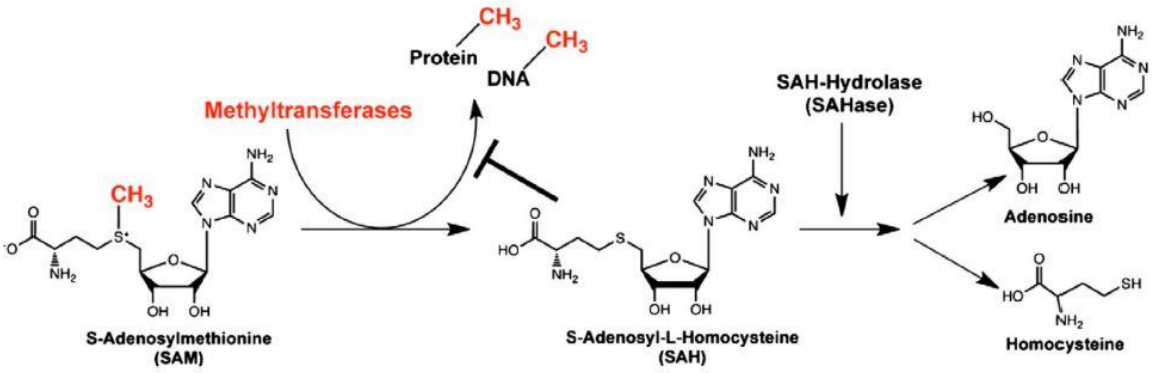

Figure 41: Biochemical pathway of protein and DNA methylation. The transfer of methyl groups from SAM to proteins or DNA leads to the conversion of SAM to SAH, which is then hydrolysed into adenosine and homocysteine by SAH-Hydrolase (SAHase or SAHH). At aberrantly high concentrations, SAH acts as an inhibitor of methyltransferases through a negative feedback loop (Lawson et al. 2012).

dependent methyltransferases, including PRMTs (Baric et al. 2004). Aberrantly high levels of SAH and a SAM/SAH imbalance in neurons could therefore cause PRMT6 inhibition and reduced HTT methylation. In this direction, a quantitative mass spectrometry analysis of R118 methylation in the brain of HD patients compared to healthy individuals would be crucial to address whether arginine methylation of HTT is reduced in HD.

5. Conclusions and future perspectives

In this study, I explored the role of arginine methylation of HTT under physiological and pathological conditions. I found that HTT is methylated at highly evolutionarily conserved arginine residues *in vivo*. HTT methylation at R118 is catalysed by PRMT6 and is crucial to recruit HTT to vesicles and facilitate its function as a scaffold for components of the molecular motor machinery. Loss of R118 methylation caused impaired anterograde axonal trafficking and enhanced neuronal toxicity. Importantly, PRMT6 upregulation improves axonal transport in the anterograde direction and rescues polyQ-expanded HTT-induced neuronal death.

These findings establish a crucial role of arginine methylation as a modulator of polyQ-expanded HTT toxicity and identify PRMT6 as a novel modifier of HD pathogenesis, strengthening the idea that arginine methylation is a key PTM in polyQ diseases and other neurodegenerative disorders. Furthermore, they reinforce the concept that the consequences of arginine methylation of mutant polyQ proteins are disease-specific and depend strikingly on the protein context, due to the capacity of arginine methylation to regulate the native function of the wild-type proteins. Indeed, PRMT6 interacts with both AR and HTT and modulates toxicity in opposite directions: arginine methylation of AR aggravates phenotype in SBMA (Scaramuzzino et al. 2015), whereas it protects from neurodegeneration in HD.

The results described in this thesis open new mechanistic and therapeutic avenues in HD. Mechanistically, it might be important to explore the functional consequences of a crosstalk between serine phosphorylation and arginine methylation in HTT. These two PTMs are often mutually exclusive when occurring in close proximity on a protein. R118 in HTT is surrounded by S116 and S120, which have previously been reported to be phosphorylated in cultured cells (Watkin et al. 2014). S116 is highly conserved throughout evolution (**Figure 12**), and serine 116-to-alanine substitution (S116A) leading to loss of phosphorylation has been shown to have protective effects against polyQ-expanded HTT toxicity. This raises the question as to whether a crosstalk exists between R118 methylation and S116 phosphorylation. In this scenario, PRMT6-mediated R118 methylation would abrogate S116 phosphorylation and lead to neuroprotection in the presence of polyQ-expanded HTT. It would be interesting to find

out which kinases are responsible for S116 and S120 phosphorylation and test whether their inhibition would increase R118 methylation and enhance protection in HD.

Therapeutically, the fact that the polyQ expansion only partially interferes with HTT-PRMT6 interaction and that polyQ-expanded HTT is still methylated by PRMT6 implies that by globally promoting arginine methylation it is possible to enhance R118 methylation of HTT. This is further supported by the normal PRMT6 expression levels in the brain of HD mice. As a proof of principle, we are planning to overexpress PRMT6 via adeno-associated viral vectors (AAV9) in cortex and striatum of HD mice and investigate whether PRMT6 upregulation results in an amelioration of HD-related neuropathological and behavioural phenotype. Finally, another interesting way of boosting arginine methylation of HTT could be to increase the levels of the methyl-donor S-adenosylmethionine (SAM) in neurons. As shown in **Figure 42**, the folate and the methionine cycles are interconnected and comprise the so-called one-carbon cycle, and the production of SAM can be increased by dietary intake of folate and vitamins B. The stimulation of arginine methylation through increased folate intake could thus offer a possibility of therapeutic intervention in HD and might alleviate disease manifestations in HD patients.

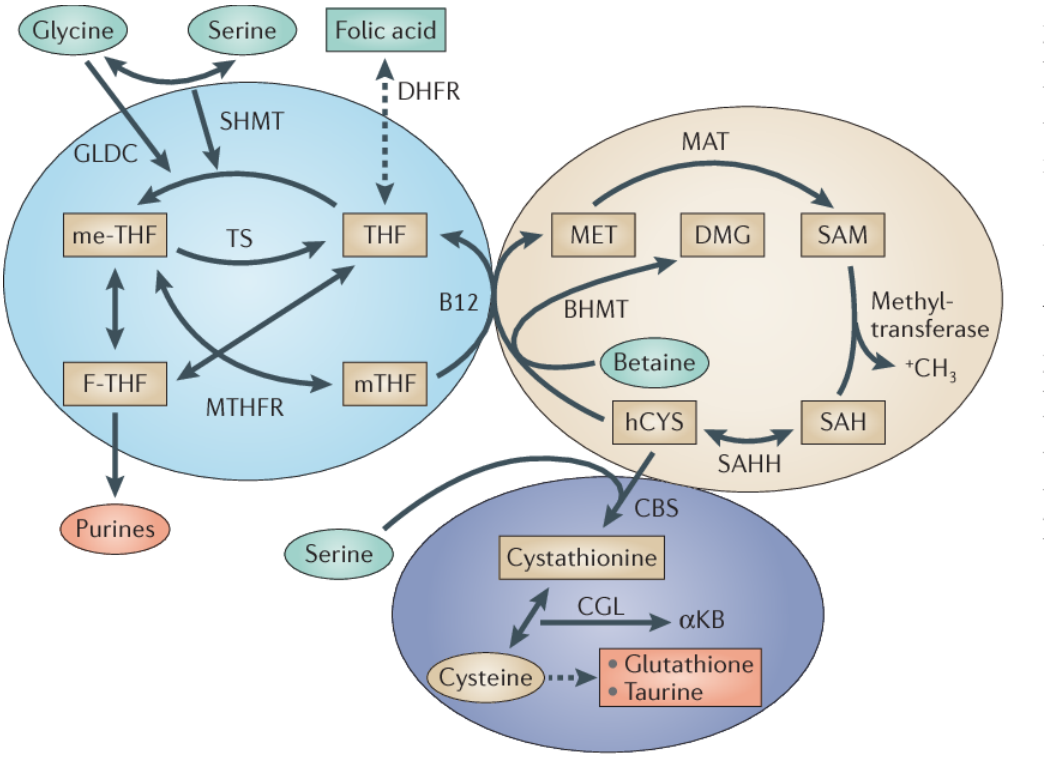

Figure 42: One-carbon cycle. The folate cycle and the methionine cycle comprise the one-carbon cycle. With the demethylation of 5-methyltetrahydrofolate (mTHF), the carbon is donated into the methionine cycle through the methylation of homocysteine (hCYS) by methionine synthase and its cofactor vitamin B12. Methionine (MET) is then converted into SAM, the substrate for methyltransferase reactions (Locasale 2013).

6. Appendix

Table 1: Mass spectrometry analysis of immunopurified vesicle-associated HTT.

The small vesicle-rich fraction was isolated from a wild-type mouse brain and HTT was immunopurified and subjected to mass spectrometry analysis. The presence of two methyl groups was observed both on R101 and R118 (highlighted in red).

Description	ΣCoverage	Σ# Proteins	Σ# Unique Peptides	Σ# PSMs	
Huntingtin OS=Mus musculus GN=Htt PE=1 SV=2 - [HD_MOUSE]	6,12	1	8	18	
Sequence	**# PSMs**	**# Proteins**	**# Protein Groups**	**Modifications**	**MH+ [Da]**
QVLDLLAQLVQLR	3	1	1		1508,91680
VPLNTTESTEEQYVSDILNYIDHGDPQVR	4	1	1		3332,58542
SLLVVSDLFTER	1	1	1		1378,75676
AVTHAIPALQPIVHDLFVLR	1	1	1		2210,27993
TAAGSAVSICQHSR	1	1	1	C10(Carbamidomethyl)	1444,69681
DRVNHCLTICENIVAQSLRNSPEFQK	1	1	1	R2(Dimethyl); T8(Phospho); R19(Dimethyl); K26(Acetyl)	3192,51084

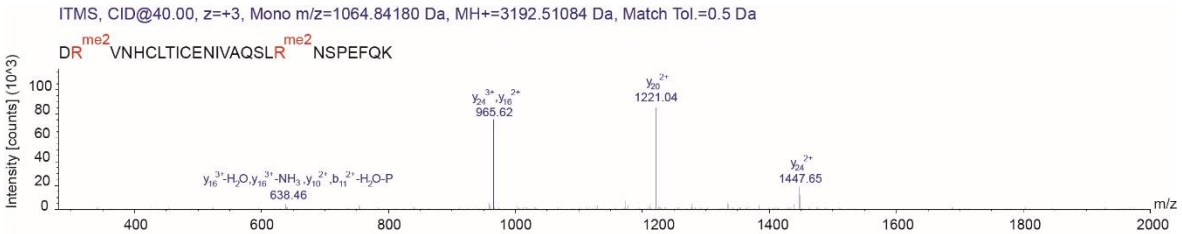

Figure S1: Mass spectrometry spectrum showing dimethylation of HTT at R101 and R118 in the small vesicle-rich fraction (P3) purified from mouse brain.

7. References

Andrew, S E, Y P Goldberg, B Kremer, H Telenius, J Theilmann, S Adam, E Starr, et al. 1993. "The Relationship between Trinucleotide (CAG) Repeat Length and Clinical Features of Huntington's Disease." *Nature Genetics* 4 (4): 398–403. https://doi.org/10.1038/ng0893-398.

Anne, S. L., F. Saudou, and S. Humbert. 2007. "Phosphorylation of Huntingtin by Cyclin-Dependent Kinase 5 Is Induced by DNA Damage and Regulates Wild-Type and Mutant Huntingtin Toxicity in Neurons." *Journal of Neuroscience* 27 (27): 7318–28. https://doi.org/10.1523/jneurosci.1831-07.2007.

Arbez, Nicolas, Tamara Ratovitski, Elaine Roby, Ekaterine Chighladze, Jacqueline C. Stewart, Mark Ren, Xiaofang Wang, Daniel J. Lavery, and Christopher A. Ross. 2017. "Post-Translational Modifications Clustering within Proteolytic Domains Decrease Mutant Huntingtin Toxicity." *Journal of Biological Chemistry* 292 (47): 19238–54. https://doi.org/10.1074/jbc.M117.782300.

Arrasate, Montserrat, Siddhartha Mitra, Erik S. Schweitzer, Mark R. Segal, and Steven Finkbeiner. 2004. "Inclusion Body Formation Reduces Levels of Mutant Huntingtin and the Risk of Neuronal Death." *Nature* 431 (7010): 805–10. https://doi.org/10.1038/nature02998.

Atanesyan, Lilit, Viola Günther, Bernhard Dichtl, Oleg Georgiev, and Walter Schaffner. 2012. "Polyglutamine Tracts as Modulators of Transcriptional Activation from Yeast to Mammals." *Biological Chemistry* 393 (1–2): 63–70. https://doi.org/10.1515/BC-2011-252.

Atwal, Randy Singh, Carly R Desmond, Nicholas Caron, Tamara Maiuri, Jianrun Xia, Simonetta Sipione, and Ray Truant. 2011. "Kinase Inhibitors Modulate Huntingtin Cell Localization and Toxicity." *Nature Chemical Biology* 7 (7): 453–60. https://doi.org/10.1038/nchembio.582.

Atwal, Randy Singh, Jianrun Xia, Deborah Pinchev, Jillian Taylor, Richard M Epand, and Ray Truant. 2007. "Huntingtin Has a Membrane Association Signal That Can Modulate Huntingtin Aggregation, Nuclear Entry and Toxicity." *Human Molecular Genetics* 16 (21): 2600–2615. https://doi.org/10.1093/hmg/ddm217.

Baric, I., K. Fumic, B. Glenn, M. Cuk, A. Schulze, J. D. Finkelstein, S. J. James, et al. 2004. "S-Adenosylhomocysteine Hydrolase Deficiency in a Human: A Genetic Disorder of Methionine Metabolism." *Proceedings of the National Academy of Sciences* 101 (12): 4234–39. https://doi.org/10.1073/pnas.0400658101.

Basso, Manuela, Jill Berlin, Li Xia, Sama F Sleiman, Brendan Ko, Renee Haskew-Layton, Eunhee Kim, et al. 2012. "Transglutaminase Inhibition Protects against Oxidative Stress-Induced Neuronal Death Downstream of Pathological ERK Activation." *The Journal of Neuroscience : The Official Journal of the Society for Neuroscience* 32 (19): 6561–69. https://doi.org/10.1523/JNEUROSCI.3353-11.2012.

Basso, Manuela, and Maria Pennuto. 2015. "Serine Phosphorylation and Arginine Methylation at the Crossroads to Neurodegeneration." *Experimental Neurology*. Academic Press Inc. https://doi.org/10.1016/j.expneurol.2015.05.003.

Bates, Gillian P, Ray Dorsey, James F Gusella, Michael R Hayden, Chris Kay, Blair R Leavitt, Martha Nance, et al. 2015. "Huntington Disease." *Nature Reviews. Disease Primers* 1 (April): 15005. https://doi.org/10.1038/nrdp.2015.5.

Bedford, Mark T., and Steven G. Clarke. 2009. "Protein Arginine Methylation in Mammals: Who, What, and Why." *Molecular Cell*. https://doi.org/10.1016/j.molcel.2008.12.013.

Benn, C. L., T. Sun, G. Sadri-Vakili, K. N. McFarland, D. P. DiRocco, G. J. Yohrling, T. W. Clark, B. Bouzou, and J.-H. J. Cha. 2008. "Huntingtin Modulates Transcription, Occupies Gene Promoters In Vivo, and Binds Directly to DNA in a Polyglutamine-Dependent Manner." *Journal of Neuroscience* 28 (42): 10720–33. https://doi.org/10.1523/JNEUROSCI.2126-08.2008.

Blanc, Roméo S., and Stéphane Richard. 2017. "Arginine Methylation: The Coming of Age." *Molecular Cell*. Cell Press. https://doi.org/10.1016/j.molcel.2016.11.003.

Block-Galarza, J, K O Chase, E Sapp, K T Vaughn, R B Vallee, M DiFiglia, and N Aronin. 1997. "Fast Transport and Retrograde Movement of Huntingtin and HAP 1 in Axons." *Neuroreport* 8 (9–10): 2247–51. http://www.ncbi.nlm.nih.gov/pubmed/9243620.

Blythe, Shelby A., Sang Wook Cha, Emmanuel Tadjuidje, Janet Heasman, and Peter S. Klein. 2010. "β-Catenin Primes Organizer Gene Expression by Recruiting a Histone H3 Arginine 8 Methyltransferase, Prmt2." *Developmental Cell* 19 (2): 220–31. https://doi.org/10.1016/j.devcel.2010.07.007.

Casadio, F., X. Lu, S. B. Pollock, G. LeRoy, B. A. Garcia, T. W. Muir, R. G. Roeder, and C. D. Allis. 2013. "H3R42me2a Is a Histone Modification with Positive Transcriptional Effects." *Proceedings of the National Academy of Sciences* 110 (37): 14894–99. https://doi.org/10.1073/pnas.1312925110.

Caterino, Marco, Tiziana Squillaro, Daniela Montesarchio, Antonio Giordano, Concetta Giancola, and Mariarosa A.B. Melone. 2018. "Huntingtin Protein: A New Option for Fixing the Huntington's Disease Countdown Clock." *Neuropharmacology* 135 (June): 126–38. https://doi.org/10.1016/j.neuropharm.2018.03.009.

Cattaneo, Elena, Chiara Zuccato, and Marzia Tartari. 2005. "NCattaneo, Elena, Chiara Zuccato, and Marzia Tartari. 2005. 'Normal Huntingtin Function: An Alternative Approach to Huntington's Disease.' Nature Reviews Neuroscience 6 (12): 919–30. Https://Doi.Org/10.1038/Nrn1806.Ormal Huntingtin Function: An Alternativ." *Nature Reviews Neuroscience* 6 (12): 919–30. https://doi.org/10.1038/nrn1806.

Caviston, J. P., J. L. Ross, S. M. Antony, M. Tokito, and E. L. F. Holzbaur. 2007. "Huntingtin Facilitates Dynein/Dynactin-Mediated Vesicle Transport." *Proceedings of the National Academy of Sciences* 104 (24): 10045–50. https://doi.org/10.1073/pnas.0610628104.

Caviston, Juliane P, and Erika L F Holzbaur. 2009. "Huntingtin as an Essential Integrator of Intracellular Vesicular Trafficking." *Trends in Cell Biology* 19 (4): 147–55. https://doi.org/10.1016/j.tcb.2009.01.005.

Chang, B., Y. Chen, Y. Zhao, and R. K. Bruick. 2007. "JMJD6 Is a Histone Arginine Demethylase." *Science* 318 (5849): 444–47. https://doi.org/10.1126/science.1145801.

Chang, Kuo-Hsuan, Yi-Chun Chen, Yih-Ru Wu, Wan-Fen Lee, and Chiung-Mei Chen. 2012. "Downregulation of Genes Involved in Metabolism and Oxidative Stress in the Peripheral Leukocytes of Huntington's Disease Patients." Edited by David R. Borchelt. *PLoS ONE* 7

(9): e46492. https://doi.org/10.1371/journal.pone.0046492.

Chen, Chen, Timothy J. Nott, Jing Jin, and Tony Pawson. 2011. "Deciphering Arginine Methylation: Tudor Tells the Tale." *Nature Reviews Molecular Cell Biology*. https://doi.org/10.1038/nrm3185.

Colin, Emilie, Diana Zala, Géraldine Liot, Hélène Rangone, Maria Borrell-Pagès, Xiao Jiang Li, Frédéric Saudou, and Sandrine Humbert. 2008. "Huntingtin Phosphorylation Acts as a Molecular Switch for Anterograde/Retrograde Transport in Neurons." *EMBO Journal* 27 (15): 2124–34. https://doi.org/10.1038/emboj.2008.133.

Desmond, Carly R., Randy Singh Atwal, Jianrun Xia, and Ray Truant. 2012. "Identification of a Karyopherin B1/B2 Proline-Tyrosine Nuclear Localization Signal in Huntingtin Protein." *Journal of Biological Chemistry* 287 (47): 39626–33. https://doi.org/10.1074/jbc.M112.412379.

Diekmann, H., O. Anichtchik, A. Fleming, M. Futter, P. Goldsmith, A. Roach, and D. C. Rubinsztein. 2009. "Decreased BDNF Levels Are a Major Contributor to the Embryonic Phenotype of Huntingtin Knockdown Zebrafish." *Journal of Neuroscience* 29 (5): 1343–49. https://doi.org/10.1523/JNEUROSCI.6039-08.2009.

DiFiglia, M, M Sena-Esteves, K Chase, E Sapp, E Pfister, M Sass, J Yoder, et al. 2007. "Therapeutic Silencing of Mutant Huntingtin with SiRNA Attenuates Striatal and Cortical Neuropathology and Behavioral Deficits." *Proceedings of the National Academy of Sciences of the United States of America* 104 (43): 17204–9. https://doi.org/10.1073/pnas.0708285104.

DiFiglia, Marian, Ellen Sapp, Kathryn Chase, Cordula Schwarz, Alison Meloni, Christine Young, Eileen Martin, et al. 1995. "Huntingtin Is a Cytoplasmic Protein Associated with Vesicles in Human and Rat Brain Neurons." *Neuron* 14 (5): 1075–81. https://doi.org/10.1016/0896-6273(95)90346-1.

Dong, Feng, Qian Li, Chao Yang, Dawei Huo, Xing Wang, Chunbo Ai, Yu Kong, et al. 2018. "PRMT2 Links Histone H3R8 Asymmetric Dimethylation to Oncogenic Activation and Tumorigenesis of Glioblastoma." *Nature Communications* 9 (1): 4552. https://doi.org/10.1038/s41467-018-06968-7.

Dragatsis, I, A Efstratiadis, and S Zeitlin. 1998. "Mouse Mutant Embryos Lacking Huntingtin Are Rescued from Lethality by Wild-Type Extraembryonic Tissues." *Development (Cambridge, England)* 125 (8): 1529–39. http://www.ncbi.nlm.nih.gov/pubmed/9502734.

Dragatsis, Ioannis, Michael S. Levine, and Scott Zeitlin. 2000. "Inactivation of Hdh in the Brain and Testis Results in Progressive Neurodegeneration and Sterility in Mice." *Nature Genetics* 26 (3): 300–306. https://doi.org/10.1038/81593.

Dunah, Anthone W, Hyunkyung Jeong, April Griffin, Yong-Man Kim, David G Standaert, Steven M Hersch, M Maral Mouradian, Anne B Young, Naoko Tanese, and Dimitri Krainc. 2002. "Sp1 and TAFII130 Transcriptional Activity Disrupted in Early Huntington's Disease." *Science (New York, N.Y.)* 296 (5576): 2238–43. https://doi.org/10.1126/science.1072613.

Duyao, M P, A B Auerbach, A Ryan, F Persichetti, G T Barnes, S M McNeil, P Ge, J P Vonsattel, J F Gusella, and A L Joyner. 1995. "Inactivation of the Mouse Huntington's Disease Gene Homolog Hdh." *Science (New York, N.Y.)* 269 (5222): 407–10. http://www.ncbi.nlm.nih.gov/pubmed/7618107.

Engelender, S, A H Sharp, V Colomer, M K Tokito, A Lanahan, P Worley, E L Holzbaur, and C A Ross. 1997. "Huntingtin-Associated Protein 1 (HAP1) Interacts with the P150Glued Subunit of Dynactin." *Human Molecular Genetics* 6 (13): 2205–12. http://www.ncbi.nlm.nih.gov/pubmed/9361024.

Eram, Mohammad S., Yudao Shen, Magdalena M. Szewczyk, Hong Wu, Guillermo Senisterra, Fengling Li, Kyle V. Butler, et al. 2016. "A Potent, Selective, and Cell-Active Inhibitor of Human Type i Protein Arginine Methyltransferases." *ACS Chemical Biology* 11 (3): 772–81. https://doi.org/10.1021/acschembio.5b00839.

Ferrante, R J, N W Kowall, M F Beal, E P Richardson, E D Bird, and J B Martin. 1985. "Selective Sparing of a Class of Striatal Neurons in Huntington's Disease." *Science (New York, N.Y.)* 230 (4725): 561–63. http://www.ncbi.nlm.nih.gov/pubmed/2931802.

Ferrante, Robert J, James K Kubilus, Junghee Lee, Hoon Ryu, Ayshe Beesen, Birgit Zucker, Karen Smith, et al. 2003. "Histone Deacetylase Inhibition by Sodium Butyrate Chemotherapy Ameliorates the Neurodegenerative Phenotype in Huntington's Disease Mice." *The Journal of Neuroscience : The Official Journal of the Society for Neuroscience* 23 (28): 9418–27. http://www.ncbi.nlm.nih.gov/pubmed/14561870.

Futter, M, H Diekmann, E Schoenmakers, O Sadiq, K Chatterjee, and D C Rubinsztein. 2009. "Wild-Type but Not Mutant Huntingtin Modulates the Transcriptional Activity of Liver X Receptors." *Journal of Medical Genetics* 46 (7): 438–46. https://doi.org/10.1136/jmg.2009.066399.

Gauthier, Laurent R, Bé Né Dicte, C Charrin, Maria Borrell-Pagè, Jim P Dompierre, Hé Lè Ne Rangone, Fabrice P Cordelière Res, et al. 2004. "Huntingtin Controls Neurotrophic Support and Survival of Neurons by Enhancing BDNF Vesicular Transport along Microtubules." *Cell*. Vol. 118. http://www.cell.com/cgi/content/.

Gayatri, Sitaram, and Mark T. Bedford. 2014. "Readers of Histone Methylarginine Marks." *Biochimica et Biophysica Acta (BBA) - Gene Regulatory Mechanisms* 1839 (8): 702–10. https://doi.org/10.1016/J.BBAGRM.2014.02.015.

Gervais, François G., Roshni Singaraja, Steven Xanthoudakis, Claire-Anne Gutekunst, Blair R. Leavitt, Martina Metzler, Abigail S. Hackam, et al. 2002. "Recruitment and Activation of Caspase-8 by the Huntingtin-Interacting Protein Hip-1 and a Novel Partner Hippi." *Nature Cell Biology* 4 (2): 95–105. https://doi.org/10.1038/ncb735.

Ghosh, Rhia, and Sarah J. Tabrizi. 2018. "Clinical Features of Huntington's Disease." In *Advances in Experimental Medicine and Biology*, 1049:1–28. Springer New York LLC. https://doi.org/10.1007/978-3-319-71779-1_1.

Godin, Juliette D., Kelly Colombo, Maria Molina-Calavita, Guy Keryer, Diana Zala, Béé Edicte C. Charrin, Paula Dietrich, et al. 2010. "Huntingtin Is Required for Mitotic Spindle Orientation and Mammalian Neurogenesis." *Neuron* 67 (3): 392–406. https://doi.org/10.1016/j.neuron.2010.06.027.

Guccione, Ernesto, Christian Bassi, Fabio Casadio, Francesca Martinato, Matteo Cesaroni, Henning Schuchlautz, Bernhard Lüscher, and Bruno Amati. 2007. "Methylation of Histone H3R2 by PRMT6 and H3K4 by an MLL Complex Are Mutually Exclusive." *Nature* 449 (7164): 933–37. https://doi.org/10.1038/nature06166.

Gunawardena, Shermali, Lu-Shiun Her, Richard G Brusch, Robert A Laymon, Ingrid R Niesman, Beth Gordesky-Gold, Louis Sintasath, Nancy M Bonini, and Lawrence S B Goldstein. 2003.

"Disruption of Axonal Transport by Loss of Huntingtin or Expression of Pathogenic PolyQ Proteins in Drosophila Transcription Factors, Caspases, and Molecular Chaper-Ones and Other Proteins, Which May Stimulate Apoptosis. We Previously Found That Expression." *Neuron*. Vol. 40. http://www.neuron.org/cgi/content/full/.

Guo, Qiang, Bin Huang, Jingdong Cheng, Manuel Seefelder, Tatjana Engler, Günter Pfeifer, Patrick Oeckl, et al. 2018. "The Cryo-Electron Microscopy Structure of Huntingtin." *Nature* 555 (7694): 117–20. https://doi.org/10.1038/nature25502.

Gusella, J F, N S Wexler, P M Conneally, S L Naylor, M A Anderson, R E Tanzi, P C Watkins, K Ottina, M R Wallace, and A Y Sakaguchi. n.d. "A Polymorphic DNA Marker Genetically Linked to Huntington's Disease." *Nature* 306 (5940): 234–38. Accessed May 12, 2019. http://www.ncbi.nlm.nih.gov/pubmed/6316146.

Harjes, Phoebe, and Erich E. Wanker. 2003. "The Hunt for Huntingtin Function: Interaction Partners Tell Many Different Stories." *Trends in Biochemical Sciences*. Elsevier Ltd. https://doi.org/10.1016/S0968-0004(03)00168-3.

Herrmann, F., P. Pably, C. Eckerich, M. T. Bedford, and F. O. Fackelmayer. 2009. "Human Protein Arginine Methyltransferases in Vivo - Distinct Properties of Eight Canonical Members of the PRMT Family." *Journal of Cell Science* 122 (5): 667–77. https://doi.org/10.1242/jcs.039933.

Hilditch-Maguire, P, F Trettel, L A Passani, A Auerbach, F Persichetti, and M E MacDonald. 2000. "Huntingtin: An Iron-Regulated Protein Essential for Normal Nuclear and Perinuclear Organelles." *Human Molecular Genetics* 9 (19): 2789–97. http://www.ncbi.nlm.nih.gov/pubmed/11092755.

Ho, L. W, R Brown, M Maxwell, A Wyttenbach, and D C Rubinsztein. 2001. "Wild Type Huntingtin Reduces the Cellular Toxicity of Mutant Huntingtin in Mammalian Cell Models of Huntington's Disease." *Journal of Medical Genetics* 38 (7): 450–52. https://doi.org/10.1136/jmg.38.7.450.

Hockly, E., V. M. Richon, B. Woodman, D. L. Smith, X. Zhou, E. Rosa, K. Sathasivam, et al. 2003. "Suberoylanilide Hydroxamic Acid, a Histone Deacetylase Inhibitor, Ameliorates Motor Deficits in a Mouse Model of Huntington's Disease." *Proceedings of the National Academy of Sciences* 100 (4): 2041–46. https://doi.org/10.1073/pnas.0437870100.

Hoffner, Guylaine, Pascal Kahlem, and Philippe Djian. 2002. "Perinuclear Localization of Huntingtin as a Consequence of Its Binding to Microtubules through an Interaction with Beta-Tubulin: Relevance to Huntington's Disease." *Journal of Cell Science* 115 (Pt 5): 941–48. http://www.ncbi.nlm.nih.gov/pubmed/11870213.

Humbert, Sandrine, Elzbieta A. Bryson, Fabrice P. Cordelières, Nathan C. Connors, Sandeep R. Datta, Steven Finkbeiner, Michael E. Greenberg, and Frédéric Saudou. 2002. "The IGF-1/Akt Pathway Is Neuroprotective in Huntington's Disease and Involves Huntingtin Phosphorylation by Akt." *Developmental Cell* 2 (6): 831–37. https://doi.org/10.1016/S1534-5807(02)00188-0.

Jayaraman, Murali, Ravindra Kodali, Bankanidhi Sahoo, Ashwani K. Thakur, Anand Mayasundari, Rakesh Mishra, Cynthia B. Peterson, and Ronald Wetzel. 2012. "Slow Amyloid Nucleation via α-Helix-Rich Oligomeric Intermediates in Short Polyglutamine-Containing Huntingtin Fragments." *Journal of Molecular Biology* 415 (5): 881–99. https://doi.org/10.1016/j.jmb.2011.12.010.

Jeong, Hyunkyung, Florian Then, Thomas J. Melia, Joseph R. Mazzulli, Libin Cui, Jeffrey N. Savas, Cindy Voisine, et al. 2009. "Acetylation Targets Mutant Huntingtin to Autophagosomes for Degradation." *Cell* 137 (1): 60–72. https://doi.org/10.1016/j.cell.2009.03.018.

Jimenez-Sanchez, Maria, Floriana Licitra, Benjamin R. Underwood, and David C. Rubinsztein. 2017. "Huntington's Disease: Mechanisms of Pathogenesis and Therapeutic Strategies." *Cold Spring Harbor Perspectives in Medicine* 7 (7): 1–22. https://doi.org/10.1101/cshperspect.a024240.

Kay, Chris, Michael R. Hayden, and Blair R. Leavitt. 2017. "Epidemiology of Huntington Disease." In *Handbook of Clinical Neurology*, 144:31–46. https://doi.org/10.1016/B978-0-12-801893-4.00003-1.

Landwehrmeyer, G. Bernhard, Sandra M. McNeil, Leon S. Dure, Pei Ge, Hitoshi Aizawa, Qin Huang, Christine M. Ambrose, et al. 1995. "Huntington's Disease Gene: Regional and Cellular Expression in Brain of Normal and Affected Individuals." *Annals of Neurology* 37 (2): 218–30. https://doi.org/10.1002/ana.410370213.

Larsen, Sara C., Kathrine B. Sylvestersen, Andreas Mund, David Lyon, Meeli Mullari, Maria V. Madsen, Jeremy A. Daniel, Lars J. Jensen, and Michael L. Nielsen. 2016. "Proteome-Wide Analysis of Arginine Monomethylation Reveals Widespread Occurrence in Human Cells." *Science Signaling* 9 (443): rs9–rs9. https://doi.org/10.1126/scisignal.aaf7329.

Leavitt, Blair R., Jeremy M. Raamsdonk, Jacqueline Shehadeh, Herman Fernandes, Zoe Murphy, Rona K. Graham, Cheryl L. Wellington, Michael R. Hayden, and Michael R Hayden. 2006. "Wild-Type Huntingtin Protects Neurons from Excitotoxicity." *Journal of Neurochemistry* 96 (4): 1121–29. https://doi.org/10.1111/j.1471-4159.2005.03605.x.

Li, S H, G Schilling, W S Young, X J Li, R L Margolis, O C Stine, M V Wagster, M H Abbott, M L Franz, and N G Ranen. 1993. "Huntington's Disease Gene (IT15) Is Widely Expressed in Human and Rat Tissues." *Neuron* 11 (5): 985–93. http://www.ncbi.nlm.nih.gov/pubmed/8240819.

Li, Shi-Hua, Anna L Cheng, Hui Zhou, Suzanne Lam, Manjula Rao, He Li, and Xiao-Jiang Li. 2002. "Interaction of Huntington Disease Protein with Transcriptional Activator Sp1." *Molecular and Cellular Biology* 22 (5): 1277–87. https://doi.org/10.1128/mcb.22.5.1277-1287.2002.

Li, Shi-Hua, Claire-Anne Gutekunst, Steven M. Hersch, and Xiao-Jiang Li. 1998. "Interaction of Huntingtin-Associated Protein with Dynactin P150 Glued." *The Journal of Neuroscience* 18 (4): 1261–69. https://doi.org/10.1523/jneurosci.18-04-01261.1998.

Liot, G., D. Zala, P. Pla, G. Mottet, M. Piel, and F. Saudou. 2013. "Mutant Huntingtin Alters Retrograde Transport of TrkB Receptors in Striatal Dendrites." *Journal of Neuroscience* 33 (15): 6298–6309. https://doi.org/10.1523/JNEUROSCI.2033-12.2013.

Luo, S., and D. C. Rubinsztein. 2009. "Huntingtin Promotes Cell Survival by Preventing Pak2 Cleavage." *Journal of Cell Science* 122 (6): 875–85. https://doi.org/10.1242/jcs.050013.

Maday, Sandra, Alison E Twelvetrees, Armen J Moughamian, and Erika L F Holzbaur. 2014. "Axonal Transport: Cargo-Specific Mechanisms of Motility and Regulation." *Neuron* 84 (2): 292–309. https://doi.org/10.1016/j.neuron.2014.10.019.

Maiuri, T., T. Woloshansky, J. Xia, and R. Truant. 2013. "The Huntingtin N17 Domain Is a Multifunctional CRM1 and Ran-Dependent Nuclear and Cilial Export Signal." *Human*

Molecular Genetics 22 (7): 1383–94. https://doi.org/10.1093/hmg/dds554.

Marques Sousa, Cristovao, and Sandrine Humbert. 2013. "Huntingtin: Here, There, Everywhere!" *Journal of Huntington's Disease* 2 (4): 395–403. https://doi.org/10.3233/JHD-130082.

McGuire, John Russel, Juan Rong, Shi-Hua Li, and Xiao-Jiang Li. 2005. "Interaction of Huntingtin-Associated Protein-1 with Kinesin Light Chain." *Journal of Biological Chemistry* 281 (6): 3552–59. https://doi.org/10.1074/jbc.m509806200.

Menalled, Liliana B, Jessica D Sison, Ying Wu, Melisa Olivieri, Xiao-Jiang Li, He Li, Scott Zeitlin, and Marie-Françoise Chesselet. 2002. "Early Motor Dysfunction and Striosomal Distribution of Huntingtin Microaggregates in Huntington's Disease Knock-in Mice." *The Journal of Neuroscience : The Official Journal of the Society for Neuroscience* 22 (18): 8266–76. http://www.ncbi.nlm.nih.gov/pubmed/12223581.

Millecamps, Stéphanie, and Jean-Pierre Julien. 2013. "Axonal Transport Deficits and Neurodegenerative Diseases." *Nature Reviews Neuroscience* 14 (3): 161–76. https://doi.org/10.1038/nrn3380.

Nasir, J, S B Floresco, J R O'Kusky, V M Diewert, J M Richman, J Zeisler, A Borowski, J D Marth, A G Phillips, and M R Hayden. 1995. "Targeted Disruption of the Huntington's Disease Gene Results in Embryonic Lethality and Behavioral and Morphological Changes in Heterozygotes." *Cell* 81 (5): 811–23. http://www.ncbi.nlm.nih.gov/pubmed/7774020.

Nucifora Jr., F. C., M Sasaki, M F Peters, H Huang, J K Cooper, M Yamada, H Takahashi, et al. 2001. "Interference by Huntingtin and Atrophin-1 with CBP-Mediated Transcription Leading to Cellular Toxicity." *Science* 291 (5512): 2423–28. https://doi.org/10.1126/science.1056784.

O'Kusky, J R, J Nasir, F Cicchetti, A Parent, and M R Hayden. 1999. "Neuronal Degeneration in the Basal Ganglia and Loss of Pallido-Subthalamic Synapses in Mice with Targeted Disruption of the Huntington's Disease Gene." *Brain Research* 818 (2): 468–79. http://www.ncbi.nlm.nih.gov/pubmed/10082833.

Ochaba, Joseph, Tamás Lukacsovich, George Csikos, Shuqiu Zheng, Julia Margulis, Lisa Salazar, Kai Mao, et al. 2014. "Potential Function for the Huntingtin Protein as a Scaffold for Selective Autophagy." *Proceedings of the National Academy of Sciences* 111 (47): 16889–94. https://doi.org/10.1073/pnas.1420103111.

Palazzolo, Isabella, Barrington G. Burnett, Jessica E. Young, Phebe L. Brenne, Albert R. La Spada, Kenneth H. Fischbeck, Brian W. Howell, and Maria Pennuto. 2007. "Akt Blocks Ligand Binding and Protects against Expanded Polyglutamine Androgen Receptor Toxicity." *Human Molecular Genetics* 16 (13): 1593–1603. https://doi.org/10.1093/hmg/ddm109.

Palazzolo, Isabella, Conor Stack, Lingling Kong, Antonio Musaro, Hiroaki Adachi, Masahisa Katsuno, Gen Sobue, et al. 2009. "Overexpression of IGF-1 in Muscle Attenuates Disease in a Mouse Model of Spinal and Bulbar Muscular Atrophy." *Neuron* 63 (3): 316–28. https://doi.org/10.1016/j.neuron.2009.07.019.

Palidwor, Gareth A, Sergey Shcherbinin, Matthew R Huska, Tamas Rasko, Ulrich Stelzl, Anup Arumughan, Raphaele Foulle, et al. 2009. "Detection of Alpha-Rod Protein Repeats Using a Neural Network and Application to Huntingtin." Edited by Philip E. Bourne. *PLoS Computational Biology* 5 (3): e1000304. https://doi.org/10.1371/journal.pcbi.1000304.

Pardo, R. 2006. “Inhibition of Calcineurin by FK506 Protects against Polyglutamine-Huntingtin Toxicity through an Increase of Huntingtin Phosphorylation at S421.” *Journal of Neuroscience* 26 (5): 1635–45. https://doi.org/10.1523/jneurosci.3706-05.2006.

Perutz, M F, and A H Windle. 2001. “Cause of Neural Death in Neurodegenerative Diseases Attributable to Expansion of Glutamine Repeats.” *Nature* 412 (6843): 143–44. https://doi.org/10.1038/35084141.

Perutz, Max F, Tony Johnson, Masashi Suzuki, and John T Finch. 1994. “Glutamine Repeats as Polar Zippers: Their Possible Role in Inherited Neurodegenerative Diseases.” *Proc. Nati. Acad. Sci. USA*. Vol. 91. https://www.pnas.org/content/pnas/91/12/5355.full.pdf.

Phalke, Sameer, Slim Mzoughi, Marco Bezzi, Nancy Jennifer, Wei Chuen Mok, Diana H. P. Low, Aye Aye Thike, et al. 2012. “P53-Independent Regulation of P21Waf1/Cip1 Expression and Senescence by PRMT6.” *Nucleic Acids Research* 40 (19): 9534–42. https://doi.org/10.1093/nar/gks858.

Quan, Xin, Wenhui Yue, Yunfeng Luo, Jianwei Cao, Hongyun Wang, Yue Wang, and Zhongbing Lu. 2015. “The Protein Arginine Methyltransferase PRMT5 Regulates Aβ-Induced Toxicity in Human Cells and Caenorhabditis Elegans Models of Alzheimer’s Disease.” *Journal of Neurochemistry* 134 (5): 969–77. https://doi.org/10.1111/jnc.13191.

Rangone, Hélène, Ghislaine Poizat, Juan Troncoso, Christopher A Ross, Marcy E MacDonald, Frédéric Saudou, and Sandrine Humbert. 2004. “The Serum- and Glucocorticoid-Induced Kinase SGK Inhibits Mutant Huntingtin-Induced Toxicity by Phosphorylating Serine 421 of Huntingtin.” *The European Journal of Neuroscience* 19 (2): 273–79. http://www.ncbi.nlm.nih.gov/pubmed/14725621.

Ratovitski, Tamara, Nicolas Arbez, Jacqueline C. Stewart, Ekaterine Chighladze, and Christopher A. Ross. 2015. “PRMT5- Mediated Symmetric Arginine Dimethylation Is Attenuated by Mutant Huntingtin and Is Impaired in Huntington’s Disease (HD).” *Cell Cycle* 14 (11): 1716–29. https://doi.org/10.1080/15384101.2015.1033595.

Ratovitski, Tamara, Robert N. O’Meally, Mali Jiang, Raghothama Chaerkady, Ekaterine Chighladze, Jacqueline C. Stewart, Xiaofang Wang, et al. 2017. “Post-Translational Modifications (PTMs), Identified on Endogenous Huntingtin, Cluster within Proteolytic Domains between HEAT Repeats.” *Journal of Proteome Research* 16 (8): 2692–2708. https://doi.org/10.1021/acs.jproteome.6b00991.

Reiner, A, N Del Mar, C A Meade, H Yang, I Dragatsis, S Zeitlin, and D Goldowitz. 2001. “Neurons Lacking Huntingtin Differentially Colonize Brain and Survive in Chimeric Mice.” *The Journal of Neuroscience : The Official Journal of the Society for Neuroscience* 21 (19): 7608–19. http://www.ncbi.nlm.nih.gov/pubmed/11567051.

Rigamonti, D, J H Bauer, C De-Fraja, L Conti, S Sipione, C Sciorati, E Clementi, et al. 2000. “Wild-Type Huntingtin Protects from Apoptosis Upstream of Caspase-3.” *The Journal of Neuroscience : The Official Journal of the Society for Neuroscience* 20 (10): 3705–13. http://www.ncbi.nlm.nih.gov/pubmed/10804212.

Rigamonti, Dorotea, Simonetta Sipione, Donato Goffredo, Chiara Zuccato, Elisa Fossale, and Elena Cattaneo. 2001. “Huntingtin’s Neuroprotective Activity Occurs via Inhibition of Procaspase-9 Processing.” *Journal of Biological Chemistry* 276 (18): 14545–48. https://doi.org/10.1074/jbc.C100044200.

Rockabrand, Erica, Natalia Slepko, Antonello Pantalone, Vidya N Nukala, Aleksey Kazantsev, J Lawrence Marsh, Patrick G Sullivan, Joan S Steffan, Stefano L Sensi, and Leslie Michels Thompson. 2007. "The First 17 Amino Acids of Huntingtin Modulate Its Sub-Cellular Localization, Aggregation and Effects on Calcium Homeostasis." *Human Molecular Genetics* 16 (1): 61–77. https://doi.org/10.1093/hmg/ddl440.

Ross, Christopher A., Elizabeth H. Aylward, Edward J. Wild, Douglas R. Langbehn, Jeffrey D. Long, John H. Warner, Rachael I. Scahill, et al. 2014. "Huntington Disease: Natural History, Biomarkers and Prospects for Therapeutics." *Nature Reviews Neurology* 10 (4): 204–16. https://doi.org/10.1038/nrneurol.2014.24.

Ross, Christopher A., Martin Kronenbuerger, Wenzhen Duan, and Russell L. Margolis. 2017. "Mechanisms Underlying Neurodegeneration in Huntington Disease: Applications to Novel Disease-Modifying Therapies." In , 15–28. https://doi.org/10.1016/B978-0-12-801893-4.00002-X.

Ross, Christopher A., and Sarah J. Tabrizi. 2011. "Huntington's Disease: From Molecular Pathogenesis to Clinical Treatment." *The Lancet Neurology*. https://doi.org/10.1016/S1474-4422(10)70245-3.

Sathasivam, K., A. Neueder, T. A. Gipson, C. Landles, A. C. Benjamin, M. K. Bondulich, D. L. Smith, et al. 2013. "Aberrant Splicing of HTT Generates the Pathogenic Exon 1 Protein in Huntington Disease." *Proceedings of the National Academy of Sciences* 110 (6): 2366–70. https://doi.org/10.1073/pnas.1221891110.

Saudou, Frédéric, Steven Finkbeiner, Didier Devys, and Michael E. Greenberg. 1998. "Huntingtin Acts in the Nucleus to Induce Apoptosis but Death Does Not Correlate with the Formation of Intranuclear Inclusions." *Cell* 95 (1): 55–66. https://doi.org/10.1016/S0092-8674(00)81782-1.

Saudou, Frédéric, and Sandrine Humbert. 2016. "The Biology of Huntingtin." *Neuron*. Cell Press. https://doi.org/10.1016/j.neuron.2016.02.003.

Scaramuzzino, Chiara, Ian Casci, Sara Parodi, Patricia M.J. Lievens, Maria J. Polanco, Carmelo Milioto, Mathilde Chivet, et al. 2015. "Protein Arginine Methyltransferase 6 Enhances Polyglutamine-Expanded Androgen Receptor Function and Toxicity in Spinal and Bulbar Muscular Atrophy." *Neuron* 85 (1): 88–100. https://doi.org/10.1016/j.neuron.2014.12.031.

Scaramuzzino, Chiara, John Monaghan, Carmelo Milioto, Nicholas A. Lanson, Astha Maltare, Tanya Aggarwal, Ian Casci, Frank O. Fackelmayer, Maria Pennuto, and Udai Bhan Pandey. 2013. "Protein Arginine Methyltransferase 1 and 8 Interact with FUS to Modify Its Sub-Cellular Distribution and Toxicity In Vitro and In Vivo." *PLoS ONE* 8 (4). https://doi.org/10.1371/journal.pone.0061576.

Schaefer, Martin H, Erich E Wanker, and Miguel A Andrade-Navarro. 2012. "Evolution and Function of CAG/Polyglutamine Repeats in Protein-Protein Interaction Networks." *Nucleic Acids Research* 40 (10): 4273–87. https://doi.org/10.1093/nar/gks011.

Schulte, Joost, and J Troy Littleton. 2011. "The Biological Function of the Huntingtin Protein and Its Relevance to Huntington's Disease Pathology." *Current Trends in Neurology* 5 (January): 65–78. http://www.ncbi.nlm.nih.gov/pubmed/22180703.

Seong, Ihn Sik, Juliana M Woda, Ji-Joon Song, Alejandro Lloret, Priyanka D Abeyrathne, Caroline J Woo, Gillian Gregory, et al. 2010. "Huntingtin Facilitates Polycomb Repressive Complex

2." *Human Molecular Genetics* 19 (4): 573–83. https://doi.org/10.1093/hmg/ddp524.

Sharma, Sorabh, and Rajeev Taliyan. 2015. "Transcriptional Dysregulation in Huntington's Disease: The Role of Histone Deacetylases." *Pharmacological Research* 100 (October): 157–69. https://doi.org/10.1016/j.phrs.2015.08.002.

Sharp, Alan H, Scott J Loev, Gabriele Schilling, Shi-Hua Li, Xiao-Jiang Li, Jun Bao, Molly V Wagster, et al. 1995. "Widespread Expression of Huntington's Disease Gene (IT15) Protein Product." *Neuron* 14 (5): 1065–74. https://doi.org/10.1016/0896-6273(95)90345-3.

Shigeoka, Toshiaki, Hosung Jung, Jane Jung, Benita Turner-Bridger, Jiyeon Ohk, Julie Qiaojin Lin, Paul S Amieux, and Christine E Holt. 2016. "Dynamic Axonal Translation in Developing and Mature Visual Circuits." *Cell* 166 (1): 181–92. https://doi.org/10.1016/j.cell.2016.05.029.

Steffan, J S, A Kazantsev, O Spasic-Boskovic, M Greenwald, Y Z Zhu, H Gohler, E E Wanker, G P Bates, D E Housman, and L M Thompson. 2000. "The Huntington's Disease Protein Interacts with P53 and CREB-Binding Protein and Represses Transcription." *Proceedings of the National Academy of Sciences of the United States of America* 97 (12): 6763–68. https://doi.org/10.1073/pnas.100110097.

Steffan, Joan S., Laszlo Bodai, Judit Pallos, Marnix Poelman, Alexander McCampbell, Barbara L. Apostol, Alexsey Kazantsev, et al. 2001. "Histone Deacetylase Inhibitors Arrest Polyglutamine-Dependent Neurodegeneration in Drosophila." *Nature* 413 (6857): 739–43. https://doi.org/10.1038/35099568.

Steffan, Joan S, Namita Agrawal, Judit Pallos, Erica Rockabrand, Lloyd C Trotman, Natalia Slepko, Katalin Illes, et al. 2004. "SUMO Modification of Huntingtin and Huntington's Disease Pathology." *Science (New York, N.Y.)* 304 (5667): 100–104. https://doi.org/10.1126/science.1092194.

Stein, Claudia, René Reiner Nötzold, Stefanie Riedl, Caroline Bouchard, and Uta Maria Bauer. 2016. "The Arginine Methyltransferase PRMT6 Cooperates with Polycomb Proteins in Regulating HOXA Gene Expression." *PLoS ONE* 11 (2): 1–19. https://doi.org/10.1371/journal.pone.0148892.

Strong, Theresa V., Danilo A. Tagle, John M. Valdes, Lawrence W. Elmer, Karina Boehm, Manju Swaroop, Kevin W. Kaatz, Francis S. Collins, and Roger L. Albin. 1993. "Widespread Expression of the Human and Rat Huntington's Disease Gene in Brain and Nonneural Tissues." *Nature Genetics* 5 (3): 259–65. https://doi.org/10.1038/ng1193-259.

Subramaniam, Srinivasa, and Solomon H Snyder. 2011. "Huntington's Disease Is a Disorder of the Corpus Striatum: Focus on Rhes (Ras Homologue Enriched in the Striatum)." *Neuropharmacology* 60 (7–8): 1187–92. https://doi.org/10.1016/j.neuropharm.2010.10.025.

Tabrizi, Sarah J., Rhia Ghosh, and Blair R. Leavitt. 2019. "Huntingtin Lowering Strategies for Disease Modification in Huntington's Disease." *Neuron*. Cell Press. https://doi.org/10.1016/j.neuron.2019.01.039.

Takano, Hiroki, and James F Gusella. 2002. "The Predominantly HEAT-like Motif Structure of Huntingtin and Its Association and Coincident Nuclear Entry with Dorsal, an NF-KB/Rel/Dorsal Family Transcription Factor." *BMC Neuroscience* 3 (October): 15. http://www.ncbi.nlm.nih.gov/pubmed/12379151.

Tartari, Marzia, Carmela Gissi, Valentina Lo Sardo, Chiara Zuccato, Ernesto Picardi, Graziano Pesole, and Elena Cattaneo. 2008. "Phylogenetic Comparison of Huntingtin Homologues Reveals the Appearance of a Primitive PolyQ in Sea Urchin." *Molecular Biology and Evolution* 25 (2): 330–38. https://doi.org/10.1093/molbev/msm258.

Taylor, Anne M, Daniela C Dieterich, Hiroshi T Ito, Sally A Kim, and Erin M Schuman. 2010. "Microfluidic Local Perfusion Chambers for the Visualization and Manipulation of Synapses." *Neuron* 66 (1): 57–68. https://doi.org/10.1016/j.neuron.2010.03.022.

Thandapani, Palaniraja, Timothy R O'Connor, Timothy L Bailey, and Stéphane Richard. 2013. "Defining the RGG/RG Motif." *Molecular Cell* 50 (5): 613–23. https://doi.org/10.1016/j.molcel.2013.05.021.

The Huntington's Disease Collaborative Research Group. "A Novel Gene Containing a Trinucleotide Repeat That Is Expanded and Unstable on Huntington's Disease Chromosomes. The Huntington's Disease Collaborative Research Group." 1993. Cell 72 (6): 971–83.

Thompson, Leslie Michels, Charity T. Aiken, Linda S. Kaltenbach, Namita Agrawal, Katalin Illes, Ali Khoshnan, Marta Martinez-Vincente, et al. 2009. "IKK Phosphorylates Huntingtin and Targets It for Degradation by the Proteasome and Lysosome." *The Journal of Cell Biology* 187 (7): 1083–99. https://doi.org/10.1083/jcb.200909067.

Tourette, Cendrine, Biao Li, Russell Bell, Shannon O'Hare, Linda S. Kaltenbach, Sean D. Mooney, and Robert E. Hughes. 2014. "A Large Scale Huntingtin Protein Interaction Network Implicates RHO GTPase Signaling Pathways in Huntington Disease." *Journal of Biological Chemistry* 289 (10): 6709–26. https://doi.org/10.1074/jbc.M113.523696.

Tradewell, Miranda L., Zhenbao Yu, Michael Tibshirani, Marie-Chloé Boulanger, Heather D. Durham, and Stéphane Richard. 2012. "Arginine Methylation by PRMT1 Regulates Nuclear-Cytoplasmic Localization and Toxicity of FUS/TLS Harbouring ALS-Linked Mutations." *Human Molecular Genetics* 21 (1): 136–49. https://doi.org/10.1093/hmg/ddr448.

Trettel, F, D Rigamonti, P Hilditch-Maguire, V C Wheeler, A H Sharp, F Persichetti, E Cattaneo, and M E MacDonald. 2000. "Dominant Phenotypes Produced by the HD Mutation in STHdh(Q111) Striatal Cells." *Human Molecular Genetics* 9 (19): 2799–2809. https://doi.org/10.1093/hmg/9.19.2799.

Tripathy, Debasmita, Beatrice Vignoli, Nandini Ramesh, Maria Jose Polanco, Marie Coutelier, Christopher D. Stephen, Marco Canossa, et al. 2017. "Mutations in TGM6 Induce the Unfolded Protein Response in SCA35." *Human Molecular Genetics* 26 (19): 3749–62. https://doi.org/10.1093/hmg/ddx259.

Trushina, E., R. B. Dyer, J. D. Badger, D. Ure, L. Eide, D. D. Tran, B. T. Vrieze, et al. 2004. "Mutant Huntingtin Impairs Axonal Trafficking in Mammalian Neurons In Vivo and In Vitro." *Molecular and Cellular Biology* 24 (18): 8195–8209. https://doi.org/10.1128/mcb.24.18.8195-8209.2004.

Twelvetrees, Alison E, Eunice Y Yuen, I Lorena Arancibia-Carcamo, Andrew F MacAskill, Philippe Rostaing, Michael J Lumb, Sandrine Humbert, et al. 2010. "Delivery of GABAARs to Synapses Is Mediated by HAP1-KIF5 and Disrupted by Mutant Huntingtin." *Neuron* 65 (1): 53–65. https://doi.org/10.1016/j.neuron.2009.12.007.

Vermeire, Jolien, Evelien Naessens, Hanne Vanderstraeten, Alessia Landi, Veronica Iannucci, Anouk Van Nuffel, Tom Taghon, Massimo Pizzato, and Bruno Verhasselt. 2012. "Quantification of Reverse Transcriptase Activity by Real-Time PCR as a Fast and Accurate Method for Titration of HIV, Lenti- and Retroviral Vectors." Edited by Gilda Tachedjian. *PloS One* 7 (12): e50859. https://doi.org/10.1371/journal.pone.0050859.

Virlogeux, Amandine, Eve Moutaux, Wilhelm Christaller, Aurélie Genoux, Julie Bruyère, Elodie Fino, Benoit Charlot, Maxime Cazorla, and Frédéric Saudou. 2018. "Reconstituting Corticostriatal Network On-a-Chip Reveals the Contribution of the Presynaptic Compartment to Huntington's Disease." *Cell Reports* 22 (1): 110–22. https://doi.org/10.1016/j.celrep.2017.12.013.

Waldmann, Tanja, Annalisa Izzo, Kinga Kamieniarz, Florian Richter, Christine Vogler, Bettina Sarg, Herbert Lindner, et al. 2011. "Methylation of H2AR29 Is a Novel Repressive PRMT6 Target." *Epigenetics and Chromatin* 4 (1): 11. https://doi.org/10.1186/1756-8935-4-11.

Waldvogel, Henry J., Eric H. Kim, Lynette J. Tippett, Jean-Paul G. Vonsattel, and Richard LM Faull. 2014. "The Neuropathology of Huntington's Disease." In , 33–80. Springer, Berlin, Heidelberg. https://doi.org/10.1007/7854_2014_354.

Warby, Simon C., Crystal N. Doty, Rona K. Graham, Jeffrey B. Carroll, Yu-Zhou Yang, Roshni R. Singaraja, Christopher M. Overall, and Michael R. Hayden. 2008. "Activated Caspase-6 and Caspase-6-Cleaved Fragments of Huntingtin Specifically Colocalize in the Nucleus." *Human Molecular Genetics* 17 (15): 2390–2404. https://doi.org/10.1093/hmg/ddn139.

Watkin, Erin E., Nicolas Arbez, Elaine Waldron-Roby, Robert O'Meally, Tamara Ratovitski, Robert N. Cole, and Christopher A. Ross. 2014. "Phosphorylation of Mutant Huntingtin at Serine 116 Modulates Neuronal Toxicity." *PLoS ONE* 9 (2). https://doi.org/10.1371/journal.pone.0088284.

White, Jacqueline K., Wojtek Auerbach, Mabel P. Duyao, Jean-Paul Vonsattel, James F Gusella, Alexandra L. Joyner, and Marcy E. MacDonald. 1997. "Huntingtin Is Required for Neurogenesis and Is Not Impaired by the Huntington's Disease CAG Expansion." *Nature Genetics* 17 (4): 404–10. https://doi.org/10.1038/ng1297-404.

Wolf, S. S. 2009. "The Protein Arginine Methyltransferase Family: An Update about Function, New Perspectives and the Physiological Role in Humans." *Cellular and Molecular Life Sciences* 66 (13): 2109–21. https://doi.org/10.1007/s00018-009-0010-x.

Wong, Y. C., and E. L. F. Holzbaur. 2014. "The Regulation of Autophagosome Dynamics by Huntingtin and HAP1 Is Disrupted by Expression of Mutant Huntingtin, Leading to Defective Cargo Degradation." *Journal of Neuroscience* 34 (4): 1293–1305. https://doi.org/10.1523/JNEUROSCI.1870-13.2014.

Xia, Jianrun, Denise H Lee, Jillian Taylor, Mark Vandelft, and Ray Truant. 2003. "Huntingtin Contains a Highly Conserved Nuclear Export Signal." *Human Molecular Genetics* 12 (12): 1393–1403. http://www.ncbi.nlm.nih.gov/pubmed/12783847.

Yanai, Anat, Kun Huang, Rujun Kang, Roshni R Singaraja, Pamela Arstikaitis, Lu Gan, Paul C Orban, et al. 2006. "Palmitoylation of Huntingtin by HIP14is Essential for Its Trafficking and Function." *Nature Neuroscience* 9 (6): 824–31. https://doi.org/10.1038/nn1702.

Zala, Diana, Maria-Victoria Hinckelmann, and Frédéric Saudou. 2013. "Huntingtin's Function in Axonal Transport Is Conserved in Drosophila Melanogaster." Edited by Andreas Bergmann. *PLoS ONE* 8 (3): e60162. https://doi.org/10.1371/journal.pone.0060162.

Zala, Diana, Maria Victoria Hinckelmann, Hua Yu, Marcel Menezes Lyra Da Cunha, Géraldine Liot, Fabrice P. Cordelières, Sergio Marco, and Frédéric Saudou. 2013. "Vesicular Glycolysis Provides On-Board Energy for Fast Axonal Transport." *Cell* 152 (3): 479–91. https://doi.org/10.1016/j.cell.2012.12.029.

Zeitlin, Scott, Jeh-Ping Liu, Deborah L. Chapman, Virginia E. Papaioannou, and Argiris Efstratiadis. 1995. "Increased Apoptosis and Early Embryonic Lethality in Mice Nullizygous for the Huntington's Disease Gene Homologue." *Nature Genetics* 11 (2): 155–63. https://doi.org/10.1038/ng1095-155.

Zhang, Yu, Blair R Leavitt, Jeremy M van Raamsdonk, Ioannis Dragatsis, Dan Goldowitz, Marcy E MacDonald, Michael R Hayden, and Robert M Friedlander. 2006. "Huntingtin Inhibits Caspase-3 Activation." *The EMBO Journal* 25 (24): 5896–5906. https://doi.org/10.1038/sj.emboj.7601445.

Zhang, Yu, Mingwei Li, Martin Drozda, Minghua Chen, Shengjun Ren, Rene O Mejia Sanchez, Blair R Leavitt, et al. 2003. "Depletion of Wild-Type Huntingtin in Mouse Models of Neurologic Diseases." *Journal of Neurochemistry* 87 (1): 101–6. http://www.ncbi.nlm.nih.gov/pubmed/12969257.

Zuccato, C., A Ciammola, D Rigamonti, B R Leavitt, D Goffredo, L Conti, M E MacDonald, et al. 2001. "Loss of Huntingtin-Mediated BDNF Gene Transcription in Huntington's Disease." *Science* 293 (5529): 493–98. https://doi.org/10.1126/science.1059581.

Zuccato, Chiara, Marzia Tartari, Andrea Crotti, Donato Goffredo, Marta Valenza, Luciano Conti, Tiziana Cataudella, et al. 2003. "Huntingtin Interacts with REST/NRSF to Modulate the Transcription of NRSE-Controlled Neuronal Genes." *Nature Genetics* 35 (1): 76–83. https://doi.org/10.1038/ng1219.

Zuccato, Chiara, Marta Valenza, and Elena Cattaneo. 2010. "Molecular Mechanisms and Potential Therapeutical Targets in Huntington's Disease." *Physiological Reviews* 90 (3): 905–81. https://doi.org/10.1152/physrev.00041.2009.